Ministry of Higher Education
and Scientific Research
University of Babylon
College of Science
Department of Applied Geology

Geophysical Engineering Study Using Seismic refraction methods For Al-Sayidah Ruqayya Hospital Site in Hilla City – Middle Iraq

A Thesis

Submitted to the College of Science University of Babylon

in Partial Fulfillment of the Requirements for the Degree of Master of Science in Applied Geology

BY

Zainab Mohammed Jawad Saify Wehaib
B.Sc. Applied Geology 2013

Higher Diploma in Science Applied Geology 2015

Supervised by

Prof. Dr. Amer Atyah Laftah Al-Khalidy

2023 A.D **1444 A.H**

DECLARATION

I certify that this thesis " **Geophysical Engineering Study Using Seismic refraction methods For Al-Sayidah Ruqayya Hospital Site in Hilla City – Middle Iraq**" has been prepared under my supervision at Applied Geology Department - College of Science / Babylon University, as partial requirement for Master degree in Science of Applied Geology.

Signature:
Supervisor: **Prof. Dr. Amer Atyah Laftah Al-Khalidy**
Date: / / 2023

Forwarding For debate
In view the available recommendations, I forward this thesis for debate by the examining committee.

Signature:
Name: **Prof. Dr. Jaffar Hussain Ali Al-Zubaydi**
Title: Head of Applied Geology Department – College of Science
Date: / / 2023

CERTIFICATION OF THE EXAMINATION COMMITTEE

We certify that we have read this thesis entitled **" Geophysical Engineering Study Using Seismic refraction methods For Al-Sayidah Ruqayya Hospital Site in Hilla City – Middle Iraq "** as Examining Committee examined the student **(Zainab Mohammed Jawad Saify)** on its content and that in our opinion it is adequate the award for the Degree of Master of Science in Applied Geology.

Signature:
Name: Dr. Jaffar Hussain Ali Al-Zubaydi
Title: Professor
Address: College of Science / University of Babylon
Date: / / 2023
(Chairman)

Signature:
Name: Dr. Munther Daher Nassif
Title: Professor
Address: College of Science / University of Diyala
Date: / / 2023
(Member)

Signature:
Name:Dr.Abdul Kareem Hussein Abd
Title: Assistant Professor
Address: College of Science / University of Babylon
Date: / / 2023
(Member)

Signature:
Name: Dr. Amer Atyah Laftah Al-Khalidy
Title: Professor
Address: College of Science University of Babylon
Date: / / 2023
(Member and Supervisor)

Approved by the Dean of the College of Science

Signature:
Name: Dr. Mohammed Mansour Al-Kafaji
Title: Professor
Address: College of Science / University of Babylon
Date: / / 2023
(Dean of College of Science)

بسم الله الرحمن الرحيم

(وَفَوْقَ كُلِّ ذِي عِلْمٍ عَلِيمٌ)

صدق الله العلي العظيم

سورة يوسف (الآية 76)

Dedication

To
My Family
With love and respect

ACKNOWLEDGMENTS

All profusion praise and thanks be to Allah for his uncountable help and strength which He gave me to achieve this work. Throughout the period of my research, I have benefited greatly from the guidance, advice, and sympathy of my teachers, and friends, to all of whom I wish to offer my warmest thanks. I would like to express my gratitude and deep thanks to my supervisor **Prof. Dr. Amer A. Al-Khalidy** for the supervision, guidance, constructive criticism and encouragement through this work.

Also I would like to thank my family for being always there with their encouragement, prayer, and patience.

ZAINAB

SUMMARY

A geophysical engineering study was conducted for the AL-Sayidah Ruqayya Hospital building project in the city of Hilla using the seismic refraction method and the Multi-channel analysis method for surface waves MASW to determine the average velocity of shear waves and their relationship to the layer thickness, foundation depth, bearing capacity and calculating the engineering parameters of the soil in the horizontal seismic refractive survey method. Where this geophysical survey was conducted using the ABEM Terraloc MK6 device, using geophones to receive seismic waves, as well as using an iron hammer weighing 10 kg to estimate seismic waves. This survey was carried out along two profiles in the seismic refraction survey to obtain the velocity of the compressive and shear waves, as the length of one track is 72m (front, reverse and central) and the dynamic elasticity parameters were calculated such as the Poison's ratio ν, the Young modulus E , the Bulk modulus B, Shear modulus μ, Lame's constant λ and a number of geometric parameters such as the Material index I_m, Concentration index I_c, Lateral pressure coefficient K_o, Effective internal friction angle Φ^o, as well as the Allowable bearing capacity Q_{all} after obtaining values for the velocities of the compressive V_p and shear V_s waves in these two tracks. Using the Reflex 2D Quick program, it is found that the first profile consists of two layers, and the second profile consists of two layers as well, as the average of velocity of the compressive waves in the first profile of the first and second layers is 277.768 and 460.001 m/sec, respectively, and the average velocity of the shear waves for the same profile and for the same first and second layers is 152.423 and 252.734 m/sec, respectively. The thickness of the first layer in the first track is 8 m. As for the second profile, the average of the compressive velocity of this profile and of the

first and second layers is 276.55 and 465.021 m/s, respectively, while the average of the shear velocities of these two layers and for the same profile are 152.149 and 250.735 m/sec, respectively. The thickness of the first layer in the second profile is 8.066 m. As for the MASW (Multi-channel analysis method), the survey was carried out in this way along only one profile and its length is 72 m to calculate the average shearing velocity and its relationship to the depth of the foundation, the thickness of the layer and the bearing capacity. Using the Reflex 2D Quick program, it is found that this track consists of two layers as well, where the value of the average for the velocity of the shear wave in the first layer is 171.6 m/sec and its thickness is 8.244 m, while the average for the shear velocity of the second layer is 272.22 m/sec. In this method, SeisImager/SW program is used to obtain photographic sections showing dispersion curves (between frequency and phase velocity) as well as to draw a one-dimensional cross section of shear velocities. The contour maps are drawn to show the distribution of shear velocity, bearing capacity, foundation depth, and layer thickness, noting the compatibility between each of them. A statistical relationship is made using SPSS program between the refractive survey and MASW method, and the correlation is high between them. Through the engineering and geophysical results, it is found that the second layer in all the profiles is the proposed layer for the construction of the engineering structure.

CONTENTS

LIST OF FIGUERS

LIST OF PLATES

LIST OF TABLES

LIST OF ABBREVIATIONS

MASW	Multi-channel Analysis Surface Waves
Remi	Micro- tremor survey method
V_P	Compressive velocity (primary)
V_S	Shear velocity
ρ	Density
ν	Poisson's ratio
E	Young modulus
K	Bulk modulus
μ	Shear modulus
λ	Lame's constant
Θ	Effective angle
I_m	Material index
I_c	Concentration index
Q_{all}	Allowable bearing capacity
q_{ul}	Ultimate bearing capacity
r_{xy}	Correlation coefficient (Pearson Correlation)

Chapter One

Introduction

CHAPTER ONE

INTRODUCTION

(1-1) Introduction:

The shallow investigation geophysical applications have a wide spread in engineering and geotechnical studies, as well as the tremendous technical development and information that we are witnessing today in the field of geophysical measurements, including the seismic method, has increased of its superiority, success and confidence its results. This development represented in the invention of measuring devices seismicity with high accuracy and speed in addition to the development acquisition methods, processing methods and interpretation methods which in turn reduced cost and time and increased the accuracy of the possible results, (Al-Heety, 2014).

The history of the use of the refractive seismic survey method in the applied field dates back to 1910, when (*L.Mintrop*) pointed out to use this method to calculate depths and determine subsurface layers types and developed this method (*Mintrop*), It became a patent registered in Germany in 1991, the first seismic exploration company is established. It is the seismic survey method Refractive is the only method available at the time that showed great effectiveness in determining salt domes (Sharma, 1986). In the early fifties this method is used in the initial investigations as a tool reconnaissance to detect underground water basins determine its extent and determine the level of groundwater (Haeni,1986). It has been noticed that this method is became more and more important in engineering applications (in situ investigations) for reasons such as: accuracy of results at shallow depths especially in determining the depth of the weathering layer low velocity seismic, determination of vertical and horizontal changes in the lithology and detecting geological structures, and the possibility of

controlling the depth of exploration. This is one of the most important features of the refractivity method, as the depth of exploration can be roughly determined by controlling the distance between the energy seismic source and seismic wave receiver which is called (geophone), depth of exploration between (1/5-1/3) from the distance between the power source and the receiver (Redpath,1973).

Seismic methods, especially the refraction seismic method, have been used to solve many problems related to civil engineering, engineering and environmental geology works.

Seismic methods are divided into two types: invasive and non-invasive. The first type requires borehole like (Cross-hole, Down hole, P-S suspension and logging), As for the second type, it is carried out on the surface like (Seismic Refraction and Reflection, Spectral Analysis of Surface Waves (SASW), Multi-channel Analysis of Surface Waves (MASW)) which enables us to calculate the velocities of the shear seismic waves (V_S), it in turn serves the engineering evaluation process for different sites (Socco et al., 2010).

Seismic wave techniques can be used to determine very useful parameters for engineering purposes, such as elastic modulus, shear modulus and Poisson's ratio. As such, geophysical techniques, like the seismic surface wave technique, offer a non-destructive way of performing geotechnical properties measurements (Clayton et al., 1995).

(1-2) Location of the study area:

The study area lies in Babylon Governorate, Hilla city, Al-Iskan neighborhood within latitudes 32º 27′ 44.85″ North and longitudes 44º 25´ 06.85″ East with an area of 4900 m^2. This location is selected to study is Al-Sayidah Ruqayya Hospital Building project Fig.(1-1).

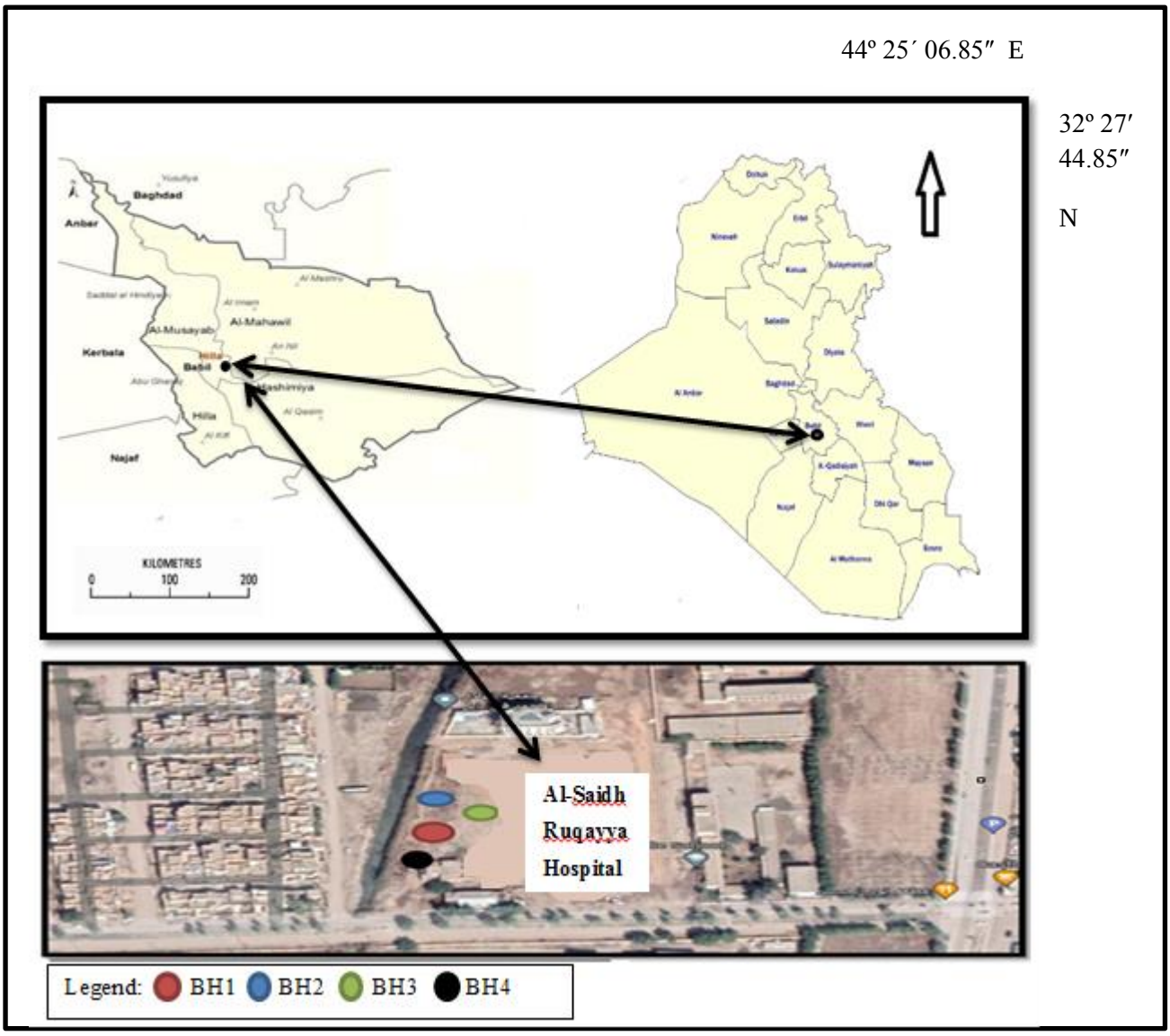

Fig (1-1): Location map of the study area satellite image of the study site.

(1-3) Aims of the study:

1- Studying the relationship between the values of the shear waves velocity with the bearing capacity of the soil and the depth of the foundation.

2- Calculation of Geotechnical parameters of the soil.

3- Drawing contour maps showing the distribution of the velocity of shear waves, bearing capacity, foundation depth and layer thickness, and observing the extent of compatibility between each of them in the study area.

4- Finding a statistical relationship (equation) in the study area that shows the comparison between the results of refraction survey method and the MASW method.

(1-4) Stratigraphy and Tectonic Setting:

The study area lies within the Mesopotamian basin as shown in Fig.(1-2) according to the tectonic zones of Iraq, where is covered by the Quaternary fluvial sediments of the Tigris and Euphrates rivers and tertiary deposit (Jassim and Goff, 2006). This area, which occupies central and southern Iraq, is a flat terrain in general with a gentle slope from northwest to southeast towards the Arabian Gulf.

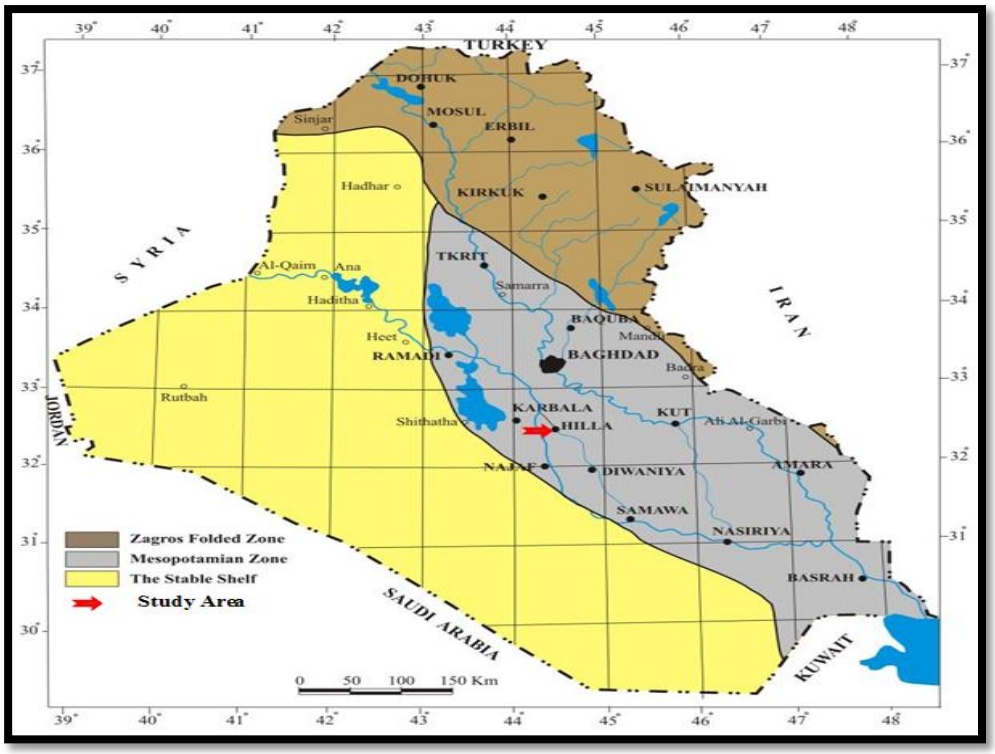

Fig (1-2): Tectonic map of Iraq (Buday and Jassim (1984)) .

The study area generally covers recent sediments from the Quaternary in the Pleistocene and Halocene, and these deposits are derived from the sediments of the Tigris and Euphrates rivers and their tributaries, it consists of a succession of well-permeable silty sand and clay layers of varying thickness, and the vertical and lateral directions change abruptly and within very short ranges, which is a distinctive feature of these sediments.

The old alluvial deposits were formed during the Pleistocene, which was characterized by a rainy and semi-rainy climate in the Middle East, more humid than the climate of the present time. Therefore, the sediments and the stratigraphic sequence depended on climate changes that led to a re-cycle of erosion and sedimentation in high areas and then sedimentation in the wide plains, and then the sediments of this period include gravel, sand, silt and clay, which are flood deposits (Budy, 1980) Fig.(1-3)

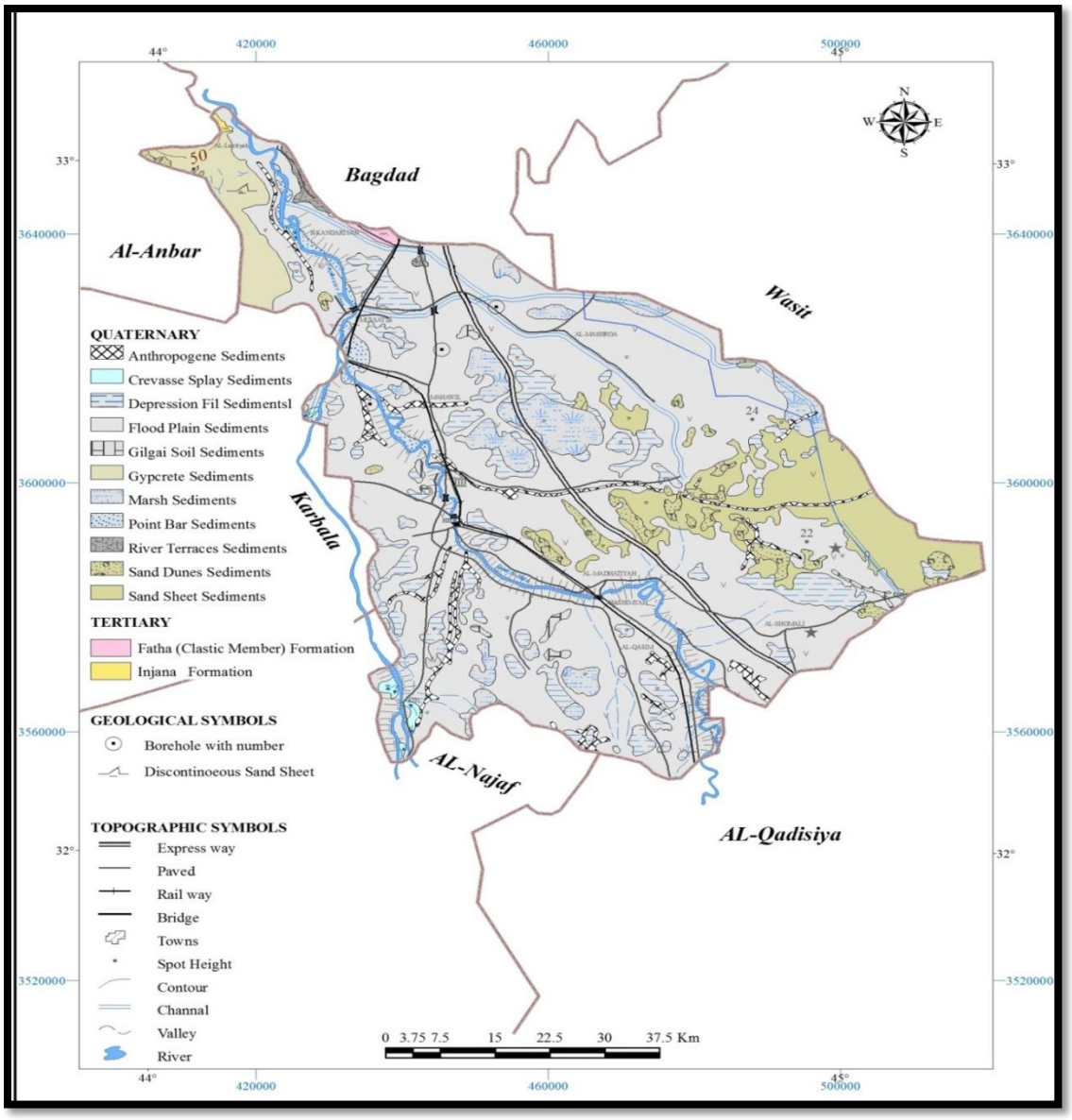

Fig.(1-3): A modified geological map of the study area (Geosurv, 2020)

Structural features are absent on the surface. It contains several subsurface structures including faults, folds, and dioptric structures that are entirely concealed beneath the Quaternary cover. Surface folds are almost absent in the Mesopotamia Plain. The Quaternary sediments are uplifted along with the structure with about (10 - 15) m relief in comparison with the surrounding. Consequently, local drainage divide lines are developed along the crests of these structures (Fouad, 2010). Subsurface folds are rather common structures within the Mesopotamia Plain. They are hidden beneath

the Quaternary cover, usually with NW _ SE trend in the central and eastern parts, following the general trend of the Zagros Fold Thrust Belt, but deviate largely in the extreme southern part where the folds are N- S trending.

The Quaternary sediments exhibit an exceptional development in the Mesopotamia Plain. They consist of gravels, sands, silts, and clays that are mainly related to the cyclic fluvial sediments of the Tigris and Euphrates Rivers, with their tributaries and distributaries. These sediments form extensive, flood plains with a complex network of natural levees and channels, and terraces. The Quaternary sediments of the Mesopotamia Plain exhibit progressive thickening from northwest to southeast (Jassim and Goff, 2006).

(1-4-1) Hydrogeology:

Available hydrogeological information of the Babylon city shows the existence of gravel, sand, silt deposits and clay content within ground water that found at different levels of the earth surface (Mashkori and Al-Naimi, 1993). The water quality vary from one site to another; however, this water is characterized by its content of high salts, total dissolved solids range from (2600 to 22224) mg/l with sulphatic and chloridic water types.

In recharge regions, water movement is generally from up to down while in discharge regions, water movement is upwards within springs zone to the west of Euphrates river at the extreme northeastern part of the southern desert, and laterally towards Mesopotamia plain (Al-Jiburi and Al-Basrawi, 2008). The direction of groundwater movement is affected by several factors, including geological, structural and topographic nature, which change the groundwater movement. Also, the quantities of percolated water depend mainly on lithology, permeability and amounts of rainfall and surface runoff, (Al-Jiburi and Al-Basrawi, 2008).

(1-5) Previous Studies:

(1-5-1) Local Studies:

Khurshid (1986) studied the behavior of refracted longitudinal and transverse waves in sedimentary rocks under cavities at the site of an engineering facility south of Baghdad to identify areas of weakness and gaps in the foundations, due to the dissolution of gypsum soil at high groundwater levels, and velocities were found for longitudinal and transverse waves, depth of layers and he measured the elasticity coefficients using (V_P), (V_S) and the density values measured in the laboratory.

Al-Rubaie (1995) Studied seismic refraction at the site of a hydroelectric station in Jabal (Makhoul/2) in Baiji District, as part of soil investigations, and it identified three layers in the study area and conducted a test of statistical relationships of field and laboratory information between the values of seismic velocities with different elasticity coefficients.

Al-Mawla (1996) conducted a geotechnical study of the rock units of the Al-Azim Dam project in the district of Al-Azim, north of Baghdad, several techniques were used to determine the thickness of layers and determine areas weaknesses, as the refractive seismic method gave the velocities of longitudinal and shear waves of the four layers of the study site and use them in calculating their geotechnical properties.

Isaac (1998) conducted a study for determining the shallow geological structures and the depth of the water level using the seismic-refractive method, four sedimentary layers in the research area were distinguished.

Al-Khafaji (2004) used seismic methods to investigate and assess the geotechnical weakness soil for the foundations of Al-Hussein Water Project Karbala. The results show that water seepage from broken pipes and their

infiltration through the soil play the great role in washing the soil and changing the water table level from one point to others. The differential washing of soil causes differential settlement beneath the buildings which appears as cracks in the walls.

AlShujairy (2008) use geotechnical and geophysical methods (refractive survey and ultrasound to study two selected sites in Baghdad and measure the velocities of seismic waves to calculate the coefficients of dynamic elasticity.

Al-Shimaree, et al., (2012) used geophysical methods such as seismic refraction, electrical survey with the assistance of the engineering information at both gas power Hilla-2 and Karbala-2 plants which located within Babylon and Karbala Governorates/Central Iraq. They are able to obtain the elastic modulus such as Poisson ratio, Young modulus, Shear modulus and Bulk modulus. As well as, they obtained on standard penetration test and bearing capacity values which performed and calculated for the studied soils. They gave five subsurface layers in these two plants, depths, thicknesses and resistivities of these layers were identified. They indicated that the subsurface layers which belonging to Karbala-2 has resistivity values higher than Hilla-2. This is due to the dry soil and high gypsum content.

AL-Awsi, et al., (2014) use seismic refraction survey in Tikrit University, Iraq for geotechnical evaluation of the soil based on P and S waves velocity and calculate the Poisson's ratio(ν), Material index (I_m) then plotted contour maps for different layers. These maps are divided into two zones, zone A represents the area which has good geotechnical properties, and zone B represents the area which has weak geotechnical properties such as loose unconsolidated sediments or weak zones. The first and third layers are fairly competent to intermediate competent layers because they have good

geotechnical properties by comparing with second and fourth layers which have poor geotechnical properties which represent incompetent layers.

There is a limited number of studies in which technology was used Multi-channels Analysis of Surface Waves (MASW):

Shakir (2012) conduct investigations for the proposed location for the metro in Najaf using geophysical methods and Multi-channels Analysis of Surface Waves (MASW) in addition to drilling exploratory wells and on-site tests for the proposed site to determine the quality of the subsurface layers and their geotechnical properties.

Al-Heety (2014) uses Multi-channels Analysis of Surface Waves (MASW) for the site of educational hospital in the Mosul University to delineate the thickness and types of the different subsurface layers and to evaluate some soil and rock engineering parameters.The seismic velocity and the dynamic and engineering parameters showed that the third layer is composed of very competent rock. Hence, this layer is the suggested layer for foundation purpose. Multi Analyses Surface Waves technique were conducted to obtain the S wave velocities. The field data are processed and interpreted by using the SeisImager™/2D software to obtain the velocities of Vp and Vs, as well as deducing the Vs from the phase velocity of Rayleigh surface wave by using MASW method. Then 2D seismic imaging sections and two 1D sections of shear waves were drawn.

(1-5-2) Regional and International Studies:

Abdel-Rahman, et al., (1994) used both (V_P) and (V_S) to calculate the Poisone ratio, the material index and the concentration index, and (V_S), was used to calculate the maximum load capacity in the new city in Minya Governorate - Republic of Egypt.

Long et and Donohue (2007) used the MASW technique to calculate the velocity of shear waves (V_S) in calculating some engineering parameters at 8 research sites in Norway.

Anbazhagan and Sitharam (2008) conducted a study to estimate the dynamic properties of subsurface soil layers (Young modulus and shear modulus) in Bangor state in India by using longitudinal and shear seismic velocities calculated by (MASW) method.

Khalil and Hanafy (2008) applied the seismic-refractive method to calculate the dynamic and geometric parameters based on the values of longitudinal and shear waves in Wadi Houran in the Sinai desert in Egypt.

Rao, et al., (2009) conducted a study on finding geometric coefficients in Faridabad and Ghaziabad in the capital, New Delhi- India, using longitudinal wave velocities (V_P) and the shear (V_S calculated from Multi-channel analysis technology for surface waves (MASW) and by dividing the region into several regions according to those transactions.

Wongpornchai, et al., (2009) conducted 2D and 3D seismic-refraction survey of the (Mai-Hia) landfill in Muynheg province in Thailand and select three layers and they calculated the velocity and depth for them.

George, et al., (2010) calculated the elastic properties of the subsurface and deep layers and thickened in parts of Akamba region in southeastern Nigeria using the seismic-refraction method.

(1-6) Office Work:

Seismic Refraction Survey and MASW Technique

1- The arrival times of the seismic waves (P,S) are picked by data with distance in the Reflex 2D Quick program.
2- The relationship between distance and time to find out the (P,S) velocity and depth were drawn using Excel software and the

interpretation of this relationship showed there are two layers in the study area.

3- The elasticity coefficients (Dynamic Yuong Modulus (E), Dynamic Shear Modulus (μ), Poisson ratio (ν), Dynamic Bulk Modulus (K) and Dynamic Lame constant (λ)) as well as the engineering properties (Material Index (I_m), Concentration Index (I_c), Coefficient of lateral earth pressure at rest (K_o), Effective angle of internal friction ($\emptyset^o$) and Allowable Bearing Capacity (Q_{all})) of the soil were calculated.

4- For MASW method Shear velocity and layer thickness are calculated by Reflex 2D Quick. Then the bearing capacity was extracted according to the depth of the foundation which is (1,2,3) m.

Chapter Two

Theoretical Background

CHAPTER TWO
THEORETICAL BACKGROUND

(2-1) Introduction:

One outstanding seismic method used for estimating ground stiffness or elastic state of the soil is the Multi-channel Surface Wave (MASW) method, which was initially discovered in Japan more than half a century ago. Initially it was called the micro-tremor survey method (Remi). The Kansas Geological Survey in the late 1990s developed electrical equipment for the (Remi) and used it for multi-channel analysis of surface waves, MASW (Park et al., 1999). MASW operates by initially measuring the seismic surface waves obtained from various types of seismic sources. The transmission velocities of these surface waves are then analyses to deduce shear wave velocity variations below the surveyed area, which are related to its geotechnical features.

MASW, which is presented by (Park et al. 1999), allows one to efficiently identify, isolate and filter noise from dispersed and reflected waves during data analysis just by using several receivers and with only one shot. It therefore becomes possible for the best fit line to be drawn on the phase angle plot. There are three main steps for the complete procedure of the MASW.

The initial step is obtaining the multi-channel field records. This is followed by the extraction of the dispersion curves and finally inverting these dispersion curves to achieve a one- or two dimensional shear wave velocity and depth profile as shown in Fig. (2.1).

When Stress, a force act on an area of body applied, the body will deform and this is the strain. A stress normal to the area is called a compressive stress and causes a shortening of the body, or a tensile stress which causes elongation, while a stress applied parallel to the area is called a shear

stress. For elastic behavior, the strain in a body is proportional to the applied stress. This linear relationship is called Hooke's law (Hasan, 2011).

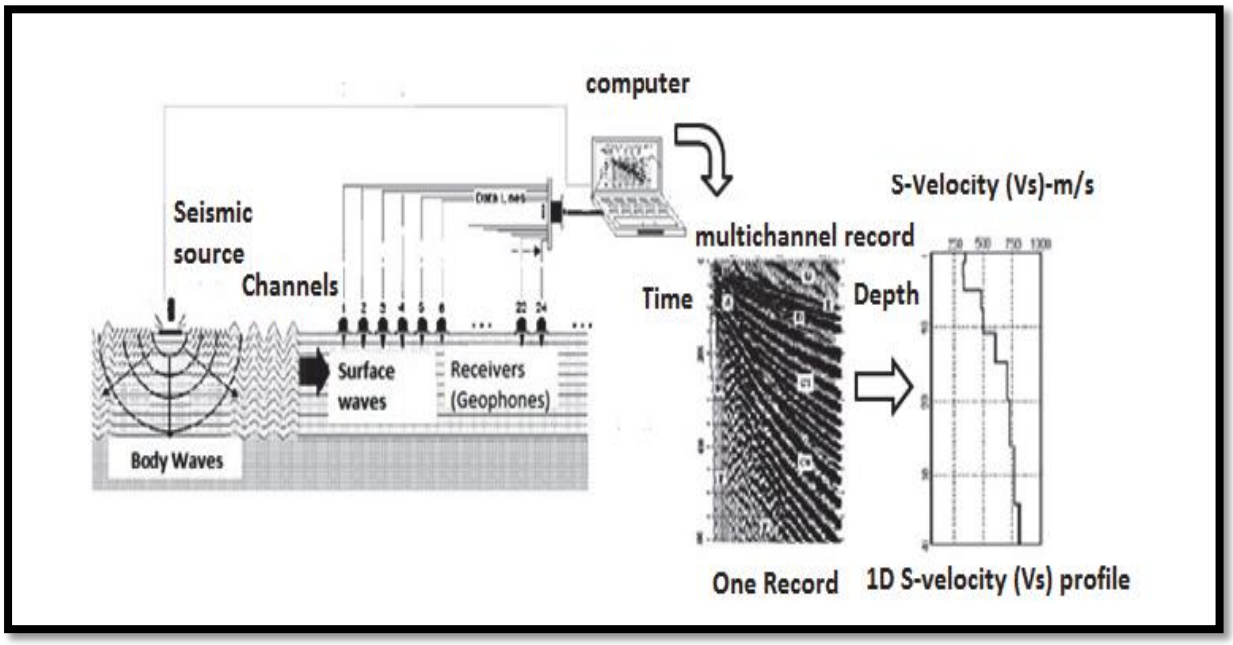

Fig.(2-1): Inverting the dispersion curves to obtain1D shear wave velocity depth profiles (after Park et al., 2007 & 1999).

(2-2) Elastic Parameters:

1- Young's modulus (E):

It is the relation between stress and longitudinal strain, Fig. (2-2).

$$E = \frac{\text{Longitudinal stress} \quad F/A}{\text{Longitudinal strain } \Delta L/L} \qquad \ldots\ldots\ldots\ldots (2\text{-}1)$$

Where F is the force, A is the area, L is length and ΔL is the change in the length.

2- Shear modulus (μ):

It is given by the ratio of shear stress (τ) divided by the shear strain (tanθ), (Barton, 2007) thus:

$$\mu = \tau / \tan \theta \quad \ldots\ldots\ldots\ldots (2\text{-}2)$$

Where θ is the shearing strain, Fig. (2-2).

3- Lame's constant (λ):

It is similar to the rigidity, (shear) modulus that is scale of hardness or force for homogeneous substance, so the elastic modulus is equal for all directions (Hasan, 2011).

$$\lambda = \mu \cdot E / (1+\mu)(1-2\mu) \quad \ldots\ldots\ldots\ldots (2\text{-}3)$$

4- Bulk modulus (K):

If a body of volume V is subjected to an uniform compressive stress in all direction, its volume will decrease by an amount of ΔV. The bulk modulus K, also called the incompressibility, is the ratio of (hydrostatic) pressure (p) to the corresponding proportional change in volume, (Gerkens, 1987). Fig. (2-2). K equation is:

$$K = \frac{P}{\Delta V/V} \quad \ldots\ldots\ldots\ldots (2\text{-}4)$$

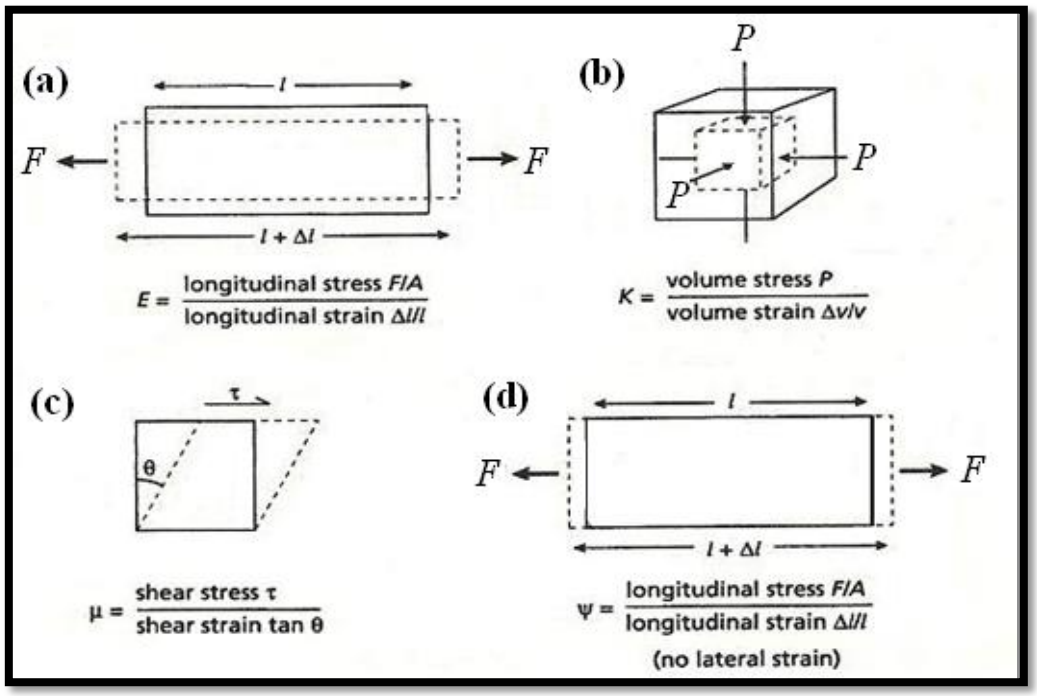

Fig. (2-2) The elastic module: (a)Young's modulus E. (b) Bulk modulus k. (c) Shear modulus μ. (d) axial modulus Ψ. After (kearey et al., 2002).

5- Poison's ratio (ν):

When a body is elongated by a tensile stress at the same time, it will be shortened in the direction perpendicular to that of the stress, vice versa. The ratio of the strain perpendicular to either type of deformation force to that in the direction of the force itself is called Poison's ratio and is designated as ν:

$$\nu = \frac{\Delta W / W \text{ Transverse strain}}{\Delta L / L \text{ Longitudinal strain}} \quad \ldots\ldots\ldots\ldots (2\text{-}5)$$

Where W is the width, ΔW is the change in the width, Fig. (2-2).

6- Axial modulus (Ψ):

It defines as the ratio of longitudinal stress to longitudinal strain in the case when there is no lateral strain; that is, when the material is constrained to deform uniaxially, (kearey, et al, 2002). Fig.(2-2).

$$\Psi = \frac{F/A}{\Delta L / L} \quad \ldots\ldots\ldots\ldots (2\text{-}6)$$

(2-3) The relationship between Bulk modulus (K) and Shear modulus (μ):

The relationship between (K) and (μ) is linear, where with increase (K), (μ) will increase, depending on the ratio between velocities of (P) wave to velocity of (S) wave (Hasan, 2011).

$$\frac{VP}{VS} = R \ldots\ldots\ldots\ldots (2\text{-}7)$$

Where R is the ratio between Vp to Vs.

$$V_p = R^* V_s \text{ ..... (2-8)}$$

$$\sqrt{\frac{K+4/3\mu}{\rho}} = R\sqrt{\frac{\mu}{\rho}} \text{ .....(2-9)}$$

$$\frac{K+4/3\mu}{\rho} = R^2 \frac{\mu}{\rho} \text{ ..... (2-10)}$$

$$K+\frac{4}{3}\mu = R^2 \mu \text{ ..... (2-11)}$$

$$K= (R^2 - \frac{4}{3}) \mu \text{ ..... (2-12)}$$

$$K= F \mu \text{ ..... (2-13)}$$

$$\text{Where F is } (R^2 - \frac{4}{3}) \text{ .....(2-14)}$$

Depending on this relationship between (K) and (μ), many curves can be drawn, from which the graph of relation is divided into zones can be drawn, each zone represents the degree of competence of soil and rock.

(2-4) The relationship between Lame's constant (λ) and Shear modulus (μ):

The relationship between (λ) and (μ) is linear, where with increase of (λ), (μ)will increase. Depending on the ratio between velocities of P wave to velocity of S wave (Hasan, 2011).

$$\frac{VP}{VS} = r \text{ ..... (2-15)}$$

Where r is the ratio between V_p to Vs.

$$V_p = r^* V_s \text{ .....(2-16)}$$

$$\sqrt{\frac{\lambda+2\mu}{\rho}} = r\sqrt{\frac{\mu}{\rho}} \text{.....(2-17)}$$

$$\frac{\lambda+2\mu}{\rho} = r^2 \frac{\mu}{\rho} \text{.....(2-18)}$$

$$\lambda+2\mu = r^2 \mu \text{ .....(2-19)}$$

$$\lambda = (r^2 - 2) \mu \text{ .....(2-20)}$$

$$\lambda = D \mu \text{ .....(2-21)}$$

$$\text{Where D is } (r^2 - 2) \text{ .....(2-22)}$$

(2-5) Seismic waves:

Following a seismic disturbance, several types of waves propagate within the earth and along its surface. The waves generated can be divided into two main categories: body waves and surface waves (Evrett, 2013).

(2-5-1) Body waves:

Body waves are transmitted through the interior of the earth, the medium of the wave, and consist of compressional waves (P-waves/ primary waves) and shear waves (S-waves/secondary waves).The particle motion associated with compressional waves is parallel to the motion of the wave itself causing stretching and compressing of elementary volume particles i.e. change in size (Evrett, 2013), as shown in Fig.(2-3).

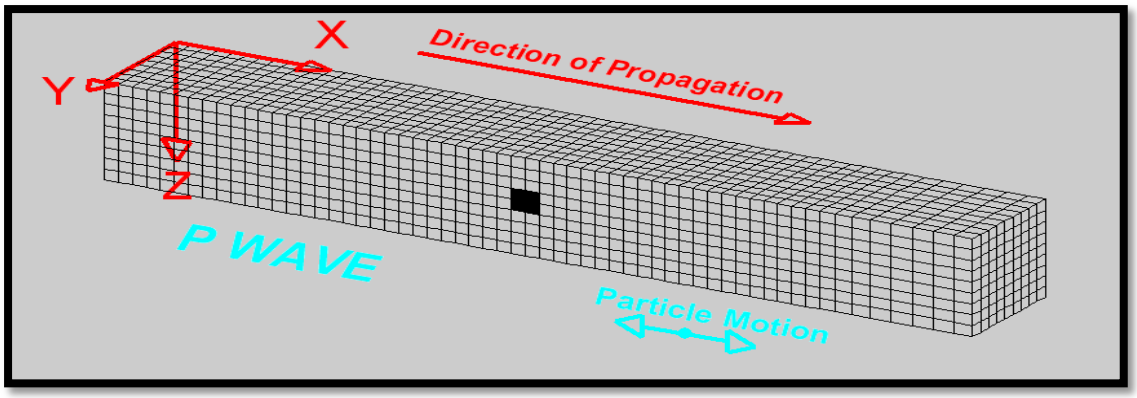

Fig. (2-3): Elastic deformation and ground particle motions associated with the passage of body waves. P-Wave. (www.geo.mtu.edu./UPSeis/waves.html)

The particle motion of shear waves is perpendicular to the direction of wave propagation and has therefore both a vertical and a horizontal component. The transverse particle motion causes shear deformation of volume elements within the medium, i.e. change in shape, (Aki & Richards, 2002; Evrett, 2013) as shown in Fig. (2-4).

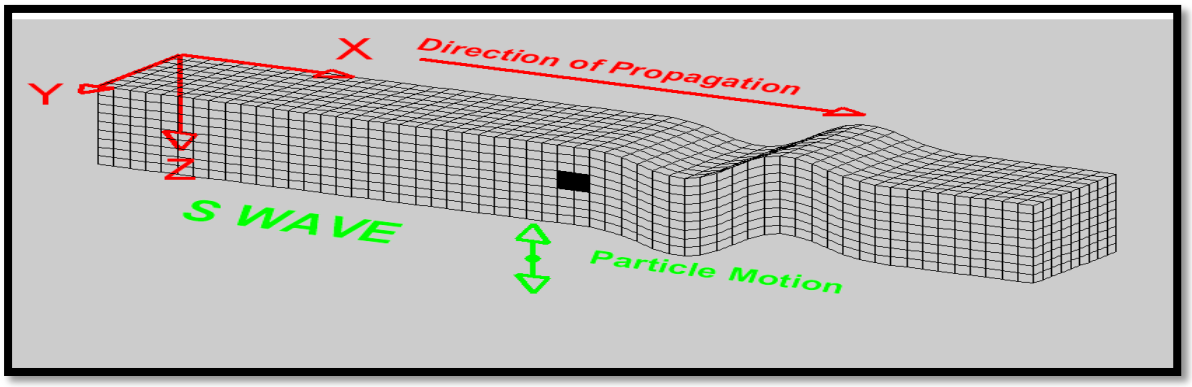

Fig. (2-4): Elastic deformation and ground particle motions associated with the passage of body waves. S-Wave. (www.geo.mtu.edu./UPSeis/waves.html)

The velocity of P and S waves related with the elastic constants and the density as follows:

$$V_P = \sqrt{\frac{\lambda+2\mu}{\rho}} = \sqrt{\frac{K+4/3\mu}{\rho}} \text{.....(2-23)}$$

$$V_S = \sqrt{\frac{\mu}{\rho}} \text{ .....(2-24)}$$

Where ρ is the density, μ is the Shear modulus, K is Bulk modulus and λ is Lame's constant. The velocities of compressional waves P in different materials illustrated in Table (2-1).

Table (2-1): Shows the velocities of compressional waves in different materials (Kearey et al,. 2002).

P wave Velocity (Km/s)	Material
0.2-1.0	Sand dry& Alluvium
0.25-1.0	Weathered layer
1.5-2.0	Sand (saturated)
1.0-2.5	Clay
1.5-2.5	Glacial till (water –saturated)
2.4-5.0	Slate & shale
2.0-6.0	Sandstone
2.0-2.5	Tertiary sandstone
2.0-6.0	Limestone
2.0-2.5	Cretaceous chalk
5.0-5.5	Carboniferous limestone
2.5-6.5	Dolomite
4.5-5.0	Salt
4.5-6.5	Anhydrite
2.0-3.5	Gypsum
1.4-1.5	Water

(2-5-2) Surface waves:

Surface waves travel along the interface between two different media, i.e. near the surface of the earth and are the results of interfering P-waves and /or S-waves (Xia et al., 2002). There are two main types of surface waves; Rayleigh waves and Love waves (Evrett, 2013). The particle motion of Rayleigh waves is in a vertical direction and reminds of rolling ocean waves (Evrett, 2013; Xia et al., 1999), as shown in Fig.(2-5).

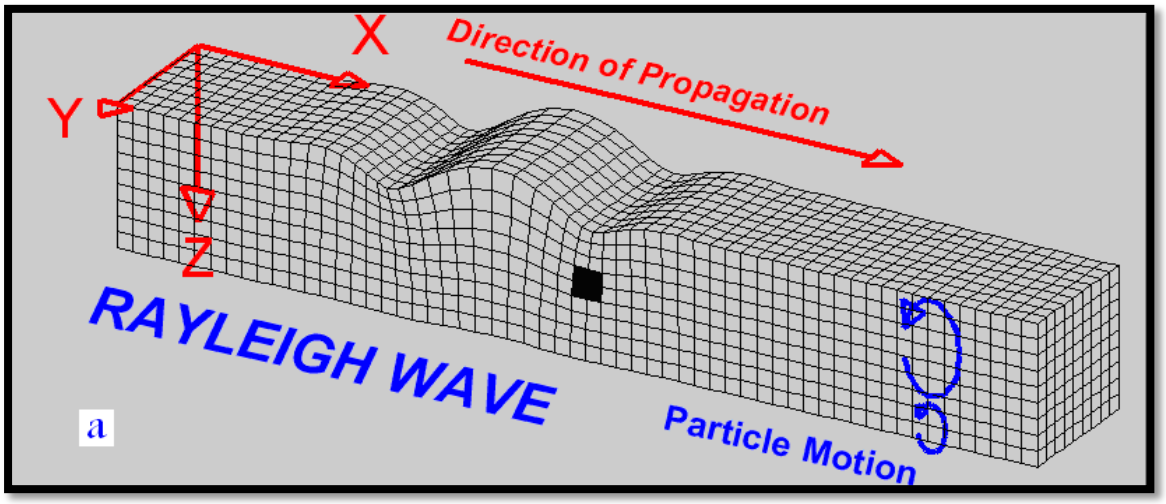

Fig. (2-5): Elastic deformations and ground particle motions associated with the passage of the surface wave. (Rayleigh wave). (www.geo.mtu.edu./UPSeis/waves.html)

The particle motion associated with Love waves is horizontal and transverse to the direction of wave propagation (Evrett, 2013), as shown in Fig. (2-6). Love waves are only generated where there is a soft (low velocity) layer overlying a stiffer layer whereas Rayleigh waves always exist in the presence of a free surface (Foti, 2000).

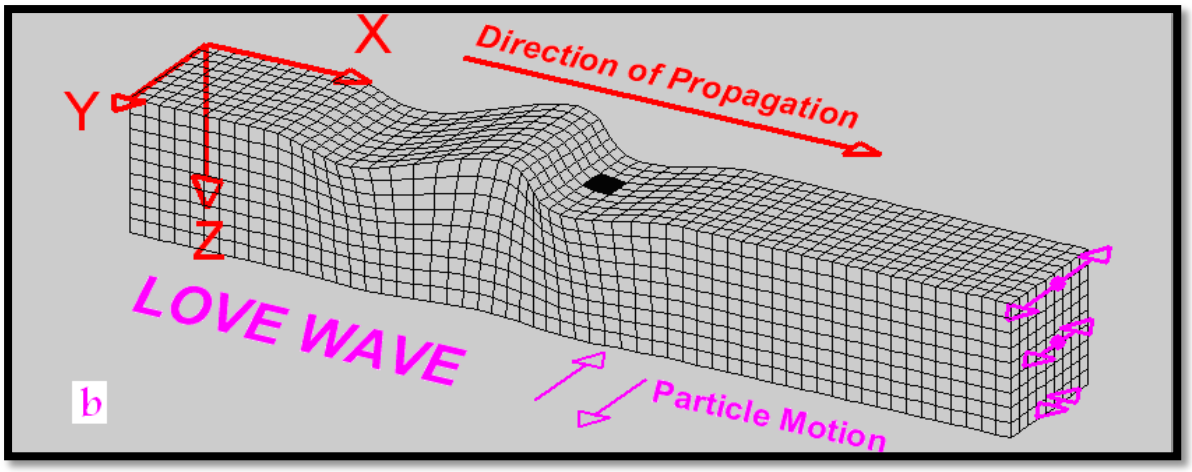

Fig. (2-6): Elastic deformations and ground particle motions associated with the passage of the surface wave. (Love wave). (www.geo.mtu.edu./UPSeis/waves.html)

(2-6) Rayleigh waves:

Rayleigh waves are the most fundamental of the surface waves (Aki & Richards, 2002) and are of great interest in near-surface geophysics as they can provide key information regarding the properties of the earth's sub-surface (Evrett, 2013; Park et al., 1997; 1999). Ground roll is a particular type of Rayleigh waves that is characterized by relatively high amplitude and low frequency and travels along or very close to the surface of the earth (Xia et al., 1999). Ground roll is the type of surface waves most effectively generated and recorded using vertical seismic sources and vertical receivers (Park et al., 1997).

A vertical seismic source, e.g. a sledgehammer impact or a vibrating plate, will radiate a combination of P-waves, S-waves and Rayleigh waves. Around two-thirds 67% of the seismic energy will typically be imparted into Rayleigh waves (principally ground roll) while 23% is imparted into S-waves and 7% into P-waves (Evrett, 2013). Resulting from their horizontal particle motion, Love waves are seldom recorded in

surveys in which only vertical sources and vertical receivers are used (Park et al., 1997).

Rayleigh waves cause surface particles of the medium to move along elliptical paths in the vertical plane consistent with the direction of wave propagation. The particle motion is retrograde elliptical near the surface, becoming prograde elliptical with increasing depth (Aki & Richards, 2002; Evrett, 2013), Fig. (2-7) (right).

The amplitude of Rayleigh waves decays exponentially with depth. At a penetration depth comparable to one wavelength, the displacement of the medium has become less than 30% of its surface value, Fig,. (2-7) (left). If it generated by a point source, the energy of the wave falls of as 1= r, where r is the distance to the seismic source (Evrett, 2013). Thus, the in-plane amplitude of a Rayleigh wave decays as $1/\sqrt{r}$ if a point source is assumed (Young & Freedman, 2008).

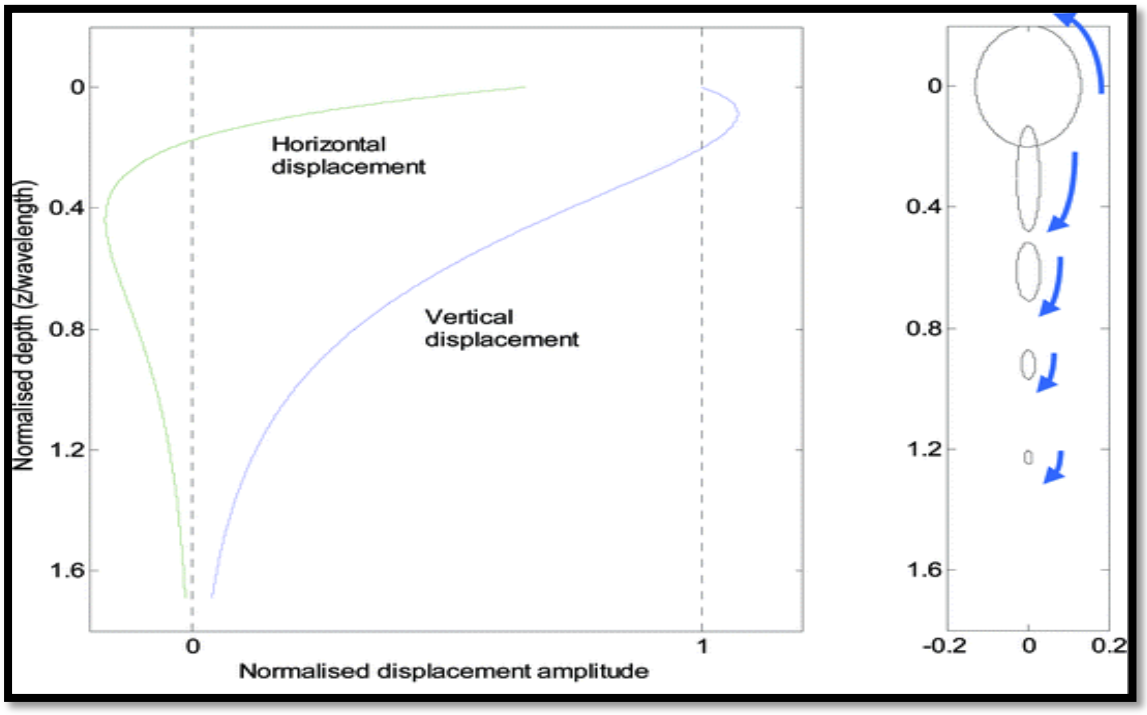

Fig.(2-7): Displacement amplitude (left) and vertical particle motion (right) of Rayleigh waves as a function of depth (Gedge & Hill, 2012).

In a homogeneous half-space, the Rayleigh wave velocity is independent of frequency, i.e. Rayleigh waves do not disperse in a homogeneous medium. However, Rayleigh waves are dispersive in a layered medium; wave components with different wavelength (and therefore different frequency) have different penetration depths and propagate at different velocities. The propagation velocity of individual frequency components is referred to as phase velocity (V_R) (Evrett, 2013; Park et al., 1997). The group velocity (V_g) of the wave is the velocity at which the wave-packet envelope propagates through the medium (Evrett, 2013). This is shown in Fig.(2-8). The blue dot moves with the phase velocity along the black path while the red wave-packet envelope propagates with the group velocity from left to right.

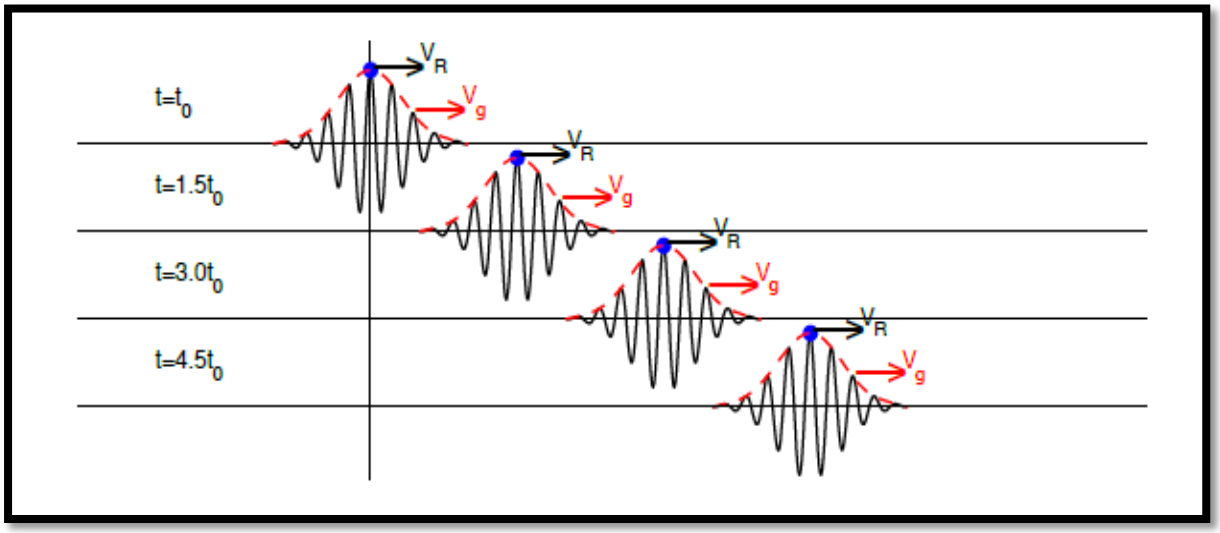

Fig. (2-8): Comparison of Rayleigh wave phase velocity (V_R) and group velocity (V_g), (Ólafsdóttir, 2014)

Dispersion of Rayleigh waves can be visualized by examining an idealized vibrating seismic source, vibrating at a single frequency f at the surface of a multilayered elastic medium. The wavelength λ of the resulting Rayleigh waves is constant and can be determined by measuring

the distance between successive peaks (or troughs) in the observed surface wave motion. A low frequency source generates long-wavelength Rayleigh waves that excite multiple layers of the medium Fig. (2-9a), while seismic sources of a higher frequency generate Rayleigh waves with shorter wavelength and shallower penetration depth (Fig.(2-9b) and (c)) (Evrett, 2013).

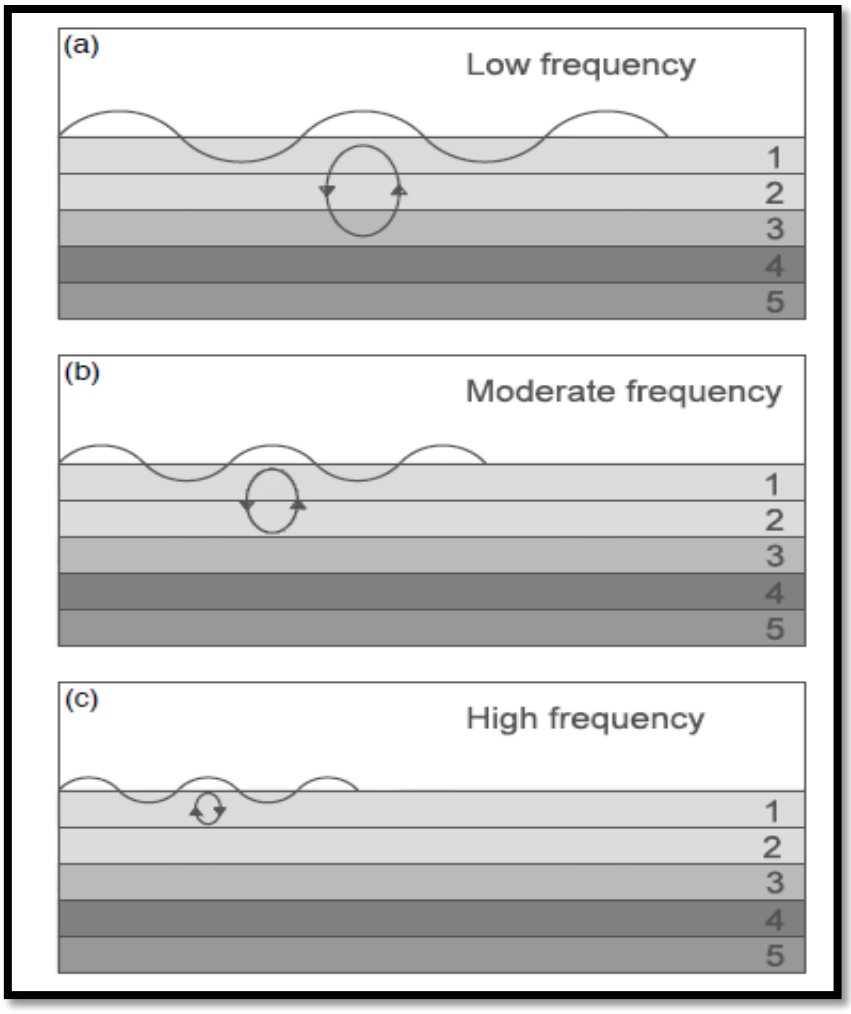

Fig.(2-9): The penetration depth of Rayleigh waves depends on their wavelength and frequency. (a) Low-frequency (long-wavelength) Rayleigh waves, penetrate deeper than Rayleigh waves of (b and c) higher frequencies (shorter wavelengths), (Ólafsdóttir, 2014).

The phase velocity of each wave component is primarily dependent on the elastic moduli of the layers that the wave component excites. Only the elastic moduli of the top-most layer have impact on the Rayleigh wave phase velocity, whereas the phase velocity of the waves depends also on the elastic properties of deeper layers Fig.(2-9 a, b and c). Each mode of a given surface wave will therefore exhibit an unique phase velocity at each frequency (Evrett, 2013; Xia et al., 2002).

Generally, seismic velocities are observed to increase with depth, i.e. waves with longer wavelengths (lower frequency) propagate faster than waves with shorter wavelengths as indicated by eq. (2-25) (Bessason & Erlingsson, 2011; Evrett 2013):

$$\lambda(f) = \frac{VR(f)}{f} \quad \ldots\ldots\ldots\ldots (2\text{-}25)$$

where f is frequency, VR (f) is the phase velocity of Rayleigh wave components of frequency f and λ (f) is the Rayleigh wave wavelength at frequency f.

A plot of frequency versus phase velocity, known as a dispersion curve, visualizes these relations Fig.(2-10 a). The shape of the dispersion curve is referred to as the dispersion characteristic of the Rayleigh wave (Evrett, 2013).

Typically multiple phase velocities exist for a given frequency, making the dispersion curve multi-modal. The mode with the lowest phase velocity (at each frequency) is termed the fundamental mode (M_0). It exists at all frequencies. Higher modes, called first mode (M_1), second mode (M_2) etc., have higher phase velocities and are only present above a cut-off frequency that depends on the mode (Evrett, 2013) Fig. (2-10 b).

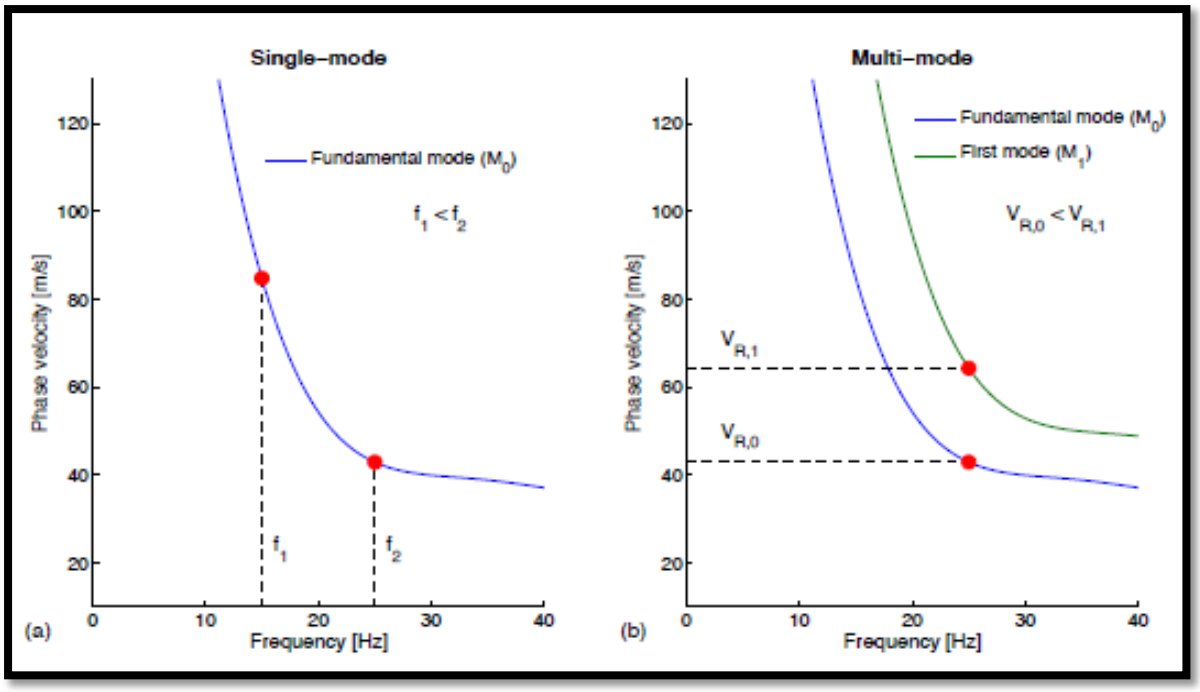

Fig. (2-10): (a) Fundamental mode dispersion curve. (b) Fundamental mode and first mode dispersion curves, (Ólafsdóttir, 2014).

(2-7) The most important physical properties of seismic waves:

1- Frequency (*f*):

It is the number of cycles (vibrations) per second and is measured in the unit Hertz, which is equal to (1/second) or 60 cycles per second, for example. Frequency is a function of the reflected or refracted medium of seismic waves (Kearey et al., 2002)

2- Wave Length (λ):

It is the distance between two adjacent peaks or troughs, it is measured in units of a meter or its parts as in Fig. (2-11).

3- Amplitude:

It is the maximum displacement a wave can reach from its line of propagation, it is measured in decibel (dB), as in Fig. (2-11),

(Kearey et al., 2002)

4- Wave Period (T):

It is the time required to complete one cycle, it is measured in units of time such as seconds or milliseconds as in Fig. (2-11). The wave period is related to the frequency through the following relationship, (Kearey et al., 2002):

$$T = \frac{1}{f} \quad \text{.....(2-26)}$$

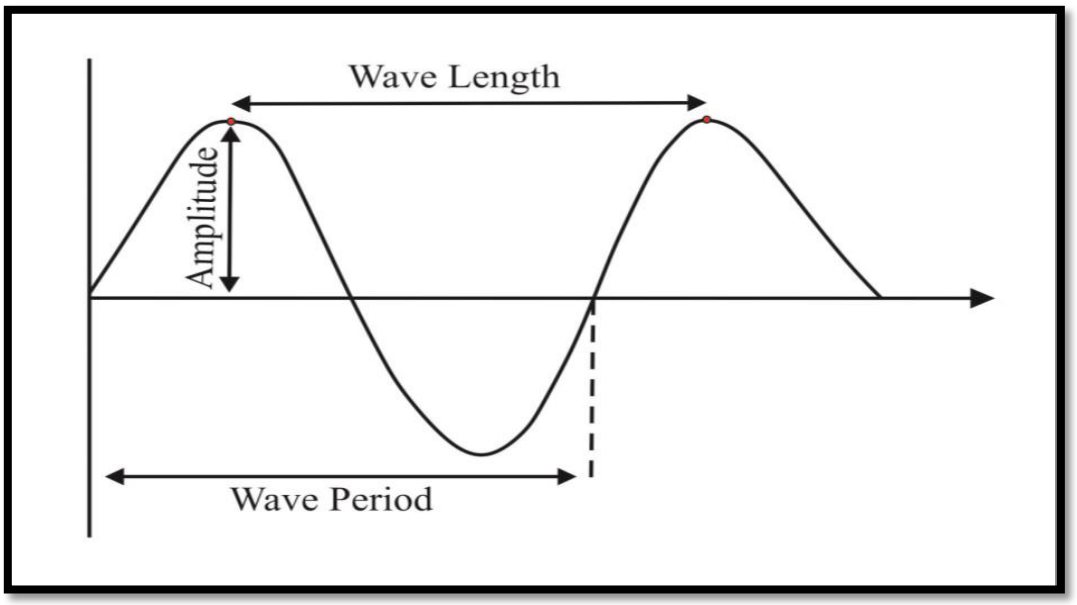

Fig.(2-11): Shows some physical properties of waves (Kearey et al., 2002).

5- Attenuation:

It is a term used to describe the phenomenon of decrease in the energy of seismic waves as they progress through the medium, as a result of the transformation of part of this energy into heat due to the inelasticity of the medium that these waves pass through, in addition, the waves suffer from a decrease in their energy as they move away from the source of their generation (Sharma, 1986).

High-frequency waves (of short wavelengths) are more weak than low-frequency waves (of long wavelengths), so they have

little ability to penetrate into great depths of the earth's crust, but what distinguishes these high-frequency waves is that they have a high resolution power, meaning It is more accurate in conveying the physical properties of the layers of rock that are reflected or refracted as well as being able to identify the thinner layers.

(2-8) Seismic Wave Velocity and Elastic Moduli:

The body wave velocities of geomaterials; shear wave velocity (V_s) and compressional wave velocity (V_P), can be directly related to the elastic moduli of the medium which the waves propagate through the relationships between the elastic moduli and the body wave velocities are widely utilized in geophysical surveys in order to gain information about the spatially distributed mechanical properties of subsoil sites (Evrett, 2013). The shear wave velocity (V_s) is especially a valuable indicator of the stress-strain behavior of soil due to its relations to the small-strain shear modulus (G_{max}) (Wair et al., 2012).

The shear modulus of soil (G) is highly dependent upon strain level as indicated by the stress-strain curve shown in Fig. (2-12), for small shear deformations the behaviour of soil is very close to being elastic, i.e. the shear modulus for small strains can be assumed to be constant at its maximum value, G_{max}. For increased deformation, the stiffness of soil diminishes as indicated by the decreasing slope of the stress-strain curve in Fig. (2-12) (Kaldal, 2007; Luna & Jadi, 2000).

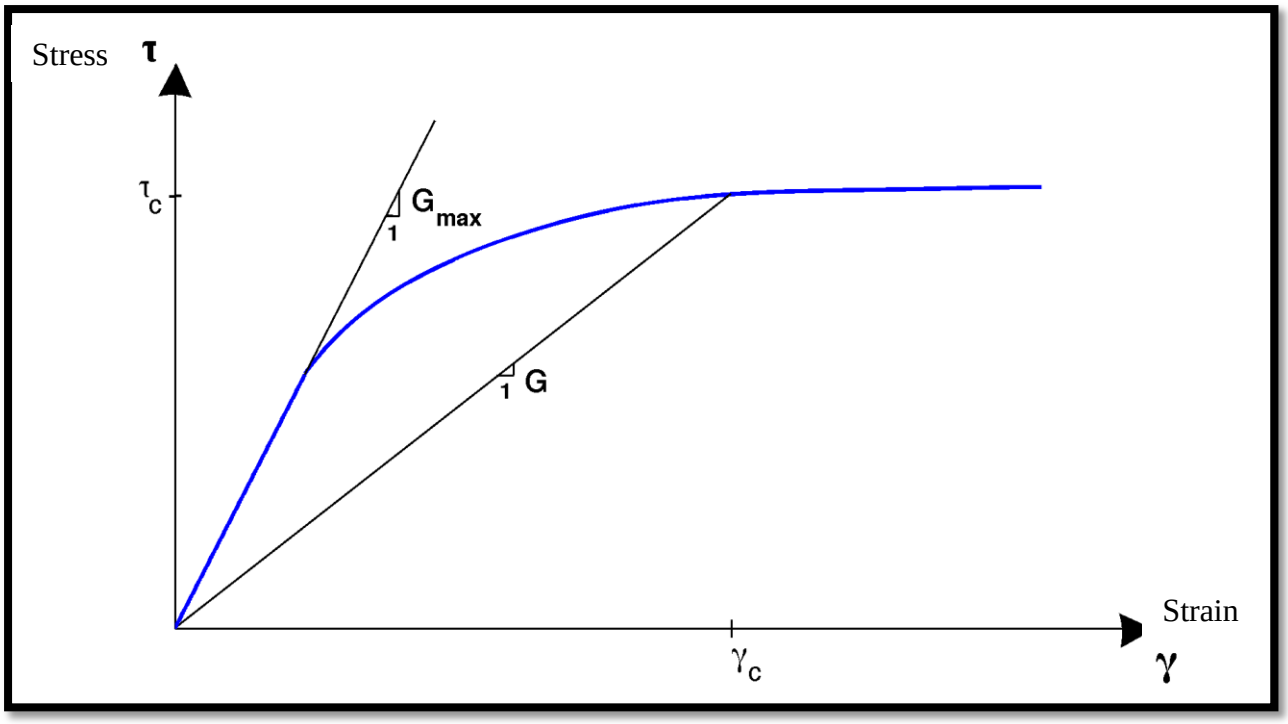

Fig. (2-12): Stress-strain curve with variation of shear modulus (G). For small shear deformations G_{max} is obtained (Ólafsdóttir, 2014).

The shear strains induced by most geophysical seismic method, such as MASW surveys, are small and well within the range where the behaviour of soil can be assumed elastic. The calculated shear wave velocity can therefore be used to infer the stiffness of the material through which the waves propagate, i.e.

$$G_{max} = \rho v_s^2 \quad \ldots\ldots\ldots\ldots (2\text{-}27)$$

where ρ is the mass density of the soil (Kaldal, 2007, Luna & Jadi, 2000). Based on the relations between the modulus of elasticity, (E) and the shear modulus (G) of homogeneous isotropic linearly elastic materials, the (small-strain) modulus of elasticity of the soil layers under study (E_{max}) can be estimated as (Evrett, 2013; Sigbjörnsson, 2007):

$$E_{max} = 2G_{max}(1+\nu) = 2\rho\, V_S^2(1+\nu) \quad \ldots\ldots\ldots\ldots (2\text{-}28)$$

where ν is Poisson's ratio. For sandy or gravelly sites, the value of the Poisson's ratio is typically in the range of ν ≈ 0.25 – 0.35 (Bessason & Erlingsson, 2011).

By solving Eq. (2-28) for V_S the following equation is obtained:

$$V_S = \sqrt{\frac{Gmax}{\rho}} = \sqrt{\frac{Emax}{2\rho(1+\nu}} \quad \text{.....(2-29)}$$

A similar expression exists for compressional wave velocity (V_P) (Evrett, 2013), i.e.

$$V_P = \sqrt{\frac{(1-\nu)Emax}{(1+\nu)(1-2\nu)\rho}} \quad \text{.....(2-30)}$$

By taking the ratio of Eqs. (2-29) and (2-30), the following relation between V_P and V_S is obtained (Evrett, 2013):

$$\frac{Vp}{Vs} = \sqrt{\frac{2(1-\nu)}{1-2\nu}} \quad \text{.....(2-31)}$$

Thus, with a known shear wave velocity and a known (or guessed) Poisson's ratio, the compressional wave velocity can estimated by Eq.(2-31).

(2-9) Seismic Waves Diffraction:

Seismic waves travel inside the earth and are subject to reflection and refraction when they hit the interface between the layers, in some cases, when there is a sharp change in the physical properties within one layer or a group of rock layers as a result of the presence of a fault or the edge of a buried river. The front of the falling wave on the sharp edge of this fault as in Fig. (2-13) will turn into a center to generate waves that spread

in all directions according to (Huygen's principle). The diffraction waves have been of great benefit in determining the subsurface faults in the seismic surveys conducted using seismic methods (Sharma, 1997).

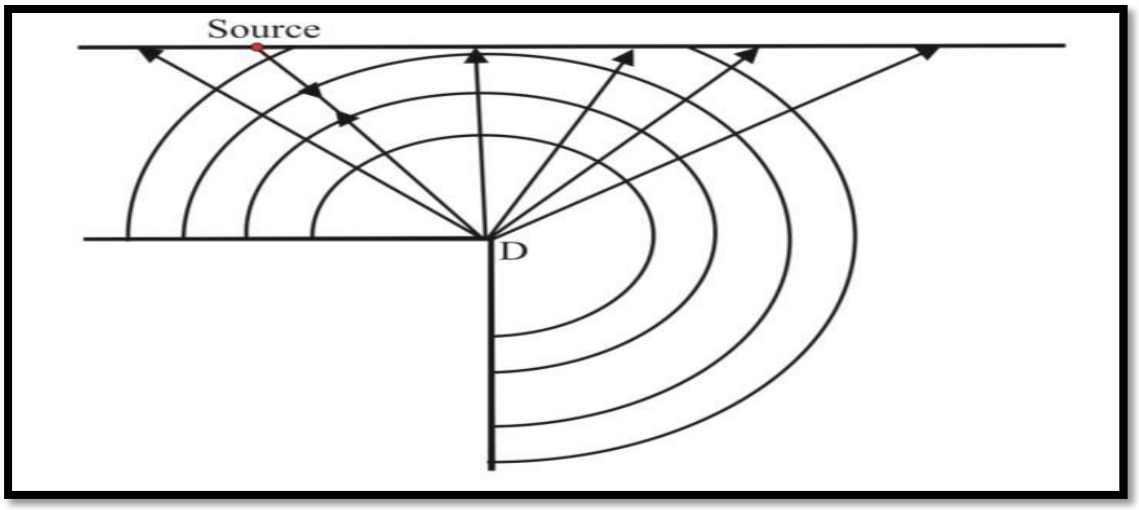

Fig.(2-13) : Shows seismic waves diffraction, developed by (Sharma,1997).

(2-10) Factors Affecting the Velocities of Seismic Waves:

1- Density:

Density is mathematically inversely proportional to velocity, but in practice is directly proportional as seismic velocities increase with increasing density the reason for this is that the coefficients of elasticity more influence on the velocity of seismic waves than the density. Through studies done by (Gardenar, et. al. 1974) and (Nafe and Drake, 1957). It was found that density (ρ) is related to velocity(V) by the following relationship:

$$\rho = 0.23\ V^{0.25} \qquad \ldots\ldots\ldots\ldots \text{(2-32)}$$

2-Porosity:

The elastic moduli are inversely proportional to porosity, where seismic velocity increase with decreasing porosity, and the porosity decrease with depth. Therefore density and velocity increase with depth, (Sharma, 1986).

3-Pores Shape

Pore shapes control the elasticity coefficients of the rock layers, and this leads to an effect on the velocity within these layers, It has been proven that the pores of oblate spheroid shapes have a greater effect on the modulus of elasticity and therefore on the velocity of the pores of spherical shapes in the case of the stability of other factors on the velocity as mentioned in (Al-Bahadily,1997).

4-Depth:

At large depths, compaction results in a reduction of porosity, increasing of seismic velocities. In addition, the elastic moduli tend to increase at higher pressures. Thus, seismic velocities in sedimentary rocks tend to be higher at greater depths.

5-Age:

Velocities tend to increase with age of sedimentary rocks, owing to cementation. As a rock becomes more cemented, its rigidity (strength) increases.

6-Fluid content:

The seismic velocity is affected by amount and type of fluid in rocks (Dobrin, 1976).

7-Lithology:

The seismic velocity in igneous and metamorphic rocks is more than sedimentary rocks . By virtue of their various compositions, texture (e.g.

grain shape and degree of sorting), and other properties, rocks differ in their elastic moduli and densities and, hence in their seismic velocities (kearey, et al., 2002).

8- Fracture and cracks effect:

Fractures and cracks lead to increasing ratio of secondary porosity in rocks, and lead to decreasing of seismic velocity in these rocks.

(2-11) Seismic Survey:

In the seismic survey an elastic pulse or a more extended elastic vibration is generated by source of energy, and the resulting motion of the ground is detected by geophone.

(2-11-1) Seismic Reflection Survey:

In this survey seismic energy pulses are reflected from subsurface and interface and recorded at near normal incidence at the surface (kearey et al., 2002).

(2-11-2) Seismic Refraction Survey:

The seismic refraction survey is considered one of the most effective methods for determining the depth of the bedrock and the ground water, the lithology type, the lateral and vertical changes in lithology, and investigating the structural features such as micro faults (Abd El-Aal and Mohamed, 2009). It has been most successful when applied to shallow depth (< 100m) problem (Green, 1974).

(2-12) Physical laws that apply to seismic refraction surveys:

(2-12-1) Huygen's Principle:

By using the concept of wave front, which is defined as the surface on which the wave motion is in the same phase, this concept is used to describe the huygen's principle, which states that "Every point on an

advancing wave front is a new source of spherical waves". The position of the wave front at a later instant can be found by constructing a surface tangent to all secondary wavelets (Gadallah and Fisher, 2009). Huygen's Principle provides a mechanism by which a propagating seismic pulse loses energy with depth.

(2-12-2) Fermat's Principle:

Fermat's principle governs the geometry of raypaths. This usually means that the ray will follow a minimum 'time path, which is the path that will allow the wavefront to move from point A to point B in the shortest amount of time. (Lay and Wallace, 1995).

(2-12-3) Snell's Law:

Snell's law for a refracted wave is the ratio of the sine of the angle of incidence and the angle of refraction is equal to the ratio of the velocities of the two media (Sjögern, 1984), Fig.(2-14).

$$\text{Sin } i / \text{Sin } r = V_1 / V_2 \quad \ldots\ldots\ldots\ldots \quad (2\text{-}33)$$

The angle r is called the angle of refraction and *i* the angle of incidence. When *i* increase there is a unique case where the angle of refraction r is 90^o and sin r = 1, where:

$$\text{Sin } i = V_1 / V_2 \ldots\ldots\ldots\ldots \quad (2\text{-}34)$$

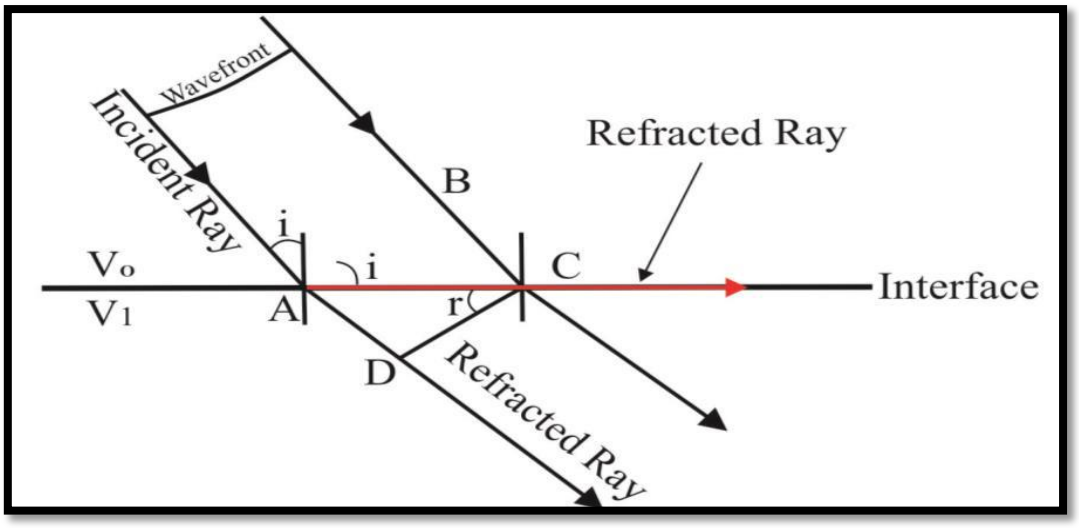

Fig. (2-14): Shows the refraction of waves according to Snell's law.

(2-13) Types of Seismic Refraction Survey Arrangements:

Depending on the position shot wave point relative to the location of the geophones, refractive seismic surveys can be carried out in five arrangements called diffusion geometry, which are as follows:

1- **Center Shooting Arrangement:**

In this type of arrangement the position shot wave generation point is at the center of the survey line, the geophones are published on both sides of it with the same number and distances and in a straight line Fig. (2-15a). This arrangement is very useful in determining the depth, true thickness and for rock layers and their position, because the arrival times of the refracted waves must be equal when they reach the geophones on either side of the generation shot point location. If it differs, then this is an indication that the rock layer is horizontal, or that it is increase thicker in one direction, or that it contains a lithological change that contributed to the delay in the arrival of the refract waves. (Kearey et al., 2002).

2- **Forward Arrangement:**

In this type of arrangement, the location of the wave generation point is at the beginning of the survey line, as in Fig. (2-15b), which is why it is called in some references the normal and is used when the survey area is small and the available geological information confirms that the layers are horizontal.

3- **Reverse Arrangement:**

It is the least used arrangement alone in refractive seismic surveys because the wave generation point is located at the end of the survey line and as in Fig. (2-15c), and for this it is called in some references the terminal or the end shot (Kearey et al., 2002).

4- **Forward- Reverse Arrangement:**

It is the most widely used arrangement in collecting data, seismic refraction surveys, and it is carried out by two shot points of wave generation, the first is at the beginning of the survey line and the second is at its end, as shown in Fig. (2-15d). This type is used for the purpose of determining the thickness and true depth of the rock layers, as well as to know its status, inclined or horizontal (Kearey et al., 2002).

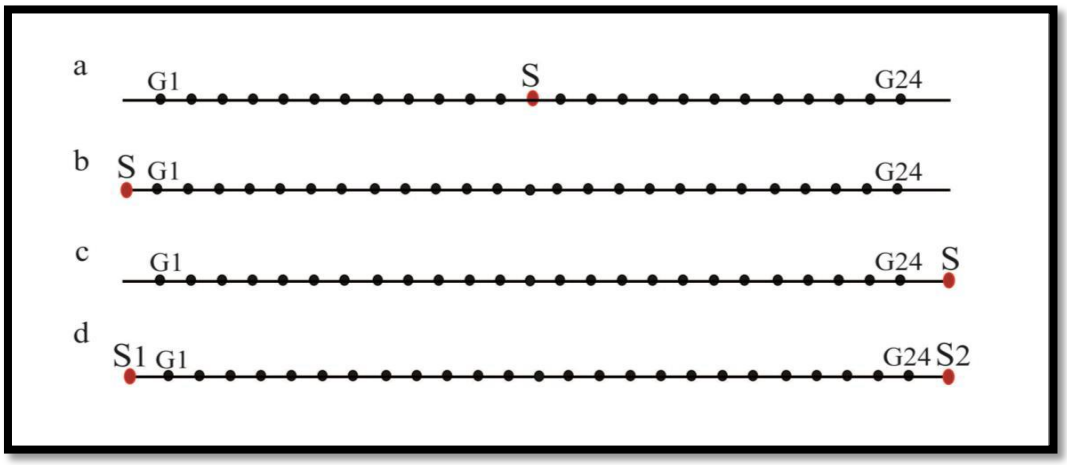

Fig (2-15): Describe the types of arrangements used in seismic refraction:(a)central,(b)Forward,(c)Reverse, (d) Forward- Reverse.

5-**Fan Arrangement:**

It is one of the most important data collection arrangements in seismic refraction surveys that is carried out in order to investigate salt domes for the exploration of hydrocarbons (oil). In this type of arrangement, the geophones are publishing in straight lines like a fan Fig. (2-16). This type is used at the beginning of the spread of the seismic refraction method in the 1930s (Sharma, 1986).

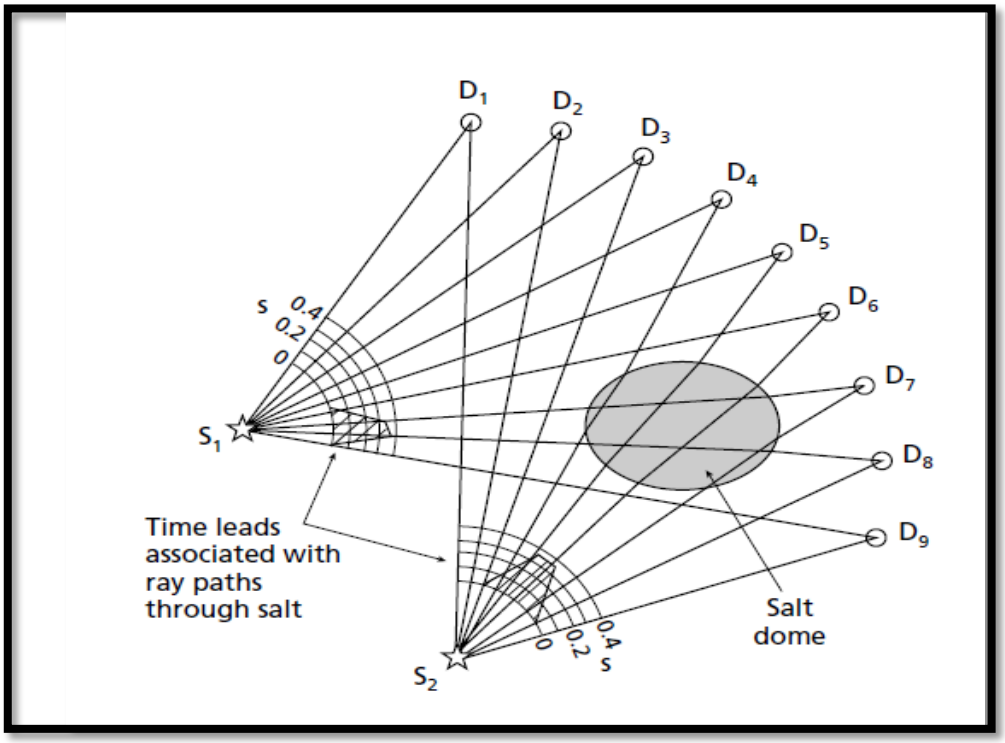

Fig.(2-16): Shows the fan arrangement used to collect field data in refractive surveys (Kearey, et. al.,2002).

(2-14) Energy Sources Used to Collect Data for a Seismic Refraction Survey:

Seismic waves are generated for refractive surveys by an energy source like: the hammer (weight 10 kg) it is used by knocking on flat plate.

The dynamite are usually used when it is intended to get rid of the weathered soil layer with low seismic velocity because it absorbs the

energy of high-frequency waves. The drop weight this type of sources is used in large surveys it is implemented by dropping an object with a large weight of hundreds of kilograms on the ground from a height of three meters or more to generate large seismic energy.

The vibrators it is one of the energy sources used in populated areas because it does not make much noise while working, lateral vibrators generate s-waves, as for vibrators with vertical vibration they generate a p- waves, and the other source is the air gun it is one of the energy sources used in marine surveys , where it works to empty the compressed air into the water generating great sound energy in marine surveys, refracted waves on the surface of the water are received through hydrophones (kearey et al., 2002).

(2-15) Calculation of the Thickness and Velocity of the Subsurface Layers:

Several methods are used to interpret time–distance curves for field refractive seismic recordings, these methods differ from each other in the geological assumption and the computational method for the velocities and depths of the layers (Kilty,et al., 1986).

The first arrival time is used to calculate the thickness and velocity of the subsurface layers, If there are two horizontal layers calculates the depths and velocities of the layers for different cases based on two methods:

a- Intercept Time(t_i): The intercept time is defined as the time obtained from extrapolating the length of the line for the time of arrival of the refracted wave on the time-distance curve at distance zero (X=0).

b- Cross-over Distance (X_{co}): It is the distance at which the direct and refracted waves have the same time of arrival, and this distance It is the point that indicates that the wave has refracted and arrived

before the direct wave Fig. (2-17), it depends on the depth of the refract and on the velocity of the first and second layers. The value of (X_{co}) is usually greater than twice the depth of the refract (Allaby, A.and Allaby M., 1999).

1- Depth (h) calculation by Intercept Time (t_i) method:

$$t_i = \frac{2h\cos\Theta}{V1} \quad \text{.....(2-35)}$$

$$t_i = \frac{2h\sqrt{(V2)^2 - (V1)^2}}{V2 * V1} \quad \text{.....(2-36)}$$

$$h = t_i\, V_2\, V_1 / 2\sqrt{(V2)^2 - (V1)^2} \quad \text{.....(2-37)}$$

2- Calculation of depth (h) by crossover distance (X_{co}) method:

$$X_{co} = 2h\sqrt{\frac{V2+V1}{V2-V1}} \quad \text{.....(2-38)}$$

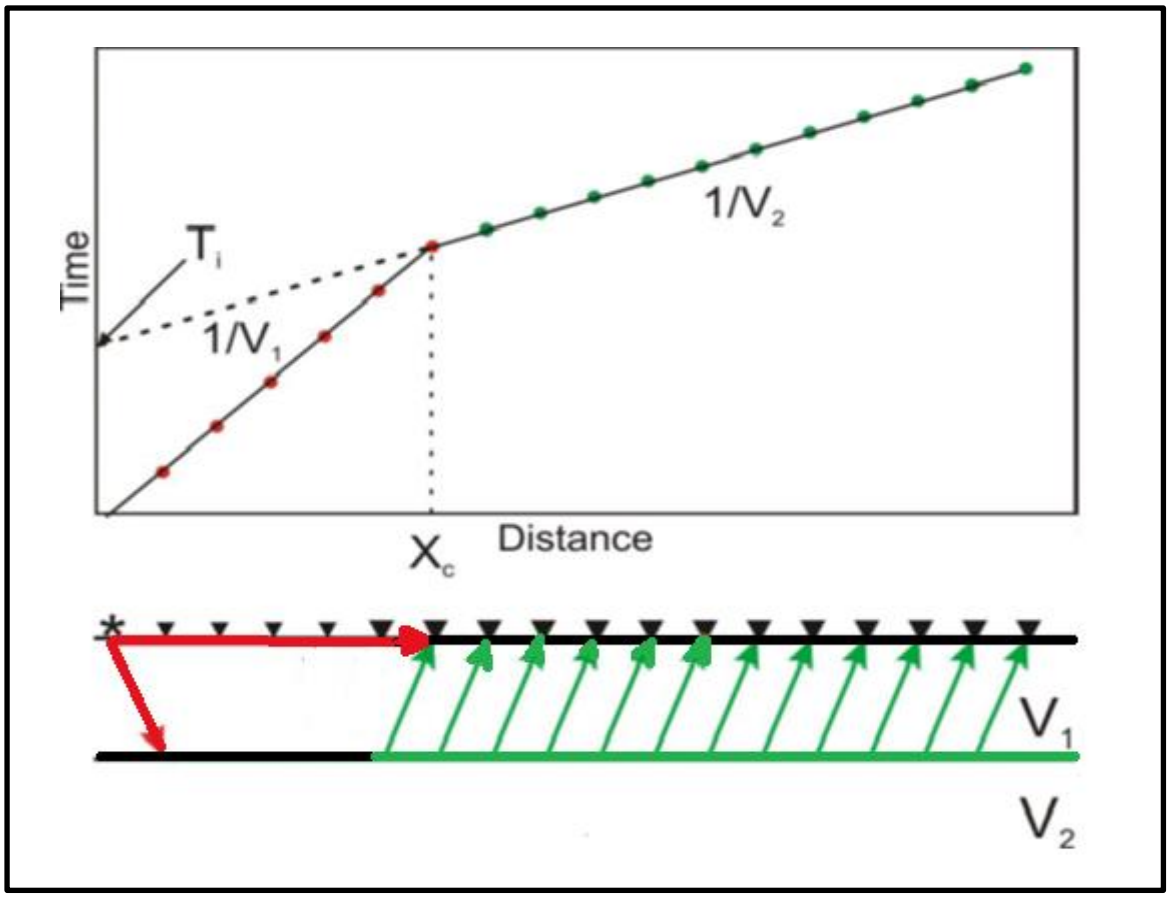

Fig.(2-17): Show Time-distance curve for direct and refracted waves of two horizontal layers (after AL-Heety, 2014; Resaercher,2023).

(2-16) Multi-channel Analysis of Surface Waves (MASW):

The Multi-channel analysis of surface waves (MASW) method is introduced by Park et al. (1999). In general, MASW surveys can be divided into active and passive surveys based on how the surface waves required for analysis are acquired. In the active MASW method, surface waves are generated actively by impulsive or vibrating seismic sources whereas the passive MASW method utilizes surface waves generated by natural sources or cultural activities, e.g. traffic (Park et al., 2007). The principal reported advantages of the MASW method are the following:

1- Data acquisition in the field using MASW method takes much less time compared to other methods. The MASW method requires only a single shot gather for one source receiver configuration, (Park et al., 1999; Xia et al., 2002).
2- The dispersion analysis involved in MASW is faster and easier to automate. Data from all receivers is processed at once (Xia et al., 2002).
3- Noise sources can be more easily identified and noise eliminated (Park et al., 1999; Xia et al., 2002). Reduction of noise leads to increased accuracy in the dispersion analysis and ultimately more precise shear wave velocity profile.
4- The maximum depth of investigation that can be achieved by using the (active) MASW method is generally around 30 m, assuming that surface waves are generated by a reasonably heavy seismic source, e.g. a sledgehammer (Park et al., 2007).
5- The MASW method makes it possible to observe multi-modal dispersion characteristics from recorded surface wave data (Park et al., 1998; Xia et al., 2003).

6- The MASW method makes it cost- and time-effective to evaluate shear wave velocity in two and/or three dimensions (Park et al., 2007; Xia et al., 2000).

(2-17) General Procedure For MASW Method:

MASW surveys can be broken down into three steps; field measurements, data processing and inversion analysis (Park et al., 1999).

1-Field measurements

Geophones are lined up in a straight, equally spaced line on the surface of the test site. A wave is generated with an impact load at one end of the lineup and the geophones record the resulting wave motion as a function of time. A single shot gather is sufficient (Park et al., 1999), Fig. (2-18a).

2-Data processing

A dispersion curve is extracted from the measured surface wave data (Park et al., 1999), Fig. (2-18b,c).

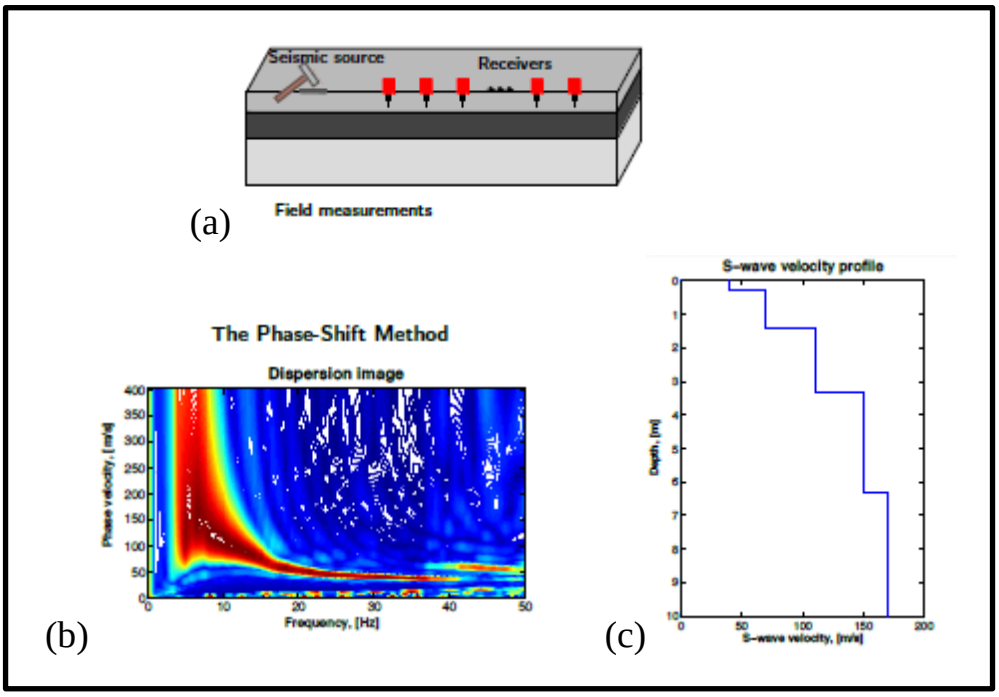

Figure (2-18): Shows (a) Field measurements by MASW method. (b,c) Data processing (Ólafsdóttir, 2014).

3-Inversion analysis

A theoretical dispersion curve for the test site is obtained, with iteration, based on an assumed number and thickness of soil layers and assumed material properties, such as shear wave velocity, for each layer (Park et al., 1999).

(2-18) Active MASW Method:

The most common acquisition data is composed of evenly-spaced vertical receivers aligned with the seismic source. This layout is often referred to as the MASW (Multichannel Analysis of Surface Waves) method.

The active MASW adopts the conventional seismic refraction mode of survey using an active seismic source such as hammers, weight drops, electromechanical shakers, and bulldozers. The maximum depth of investigation is 20-30m. This can vary with site and active source used. Waves can be best generated in the flat ground and if the vertical rise of the surface is greater than 10% of the receiver propagation length, it causes a hindrance to the wave generation. The maximum depth of penetration is determined by the longest wavelength of the surface waves. The longest wavelengths generated depend on the impact power of the source. Greater

is the impact power, longer will be the wavelength and greater will be the depth of penetration. Although the impact source such as a heavy weight drop can generate a longer wavelength of surface waves, these are very costly and not convenient for field operation. Therefore a controlled type seismic source such as a sledge hammer is used in an active survey. Metallic plates are conventionally used for impacts. However, recent studies revealed that the non-metallic plates such as a firm rubber plate

can generate stronger energy at the lower frequency part of the plates [http://www.masw.com/index.html].

The vertical, low frequency geophones <4.5 Hz are always recommended. Land streamer geophone proved to be efficient and convenient in field operation and can speed up the data acquisition in field. Length of the receiver propagation is directly related to longest wavelength which in turn determines the maximum depth of investigation. Receiver spacing is related to the shortest wavelength generated. In field, the receiver spread is limited up to 50-100m. If it is too long, the surface waves attenuate. The source and receiver spread distance (Park et. al., 2001) is one of the variables that affect the horizontal resolution of the dispersion curve. Long recording time is discouraged in the active survey because it can increase the chance of recording ambient noise. When more channels are available, the receiver spacing can be shortened which will help in obtaining a high signal to noise ratio (A high signal-to-noise ratio indicates the elimination of the influence of the signals apart from that generated by the active source), which, in turn, helps in obtaining a high resolution. Twenty four, or more, geophones are laid out in a linear array and connected to a multi-channel seismograph, collecting data simultaneously in all geophones. Active MASW utilizes surface waves mainly Rayleigh waves which are characterized by elliptical retrograde particle motion. Different types of waves are recorded through multichannel array. Dispersion nature of different types of waves is imaged through wave-field transformation of seismic record by frequency wavenumber (f-k). Certain noise wave fields such as back and side- dispersion surface waves and several types of body waves are automatically filtered out during transformation. From the dispersion image, a dispersion curve of the fundamental mode of Rayleigh waves is selected, which is then inverted for a 1D V_s profile.

Chapter Three

Instrumentation and Field Work

CHAPTER THREE

INSTRUMENTATION AND FIELD WORK

(3-1) Preface:

The applied seismic method depends on the generation of oscillating seismic waves in a specific area on the earth's surface, then receiving the refracted waves returning to the surface by the earth's receivers and calculating the first arrival time of these waves and determining their velocity. This method has become an effective method in seismology (Sharma, 1986). To explore the earth's interior, this method has shown its superior ability to determine the depths and types of rocks below the earth's surface.

(3-2) Used Instrumentation and its Accessories:

The digital seismograph *(Terraloc Mark 6)* is used in this study, and this equipment is from a Swedish company (ABEM Instrument) (AB), plate (3-1). It is multi-channel (12) channels. It is a device with high accuracy in seismic recordings of shallow depths. The seismograph consists of a case made of a durable aluminum alloy and contains two control panels of 28 keys, a screen of 8.4 inches, a processor AMD GX1- 12, a random access memory (RAM) of 256 MB, and a hard disk of at least 10 gigabyte used to record data. The weight of the seismograph is about 16 kg. Geophones are used. Results can be shown survey directly in the field through the seismograph screen after the measurement process is completed and the data can be transferred from a seismograph to a personal computer PC through the serial port. The seismograph has two systems, the first system is DOS, and the second is Windows XP (ABEM Instruction Manual, 2009).

Plate (3-1): Shows Terraloc Mark 6(ABEM Instruction) device.

The accessories of Seismograph (Terraloc MK 6) are source 10kg hammer weight, geophones one of them can be used as a trigger, it is planted near the power source, cable to connect the geophones, rubber plastic, measurement tape, car battery and shovel, plate (3-2).

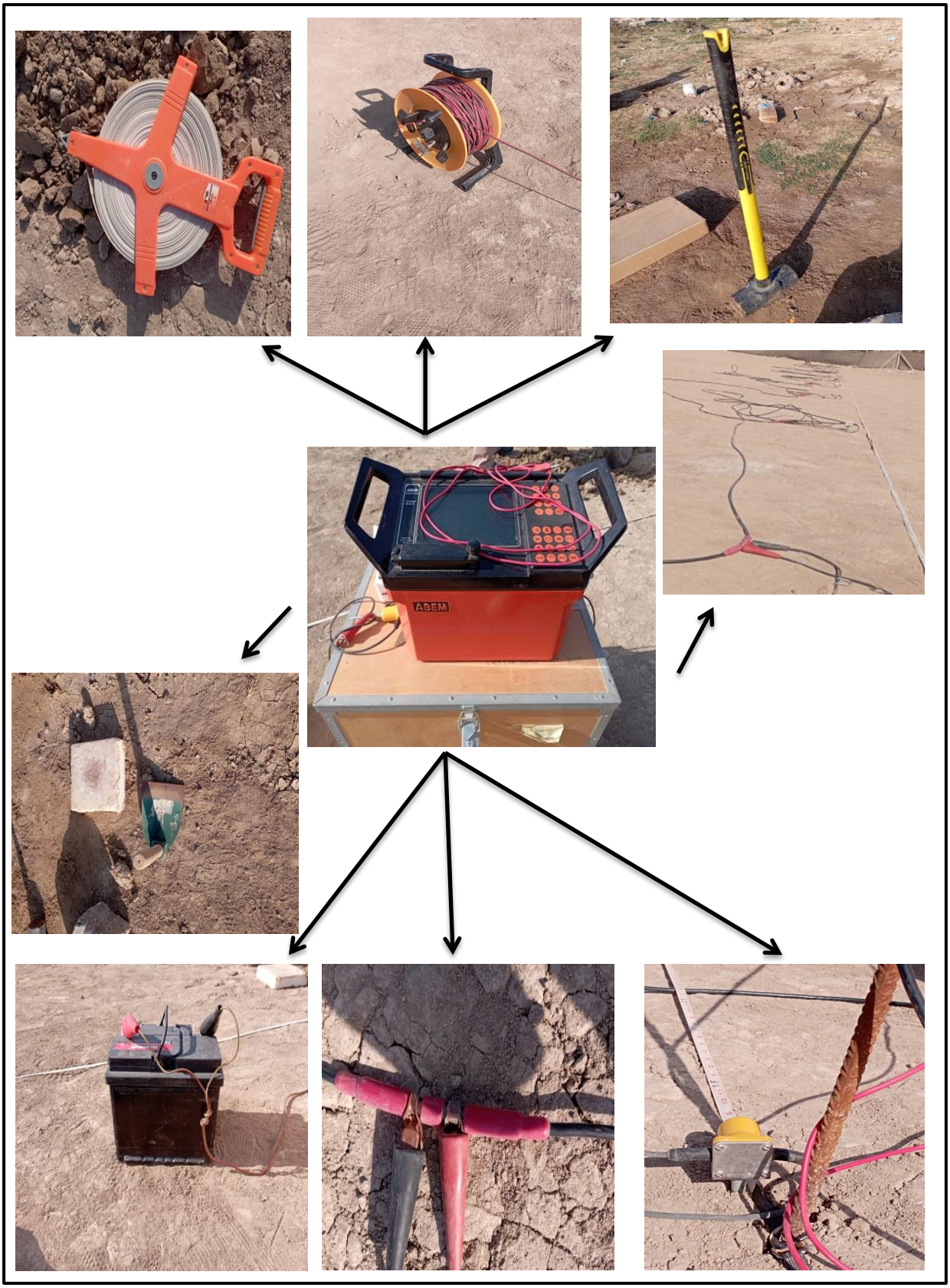

Plate (3-2): Shows the device used in this study and its accessories.

(3-3) Geophones:

For field recording, natural frequency geophones were used. These geophones convert the mechanical signal into an electrical signal, the connecting wires transmitted the signal to the seismograph and recorded.

The geophone is the unit connected directly with the ground, It consists of a coil and magnet placed inside a tapered plastic or metal box spike at one end is the coil or magnet fixed rigidly to the box, and the other has an inertia. . Instilled the well-pointed part is in the ground, and when vibrations are transmitted inside the ground, the geophone responds for seismic disturbances, it vibrates accordingly, and the inertial part remains constant, so a displacement is produced relative between them, which results in an electromotive force, which generates simple electrical signals, and then is transmitted by wires to the capture devices and is amplified by the amplifier and then it is recorded (AL-Heety,2014). There are two types of ground geophones for longitudinal and shear waves (P,S) recording has been used for seismic refraction, and one type of geophone for shear wave (S) recording has been used for MASW method, plates (3-3a),(3-3b) and Fig. (3-1).

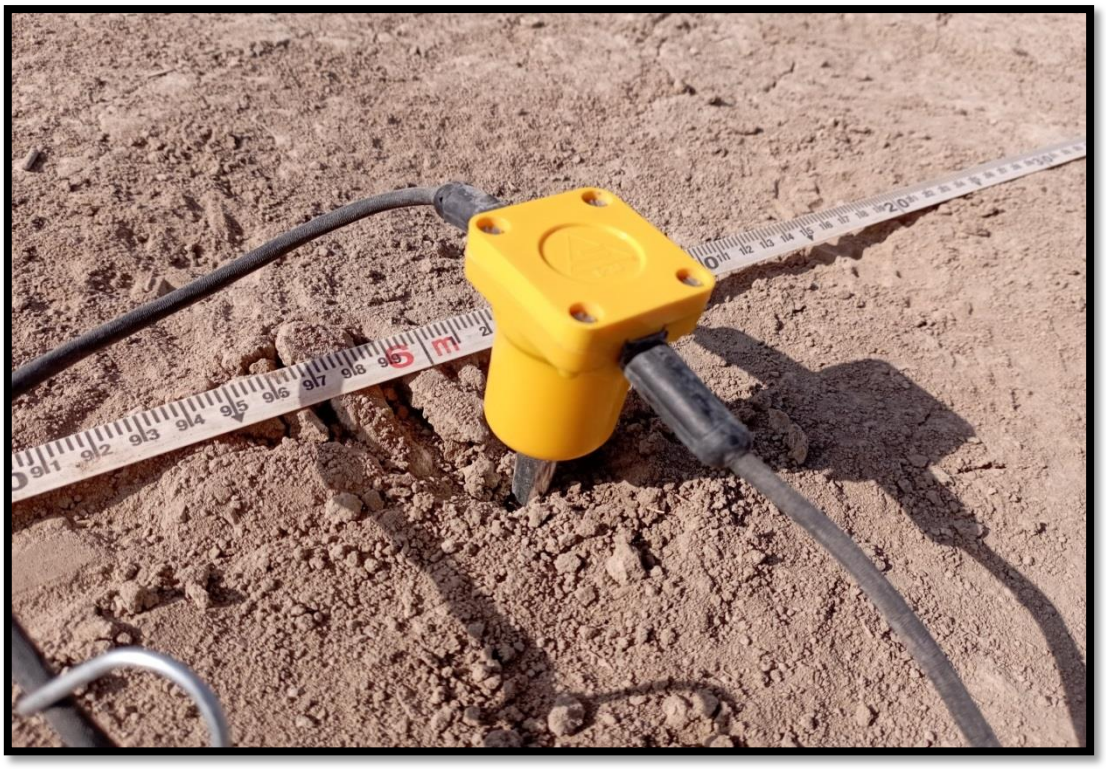

Plate (3-3a): Shows geophone P to measure P wave in seismic refraction.

Plate (3-3b): Shows geophone S to measure S wave in seismic refraction and MASW method.

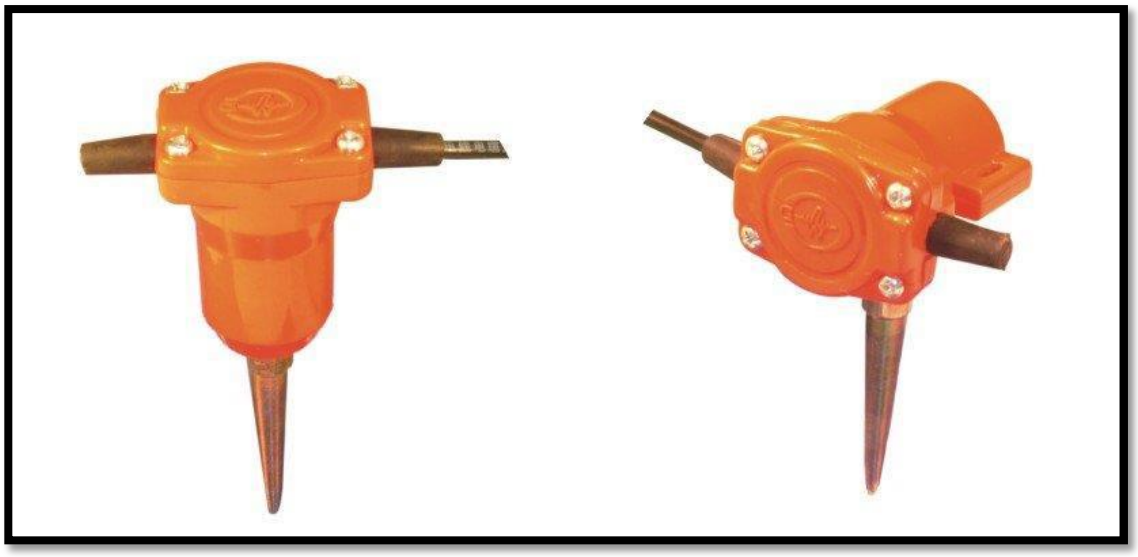

Fig. (3-1): Shows geophone (P) at the left and geophone (S) at the right, (http://www.hinageo.en.alibaba.com).

(3-4) Survey Technology and Field Work:

Field work started on 30/11/2021. Where the coordinates of the area are taken, a satellite visual image of the study area is obtained through a program (Google Earth) in order to determine the tracks on it.

The necessary equipment is provided to carry out the survey process, including the hammer with a weight of 10 kg, as well as the stone plate, the measuring tape, the seismograph and its battery, and the geophones (P,S).

Then the field work began by installing the seismograph, fixing the location of the geophones, and taking a distance of 72 m, which represents the length of the profile two profiles for the refractive survey. The wave was generated in three locations front, reverse and center in order to place the geophones, with the length of one profile being 72 m, and one profile for MASW method, Fig.(3-2).

Fig. (3-2): Shows a satellite image showing the profiles (Seismic Refraction and MASW profile) and locations of the boreholes in the study area.

After the geophones (geophones P) were installed, in which there were 24 geophones12 geophones for each half profile in their designated location, these geophones are connected with a cable, plate (3-4) in order to transfer mechanical energy and convert it into an electrical signal, this signal is transmitted to the seismograph and recorded, where this happens after the process of hammering by10 kg hammer on the rubber plastic (three times)

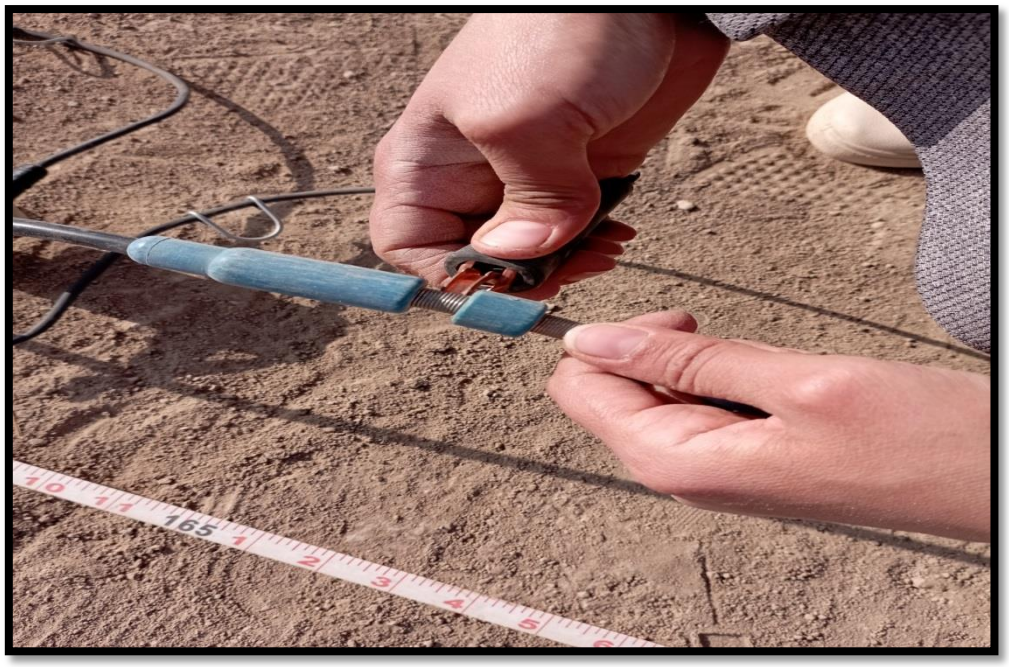

Plate (3-4): Shows the process of connecting the geophone (P,S) to the cable to convert the signal into a seismograph.

The length of the profiles are 72 m. Where the distance between the geophone and the hammer represented by X is 3 m, as for the distance between geophone and another geophone it is also 3 m represented by dx. Where the survey began in the front direction, then the middle, and then the reverse.

The hammering process on the rubber plastic is in the vertical direction in the case of generating p waves plate (3-5) in seismic refraction. The wave was generated in three locations front, reverse and center.

Plate (3-5): Shows spreading geophones P and the direction of hammering in Seismic Refraction.

Two holes are drilled in each half of the profile and one in the middle (for reading on this site) to place the rubber plastic and change the location of this rubber inside the hole, thus changing the direction of the hammer blow in relation to the location of the rubber plastic ,this is for generated S waves.

The hammering process on the rubber plastic is in the lateral and oblique direction in the case of generating S waves plate (3-5) in seismic refraction. The wave was generated in three locations front, reverse and center.

Then the office work is done for the seismic refraction survey.

Plate (3-6): Shows spreading geophones (S), the direction of the rubber plastic and the direction of hammering in Seismic Refraction.

The diffusion geometry for recording longitudinal (P) and shear (transverse) (S) waves can be noted in Fig.(3-3a) (3-3b).

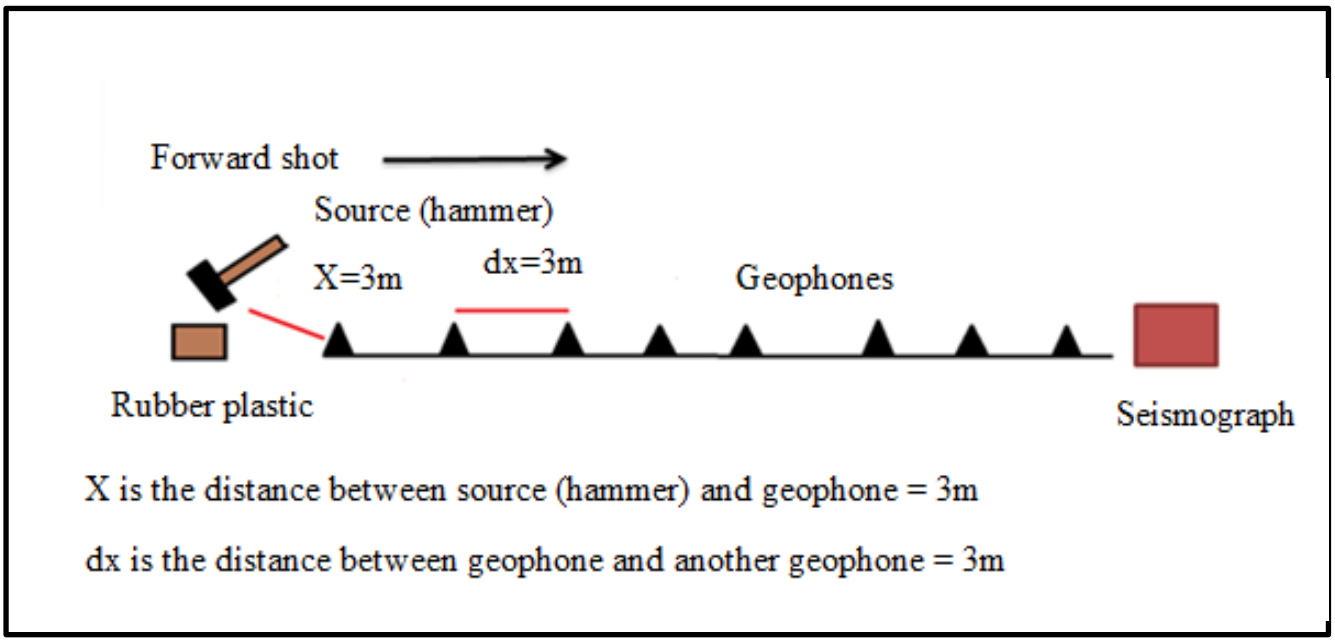

Fig. (3-3a): Shows the diffusion geometry for recording longitudinal (P) and shear (S) waves (Forward direction), (Researcher).

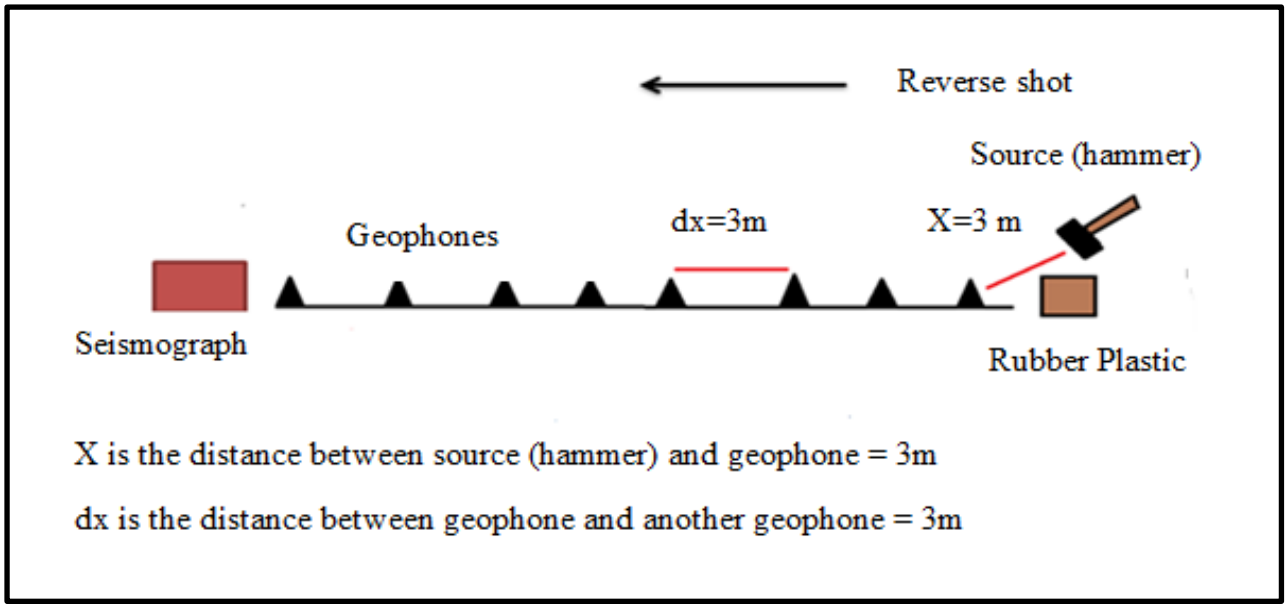

Fig. (3-3b): Shows the diffusion geometry for recording longitudinal (P) and shear (S) waves (Reverse direction), (Researcher).

As for the field work for the MASW method, which is considered as one of the modern methods in geophysics and means Multi-channel Analysis of Surface Waveswhere the survey began with the deployment of geophones (geophones S), which are represented by the destructive Rayleigh waves, where the number of geophones is 24 geophones and the length of the profile is 72 m. The distance between geophone and another geophone is 3 m represented by dx, while the distance between the geophone and the 10 kg hammer is 4 m represented by X, plate (3-7).

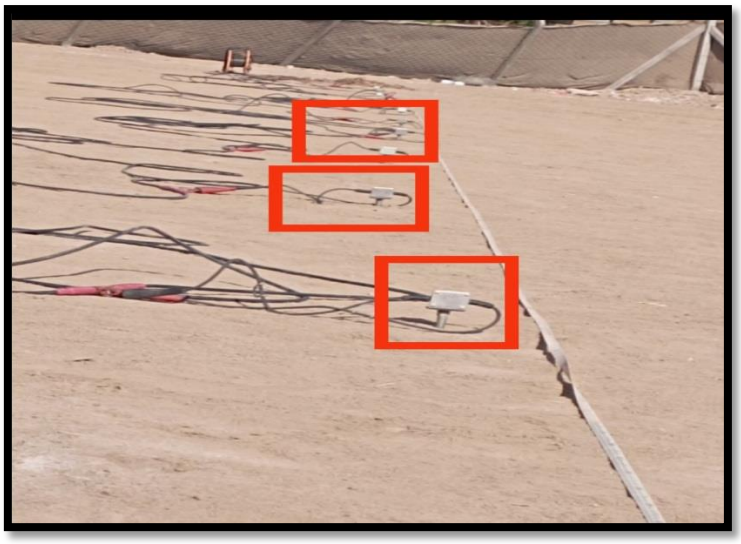

Plate (3-7): Shows the diffusion of geophones (S) in the MASW method.

Two holes are drilled and one in the middle (for reading on this site) in each half of the profile in order to place the rubber plastic in it and change the location of this rubber inside the hole and thus change the direction of the blow with the hammer relative to the location of the rubber plastic, plate (3-8).

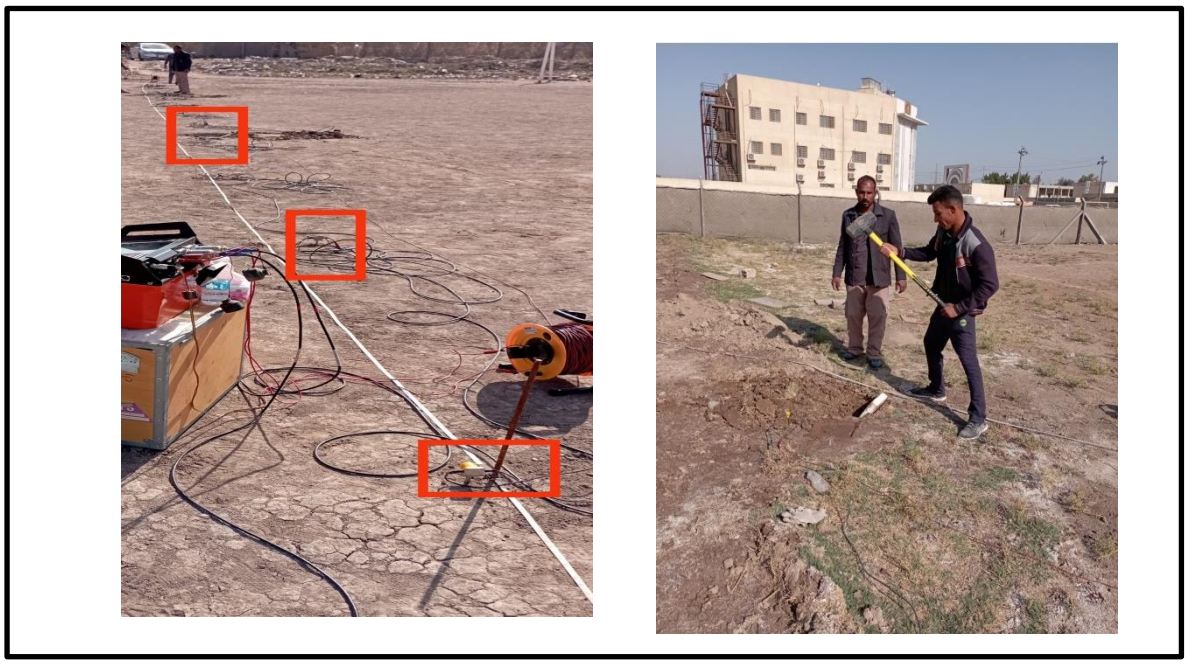

Plate (3-8): Shows spreading geophones (S), and the direction of the rubber plastic and the direction of hammering in MASW method.

The hammering process on the rubber plastic is in the lateral and oblique direction. This rubber plastic is hammered three times by means of a hammer, in order to record the readings after the transmission of mechanical energy and convert it into an electrical signal, in the case of generating S waves in MASW method Then the office work is done for the MASW method.

The diffusion geometry for recording MASW method can be noted in Fig.(3-4).

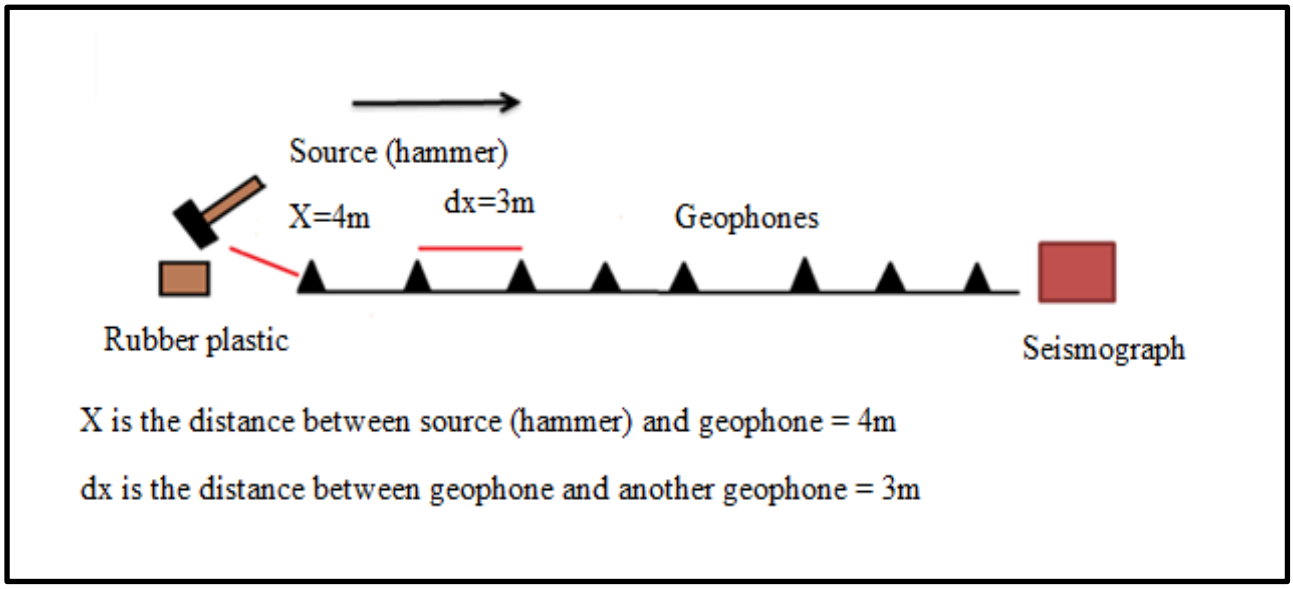

Fig. (3-4): Shows the diffusion geometry for recording MASW method, (Researcher).

Chapter Four

The Results and Interpretation

CHAPTER FOUR

THE RESULTS AND INTERPRETATION

(4-1) Preface:

The basic principle of seismic refraction survey is to use the picked first arrival times from the seismic survey data and drawing time-distance curves for the survey area, each arrival time is attributed preliminary to a specific refractor surface and estimate the depth, velocity, shape and extension of the fracture layers, and then estimate the velocity of each fracture, (Jeraisy,1992).

The choice of the optimal method for interpreting the seismic data depends on the nature of the subsurface, (Dobrin,1976).

The velocities of seismic waves depend on the modulus of elasticity of the rock layers in which they travel therefore, these coefficients are calculated depending on the compressive and shear velocities and the calculated density.

Shear waves are the most important waves in engineering studies for estimating geotechnical properties, (Foti et al., 2011). Despite the difficulty of generating and capturing these waves, recent studies have confirmed that its use in finding mathematical relationships for many geotechnical properties because the velocities of these waves are a direct indication of soil stiffness it has been observed that its applications are constantly increasing in geotechnical engineering and site studies, (Roma, 2001).

As for the MASW method, it can simply be described as recording data for Rayleigh waves, (Foti, et al., 2003).

(4-2) Processing of Seismic Data:

This stage aims to obtain a high signal ratio with the least amount of noise to be able to interpret the data correctly. With several factors that cause noise in the study area including the movement resulting from the rapid traffic of cars to the street near the study site and air movement and other factors.

A number of the seismic recordings of the study site had a percentage of noise and were processed using the Reflex 2D Quick program.

(4-3) Interpretation of Seismic Data:

Most of the interpretation methods assume that the layers have a constant velocity and that the seismic velocity of the layers increases with depth,(Mota,1954). Some methods of interpretation assume that the refractor surface is flat, while others assume that this surface is irregular (Palmer,1981) & (Hagedoorn,1959).

Interpretation of the seismic data includes calculating the depths and calculating the different velocities of the layers in addition to calculating its engineering coefficients.

The accuracy of the interpretation depends on:

1- Interpreter:

An interpreter who has a scientific and applied background and the ability to link seismic information various other information obtained from various sources is practical the interpretation process is more comprehensive and accurate.

2- Geological and Geophysical Data: Information includes that obtained from previous studies of the area that are relevant to the geology of the area and its tectonic situation.
3- Other Data:

   It includes field observations, as some information about the type of soil from the area to be studied (Al-Sayidah Ruqayya Hospital).

Before proceeding to the interpretation of the results, it should be known that the results of the study are compared with the results of the boreholes that are drilled in the study area (four boreholes) and that are drilled by Al-Ma'awal company for soil investigations. This information is obtained through a report belonging to the Holy Hussainiya Shrine (2021) of the study area Fig.(4-1), (4-2).

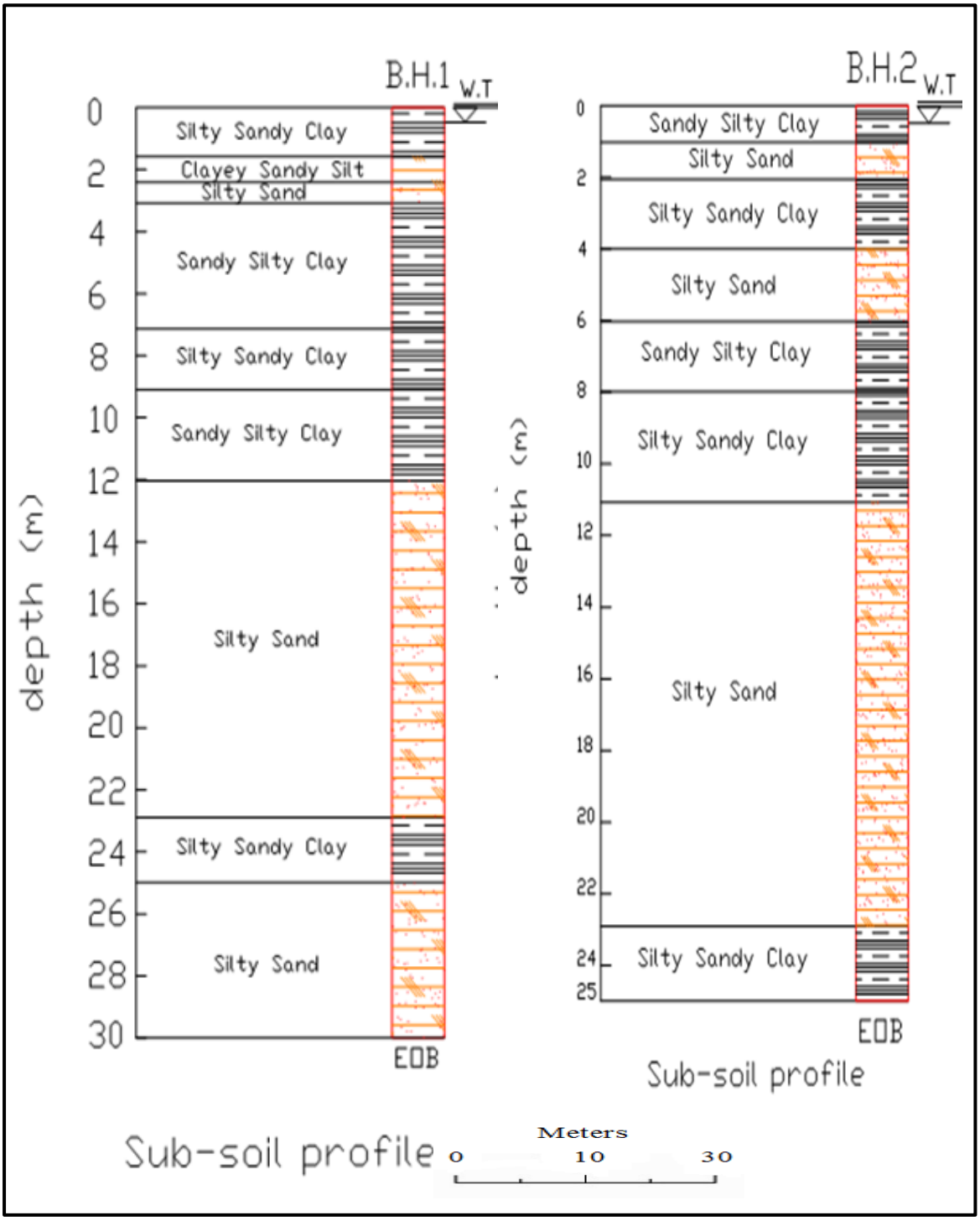

Fig.(4-1): Soil profile through boreholes (1,2)

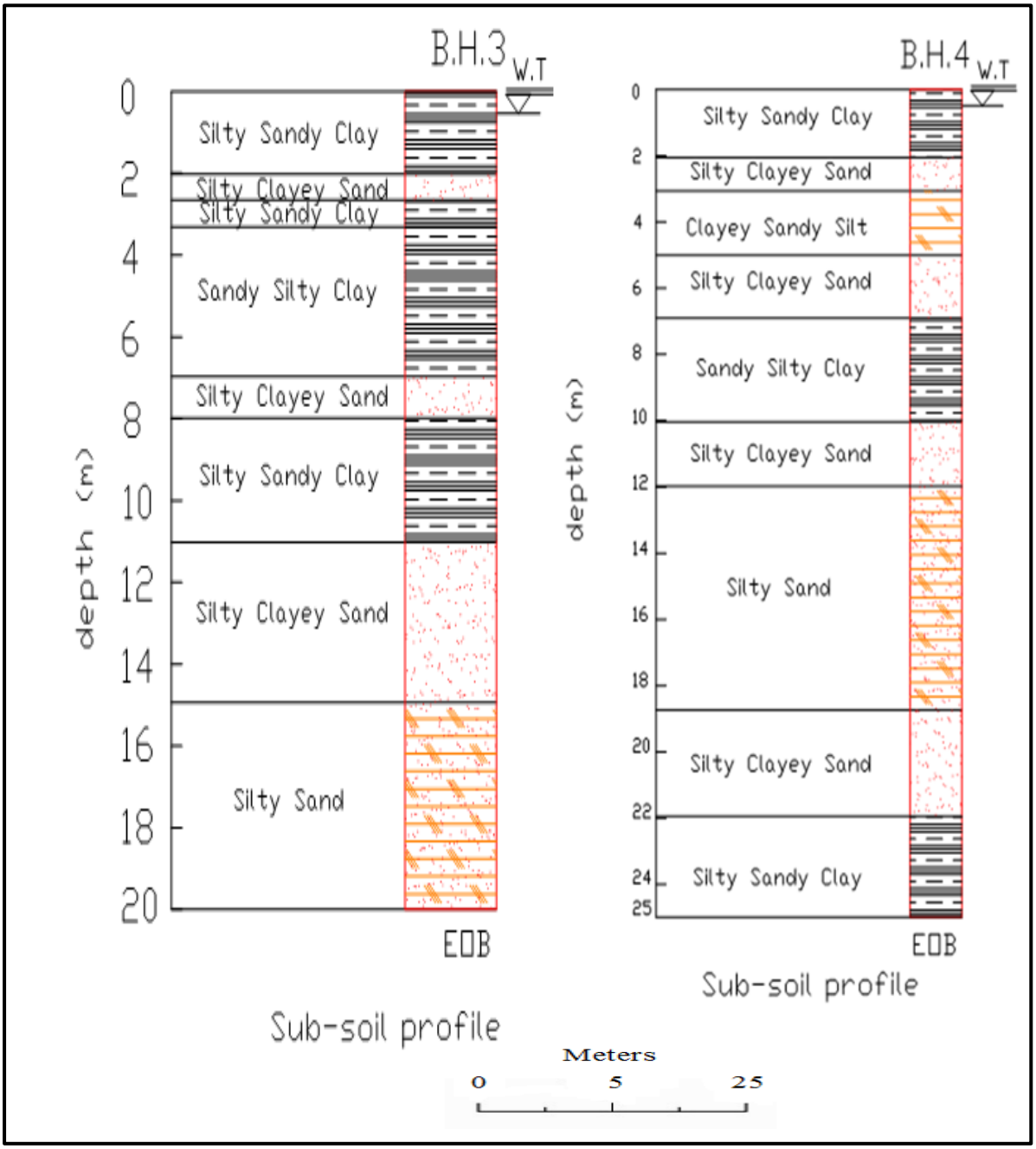

Fig.(4-2): Soil profile through boreholes (3,4)

(4-4) First Break Picking:

The first interpretation is to capture the initial arrival times of the seismic waves for each trace (Sharma,1997; Dobrin and Savit,1988; Haeni,1986 ; Parasnis,1972). And when the source power is sufficient with the least amount of noise, the first break sudden the seismic trace will be easy to determine.

picking first arrival times of seismic wave data are performed, Fig.(4-3a,b) through Reflex 2D Quick program. And the Fig.(4-4a,b) illustrated time-distance curve. The first step in the program is the process of picking the first arrival times and calculating the seismic velocity (two velocities) in the layers (2 layers of the study area) and extracting the depth (m) automatically, then downloading the distance values (m) with time (msec.) (manually) and drawing this relationship in the Excel program, Fig.(4-5). The resulting curve can represent the number of subsurface layers. Also for MASW method picking first arrival times of seismic wave data are performed through Reflex 2D Quick program. The process is picking the first arrival times and calculating the seismic velocity (shear velocity) that representing Rayleigh wave and extracting the depth (m) automatically downloading the distance values (m) with time (msec.) (manually) and drawing this relationship in the Excel program.

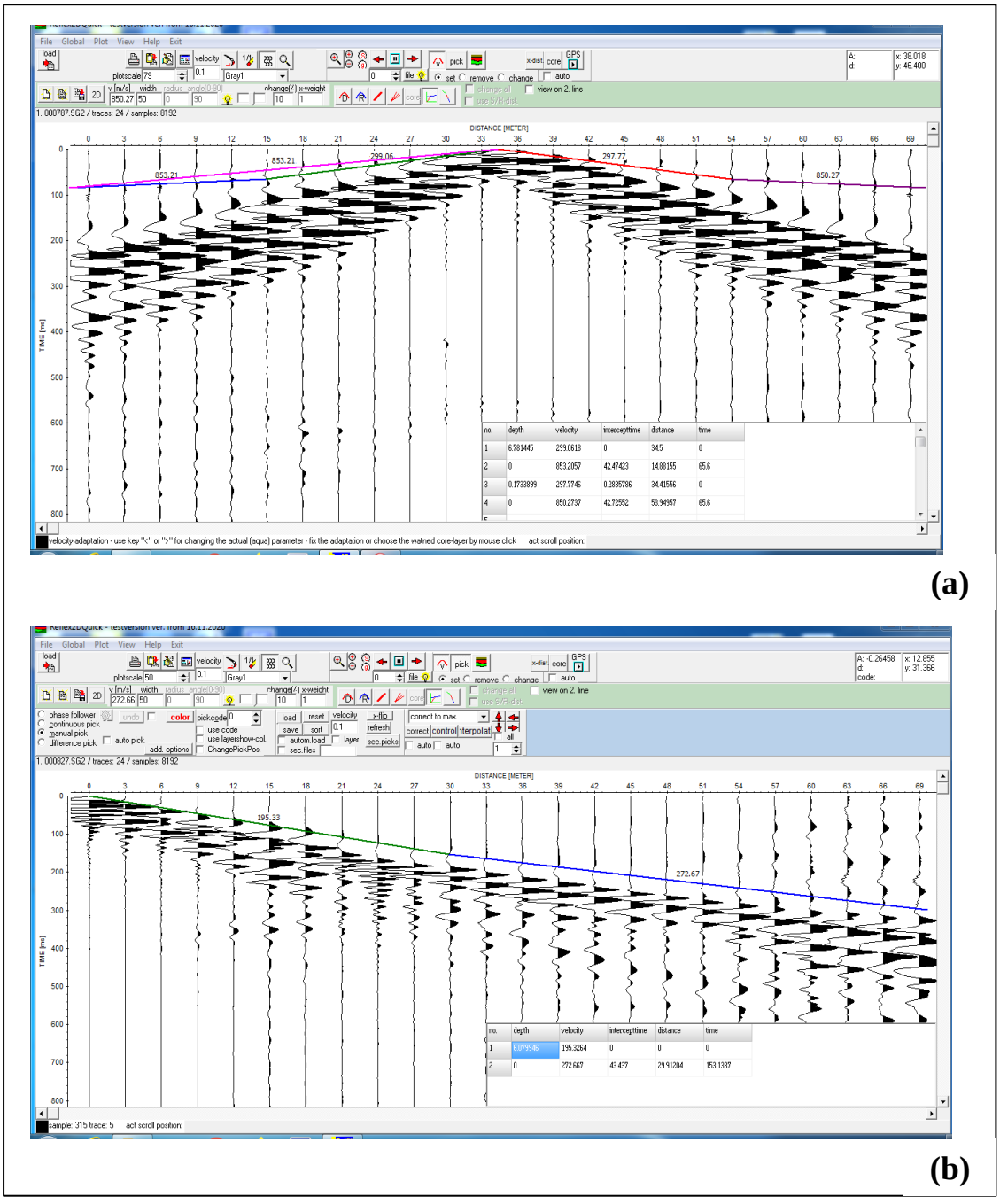

Fig. (4-3a,b): Shows two models of seismic trace in the study area.

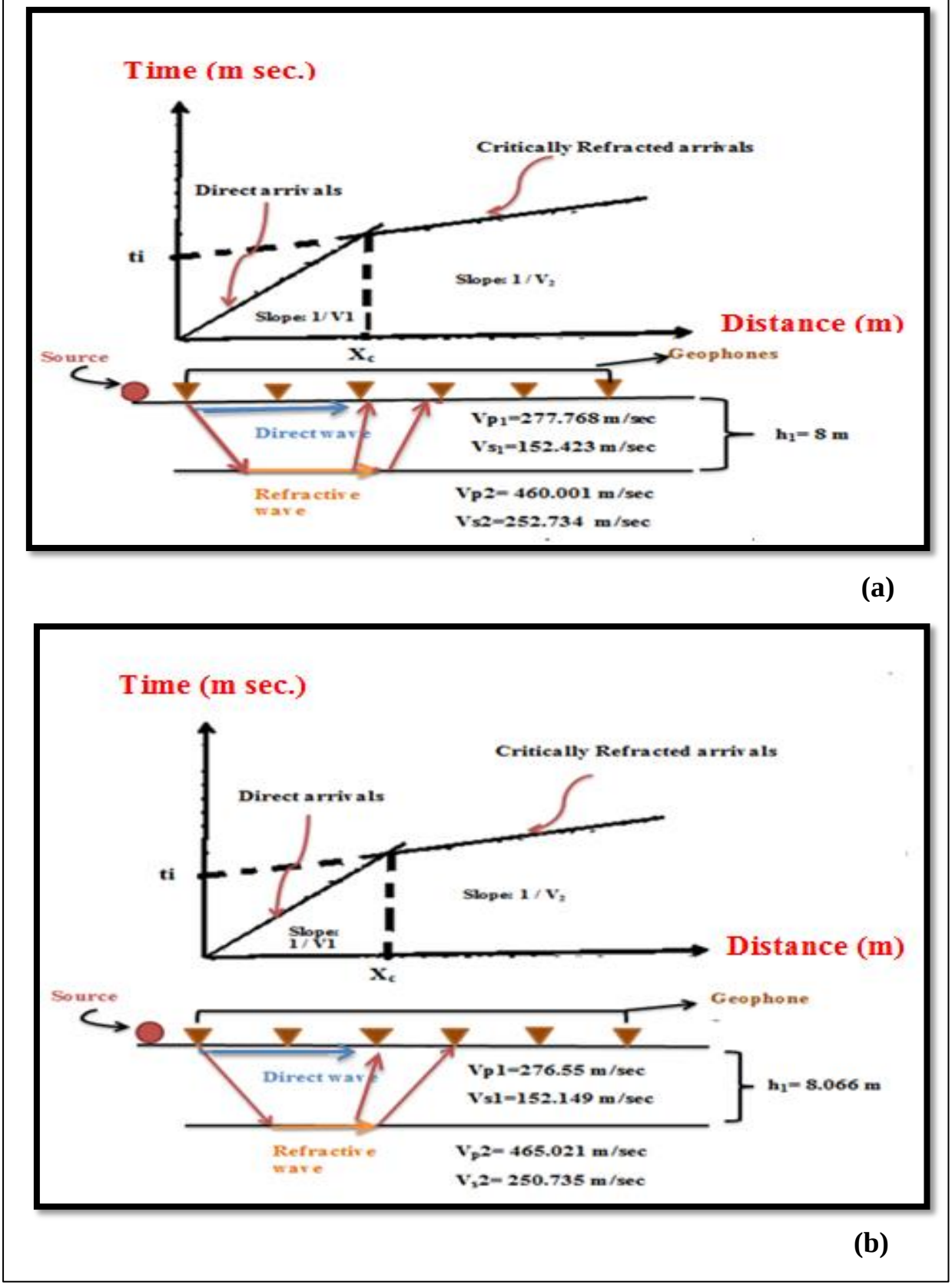

Fig.(4-4):Shows Time-Distance Curve for received waves (Refractive survey) for (a) First profile (b) Second profile, (Researcher)

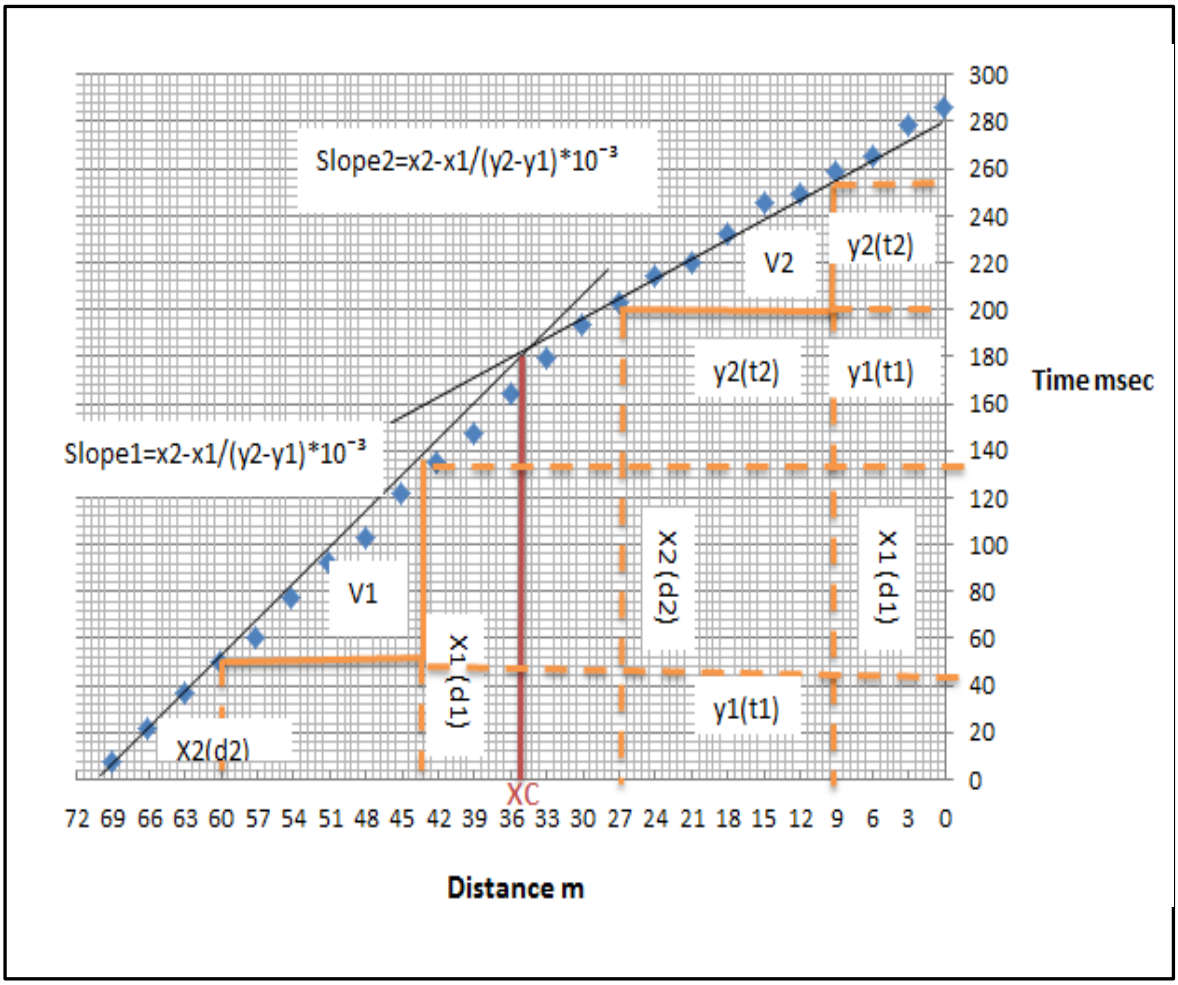

Fig. (4-5): Shows the relationship between distance and time (Forward direction- profile one) for refractive survey.

(4-5) Refractive Seismic Survey and its Interpretation:

(4-5-1) Density Value Calculation:

There is a direct correlation between seismic velocity and the density and ripability of subsurface materials as shown in Fig (4-2) . The bulk density ρ can be given as (Uyanik, 2010).

$$(\rho_1 = 16 + 0.002V_{p1} = 16.45\ kN/m^3)\ /9.8 \ldots\ldots\ldots\ldots (4\text{-}1)$$
$$(\rho_2 = 16 + 0.002V_{p2} = 17.10\ kN/m^3)\ /9.8 \ldots\ldots\ldots\ldots (4\text{-}2)$$

and the figure (4-6) illustrates this relationship.

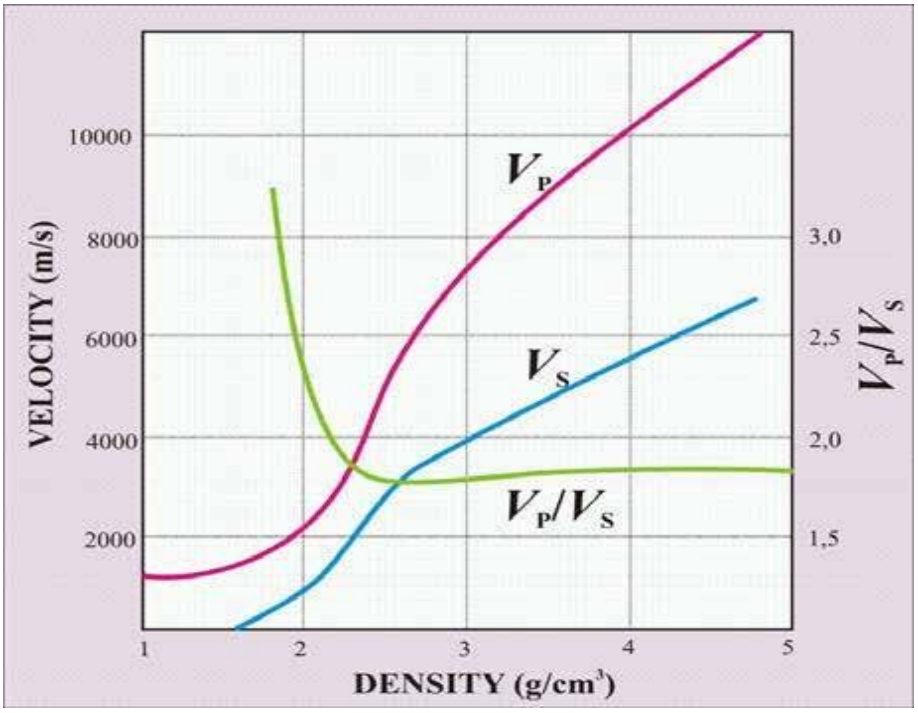

Fig (4-6): Shows the relations between P wave velocity (V_P), S wave velocity (V_S), and their ratio (V_P/V_S) and density (after Barton, 1986).

From the two equations (4-1),(4-2), the density value is calculated for the first layer and the second layer, respectively, for the two profiles.

The table (4-1) below shows the density values with the average velocities of the longitudinal (V_p) and shear (V_s) seismic, respectively.

Table (4-1): Shows density values and averages of velocities (P,S) for the two profiles and for two layers.

Profile No.		V_p Avg. (m/sec)	V_s Avg. (m/sec)	ρ (gm/cm^3)
1	First layer	277.768	152.423	1.689
	Second layer	460.001	252.734	1.72
2	First layer	276.55	152.149	1.689
	Second layer	465.021	250.735	1.72

Through the table (4-1) and according to the density values, the first layer represents the superficial soil in both profiles, its density is (1.689 gm/cm^3) also the second layer represents superficial soil in both profiles, its density are (1.72) gm/cm^3.

The density of the elastic medium in which the seismic wave propagates is one of the influencing factors at seismic velocities. And any increase in density by a certain percentage leads to an increase in elasticity many times over the ratio leads to an increase in velocity, or an error in the density measurement of the elastic medium that is being transmitted during which the seismic wave leads to many times the error in the values of the elastic modulus. And ratio the error in density measurement for subsurface soil models increases as we get closer to the surface of the ground especially for layers with a lateral shift (Bowles,1984).

(4-5-2) Evaluation of the Geotechnical Properties:

The process of on-site geotechnical evaluation is of great importance in

civil engineering works as construction important strategic or industrial facilities, dams, hydroelectric stations, bridges and high ways and others, and this is done depending on the measurement of the geotechnical properties of the soil and the geological layers below the surface.

Geotechnical properties and elasticity coefficients were measured based on the velocities of seismic waves (V_p) and (V_s) and the measured density, and based on the relationships shown in the table (4-2).

Table (4-2): Shows equations used in calculating elasticity coefficients.

Elastic Module	Used Formula	Reference
Poisson's Ratio(ν)	$\nu = 1/2[1-1/(V_p / V_s)^2-1]$	Davis and Schultheiss,1980 in Khorshid, et al. 2006
Young's Modulus (E)	$E=2V_s^2\rho(1+\nu)$	
Shear Modulus (μ)	$\mu = \rho V_s^2$	
Bulk modulus (K)	$K = \rho V_p^2-4/3\mu$	
Lame's Constants (λ)	$\lambda = \rho V_p^2-2V_s^2$	

1- Poisson's Ratio(ν):

The value of this ratio for the first layer in the first profile is 0.285, while in the second layer for the same profile is 0.284 . As for the first layer in the second profile, the Poisson's ratio was 0.283 . Poisson's ratio of the second layer in the same profile was 0.295 .

In the first and the second profiles (first layer and second layer in the profiles) the soil type is dense sand according to the table (4-3) of sandy soil, also the type of soil according to the table (4-4) of clay soil is Sandy clay and silt.

Also for the same profiles and same layers and according to Poisson's ratio the soil description parameter is Fairly to Moderate Competent materials, table (4-5).

Table (4-3): Shows classification of the soil according to the Poisson's Ratio (ν), Gercek (2006):

Soil Type	Poisson's Ratio (ν)
Loose sand	0.20 - 0.40
Medium dense sand	0.25 - 0.40
Dense Sand	0.30 - 0.45
Silty Sand	0.20 - 0.40
Sand and Gravel	0.15 - 0.35

Table (4-4): Shows classification of the soil according to the Poisson's Ratio (ν), Bowles (1996), Subramanian (2008):

Description	Poisson's ratio
Clay (saturated)	0.4 – 0.5
Clay (unsaturated)	0.1 – 0.3
Sandy clay	0.2 – 0.3
Silt	0.3 – 0.35
Sand, gravelly sand	0.3 – 0.4
Dense sand	0.2 – 0.4
Rock	0.1 – 0.4

Table (4-5): Shows classification of the soil according to the Poisson's Ratio (ν) Birch (1966), Gassman (1973), Tatham (1982), Sheriff and Geldart (1986).

Soil description parameter	Incompetent to slightly competent	Fairly to Moderate competent	Competent materials	Very high competent materials
Poisson's Ratio (ν)	0.41- 0.49	0 . 35 - 0.27	0.25-0.16	0.12-0.03

2-Young's Modulus (E):

The value of this parameter of the first layer in the first profile is 100.847 Mpa, while for the second layer in the same profile was 282.131 Mpa.

In the second profile the value of this parameter in the first layer is 100.328 Mpa and in the second layer in the same track is 280.064 Mpa.

Young's modulus is directly proportional to the velocity of wave transmission, meaning that this coefficient increase in the velocities of seismic waves and the increase in the stiffness of rock.

3-Shear Modulus (μ):

The highest value of this parameter is in the second layer of the first profile 39.240 Mpa, while in the first layer for the same profile is 109.864Mpa.

In the first layer from the second profile the value of Shear modulus is 39.099 Mpa, while the second layer from the same track is 108.133 Mpa.

The relationship of this coefficient with depth and with seismic velocities increases with increasing velocities of seismic waves and is directly proportional to them and depth.

4-Bulk modulus (K):

The values of this coefficient ranged for the first and second layer for the first profile 130.314 – 363.807 Mpa respectively, while in the second profile for the first layer is 129.122 Mpa and of the second profile is 371.796 MPa.

5-Lame's Constants (λ):

The value of this coefficient in the first layer for the first profile 83.849 Mpa, but in the second layer for the same profile is 236.204 Mpa.

For the second profile the value of the Lame's constant in the first layer is 82.875 Mpa, while in the second layer for the same profile the value is 246.204 Mpa.

From observing these values the behavior of this parameter it is similar to the modulus of shear and Young that it increases with the increase in the stiffness of the rocks.

(4-5-3) Geotechnical Parameters:

1- Material Index (I_m):

This coefficient is defined geometrically as the value used to determine the quality and efficiency of materials for building foundations, As for Abd Al-Rahman (1989) he defined it as an expression of the degree of hardness relying on its flexible transactions. This coefficient has to do with the composition of the material and the degree of cohesion and fracturing, joints and the presence or absence of fluid in the spaces, this in turn affects the nature of the medium and the velocities of seismic waves.

Abd El-Rahman (1994) derived the equation (4-3) in terms of longitudinal and shear velocities, which were used in calculating this parameter in this study:

$$I_m = 3(v_s/v_p)^2 - 1/1-(v_s/v_p)^2 \ldots\ldots\ldots\ldots \quad (4\text{-}3)$$

The values of this parameter range between -0.142 and -0.143 in the first and second layer respectively from the first profile . In the second track the values of this parameter range between -0.18 and -0.17 in the first and

second layer respectively. These values indicated a clear decrease at the layers.

The first and the second layers, which are intermediately competent table (4-6) and, or had a relatively low value in the first layer from the first profiles.

Table (4-6): Shows classification of soil competence depending on I_m (Abd Al-Rahman,1994).

I_m	Degree of Competent
(-1)-(-0.5)	Non- less competent
(-0.5)-0	Intermediately competent
0-0.5	Competent
0.5-1	Highly competent

2- Concentration Index(I_c):

One of the important engineering coefficients that indicate the degree of competence of a material which are used to measure the efficiency of the foundations and many more civil engineering purposes. This parameter depends mainly on the elasticity coefficients of the materials and the pressure distribution in the depths.

Abd El-Rahman (1991) developed an equation to calculate this coefficient in terms of the values of longitudinal wave velocities and shear velocities V_p,V_s, according to the following equation:

$$I_c = [3-4(v_s^2/v_p^2)]/[1-2(v_s^2/v_p^2] \ldots\ldots\ldots\ldots (4\text{-}4)$$

The values of this parameter for the first and second layers of the first profile are 4.51 and 4.516, respectively. And for the second profile are 4.53 and 4.436 for the first and second layers, respectively.

The measured concentration coefficient values was compared with the ranges set by Abd El-Rahman (1989) where the table (4-7) shows that, its value increases with the increase in the stiffness of the rocks it showed that the first layer of the two tracks is (fairly to moderate competent)

3- Coefficient of lateral earth pressure at rest (K_o):

It is one of the most important geotechnical transactions from an engineering point of view. (Bowles ,1982) noticed The value of this coefficient is higher in fine soils than in coarse soils and its value in loose, non-cohesive soils is large, and the value of this coefficient decreases with increasing overburden pressure.

Abd El-Rahman (1991) indicated that there is a relationship between longitudinal and shear wave velocities, and the value of this coefficient was calculated using the relationship (4-5):

$$K_0 = 1\text{-}2(v_s/v_p)^2 \ldots\ldots\ldots\ldots \text{(4-5)}$$

The values of this coefficient for the first layer is 0.398 and for the second layer is 0.397 from the first profile, as for the second profile for the first layer is 0.395 and the second layer for the same profile is 0.419 . Which indicates that the soil is moderate competent to competent (good compacted) of the first and the second layer from to tracks, by comparing it with the range determined by Abd El-Rahman, 1989) (Table 4-7).

Table (4-7): Shows ranges of concentration index values and lateral earth pressure with the degree of soil stiffness.

Soil description parameter	**Weak**		**Fair**		**Good**
	Incompetent		Fairly competent		Competent
	Very Soft	Soft	Fairly competent	Moderate competent	Compacted
Concentration Index (I_c)	3.5-4.0	4.0-4.5	4.5-5.0	5.0-5.5	5.5-6.0
Lateral earth pressure (K_o)	0.7-0.61	0.61-0.52	0.52-0.43	0.43-0.34	0.34-0.25

4- Effective Angle of Internal Friction (Ø):

It is one of the important geotechnical elements that can be measured in the laboratory using Moho's circles for Triaxial test and it is the angle of inclination of the tangent to this of the Moho's circles. Which are circles it diameters represent the difference between horizontal and vertical stresses.

Øº is widely used in evaluating the engineering properties of soils and rocks that represent their resistance to static and dynamic loads. It can be calculated in terms of the velocities of the longitudinal and shear seismic waves according to (Bowles,1988) the following relationship:

$$\text{Sin } Ø = 2(v_s/v_p)^2 \ldots\ldots\ldots\ldots \text{ (4-6)}$$

One of the factors affecting the value of (Øº) is the texture, density and water content, the granular shape of the components of the mineral composition, as the (Øº) increases with increasing density and hardness.

The values of (Øº) varied for the first profile and for the first and second layers, respectively which were 37.013 and 37.085, while in the second profile are 37.228 and 35.520 for the first and second layers respectively.

It decreases in the loose layers and increases in its value in the solid layers, and this reflects the hardness of the (first layer) of the first and second profiles. Table (4-8) show range of Øº for several soil types.

Table (4-8): Typical range of true angle of internal frictions Øº values for several soil types. (after Bowles, 1988).

Soil type	Øº		Soil type	Øº	
	Loose	**Dense**		**Loose**	**Dense**
Gravel	32 – 36	35 – 50	Fine sand	27 – 33	33 – 39
Coarse sand	32 – 38	35 – 48	Sandy gravel	30 – 38	36 – 45
Clayey sand	28 – 32	35 - 40	Gravely sand	30 – 38	36 – 50
Silty sand	28 – 32	32 - 38	Silt	20 – 30	25 - 32

5- Allowable and Ultimate Bearing Capacity (q_{all} and q_u):

Allowable bearing capacity is the ultimate bearing capacity divided by a reasonable factor of safety.

The ultimate bearing capacity is one of the important characteristics of engineering projects that is a measure of the bearing of the rocks under the foundations it expresses the resistance of the soil to the stresses resulting from the dynamic and static loads generated by the various engineering constructions. When designing engineering facilities, the amount of q_u is calculated because if the generated stresses are higher than q_u deformation and creep of the layers will occur, which leads to engineering problems such as settlement, (Bowles,1984).

A number of researchers have attempted to link this geotechnical characteristic important with shear wave velocities because they are important in engineering studies through their relationship the coefficient

of hardness which determines the hardness and durability of soils and rocks.

Abd-AL-Rahman et al.,(1994) found the following relationship with the velocities of the compression waves:

$$Q_{all} = 1/3\ (V_P / 240)^{2.38} \ldots\ldots\ldots\ldots (4\text{-}7)$$

This equation (4-7) is very important because the allowable bearing capacity along seismic tracks can be calculated by using this equation. The Q_{all} is measured in Ton/m^2.

The allowable bearing capacity Q_{all} of the first layer of the first and second tracks are 0.471 kg/cm^2 and 0.466 kg/cm^2, respectively, while for the second layer the allowable bearing capacity are 1.606 kg/cm^2 and 1.607 kg/cm^2 for the first and second tracks, respectively. Because the value of Q_{all} is low for the first layer of the first and second profiles, and this is due to its lack of rigidity, which caused the values of the transverse wave velocities to drop.

As for the second layer of the first and second profiles it was better, the values of the allowable bearing capacity are higher which reflects its high rigidity and this is consistent with other engineering parameters that were calculated for the subsurface layers in the study area.

And the value of the elastic and geotechnical parameters with density and Vp ,Vs illustrated in table (4-9).

Table (4-9):Shows the values of (V_p avg. , V_s avg. and density), Elastic Modulus and Geotechnical Parameters.

Profile No.		V_p avg. m/sec	V_s avg. m/sec	ρ gm/cm^3	Elastic Modulus.					Geotechnical Parameters				
					ν	E Mpa	μ Mpa	K Mpa	λ Mpa	I_m	I_c	K_o	ø°	Q_{all} Ton/m^2
1	First layer	277.768	152.423	1.689	0.285	100.847	39.240	130.314	83.849	-0.142	4.51	0.398	37.013	4.71
	Second layer	460.001	252.734	1.72	0.284	282.131	109.864	363.807	236.204	-0.143	4.516	0.397	37.085	16.06
2	First layer	276.55	152.149	1.689	0.283	100.328	39.099	129.122	82.875	-0.18	4.53	0.395	37.228	4.66
	Second layer	465.021	250.735	1.72	0.295	280.064	108.133	371.796	246.204	-0.17	4.436	0.419	35.520	16.07

(4-6) Shear Waves Data Collection:

Shear wave data is obtained by horizontal seismic refraction survey, similar to obtaining longitudinal waves with different geophones as well as using the Multi-Channel Analysis of Surface Waves (MASW), which is data recording for Rayleigh waves.

(4-7) Principle of MASW Method:

This method is considered nondestructive and one of the seismic methods. This method uses the properties of Rayleigh waves (Park et al., 1999) to obtain the shear wave velocities that are used in shallow depth applications related to environmental works and geotechnical engineering and to calculate the one-dimensional model (1D) for shear wave velocities (V_S).

This technique can be divided into two types, the first type is (Active MASW) and the second type is (Passive MASW).

The first type (Active MASW) allows us to measure the apparent dispersion curve or phase velocity within a frequency range greater than the second type (Passive MASW), as well as at a lower depth than the second type, where the first type (active) gives information about the shallow layers and depends on the ground hardness and the length of the diffusion. As for the second type (Passive MASW), it allows us to measure at lower frequencies than the first type, and at greater depths than the first type, depending also on the hardness of the earth (Roma, 2001). In this study, the first type (Active MASW) was used.

(4-8) Depth of Foundation:

The depth of foundation is depending on the nature, texture, type bearing capacity of the soil, and water table of groundwater. The depth of

foundation prefers to be not more than the depth of groundwater, to prevent some construction problems.

(4-9) Bearing Capacity and its Relationship with Foundation Depth and Shear Velocity:

According to Meyerhof's: For foundation on the ground, according to Meyerhof's general bearing capacity equation (1963) which will provide the most consistent results:

$$q_{ult} = C\, N_c\, S_c d_C + \gamma\, D_f\, N_q s_q\, d_q + 0.5\, \gamma_{sub}\, B\, N_\gamma\, s_\gamma\, d_\gamma \quad \ldots\ldots\ldots (4\text{-}8)$$

where:

q_{ult} : Ultimate bearing capacity.

C : cohesion.

γ : effective unit weight considering the water table effect.

B: footing width.

γ_{sub} : unit weight saturated.

N_c ,N_q, N_γ : Bearing capacity factor.

S_c, S_q ,S_γ : Shape factors.

d_c , d_q , d_γ : Depth factors.

For the transition to safety bearing capacity this value is divided into 3 safety numbers; factor of safety (Fs).

$$Qall = qult / Fs \quad T/m^2 \; Fs=3 \quad \ldots\ldots\ldots\ldots (4\text{-}9)$$

The allowable bearing capacity for the foundation from Meyerhof's equation ,Table (4-10):

And the table (4-11) show the results of MASW methods

Table (4-10): Show the depth of foundation bearing capacity according to Meyerhof's equation (Report of Holy Hussainiya Shrine, 2021) .

Df= The depth of foundation (m)	**allowable bearing capacity T/m^2**
1	**(4.46) T/m^2**
2	**(5.27) T/m^2**
3	**(5.96) T/m^2**

Table (4-11): Show the depth of foundation, bearing capacity, depth and MASW (V_s).

	VS_2 MASW m/sec	**Depth of Foundation m**	**Bearing Capacity T/m2**	**Depth m**	**Vs_1 MASW m/sec**
	317.50	1 2 3	4.46 5.27 5.96	10.398	161.96
	323.66	1 2 3	4.46 5.27 5.96	10.061	162.05
	295.24	1 2 3	4.46 5.27 5.96	11.231	166.05
	288.37	1 2 3	4.46 5.27 5.96	5.729	174.76
	292.98	1 2 3	4.46 5.27 5.96	5.749	177.38
	293.57	1 2 3	4.46 5.27 5.96	6.101	187.40
Avarage	301.88			8.211	171.6

(4-10) Processing and Interpretation of MASW:

MASW data is analyzed using the SeisImager/SW program. The processing operations consist of extracting the dispersion properties (the velocity phase of the dominant Rayleigh waves as a function of frequency) and this is done by analyzing the primary data of the survey and using Fourier transforms then we plot the dispersion curve by using

the F-K transformations that which enables us to plot the dominant data, (Dal Maoro et. al, 2003).

The following figure (4-7) shows the dispersion curve between frequency and phase velocities of the studied track (MASW profile), and the figures (4-8 to 4-13) show one-dimensional sections of the shear velocities and contour maps .

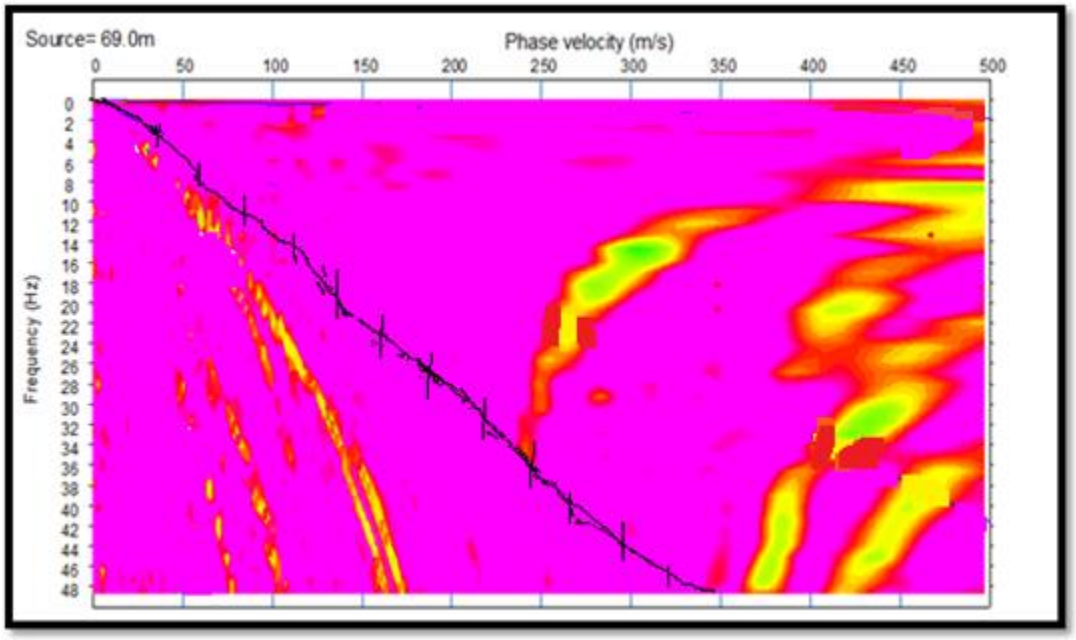

Fig.(4-7): Shows dispersion curve between frequency and phase velocities for MASW method.

The figure (4-7) shows a stage of data processing for MASW method, which is the spectral analysis and capture of dispersion curves for the phase velocities of Rayleigh waves, where the change in the phase velocity of surface waves is calculated, where the change in the velocity of waves at each wavelength is called the phase velocity, then the dispersion curve is plotted and represents the relationship between phase velocity and frequency. Rayleigh waves are characterized by the phenomenon of dispersion (spreading) that occurs as a result of the change in the phase velocity and frequency of surface waves during their

transmission between the surface layers. The dispersion curves show a good curve for the normal modes in the low velocity surface layers, which descend from the high phase velocities of low frequencies to the phase velocities of high frequencies. This stage is done automatically using the SeisImager/SW program.

The processing consists of extracting the dispersion characteristics (Phase velocity of dominant Rayleigh waves as a function of frequency) and this is done by analyzing the primary data of the survey that are affected by the seismic events Fourier transforms and then drawing the dispersion curves using (f-k) transformations. The (f-k) transformations always give a picture of the surface wave spreading shape and the dispersion curves are presented as a phase velocity with frequency.

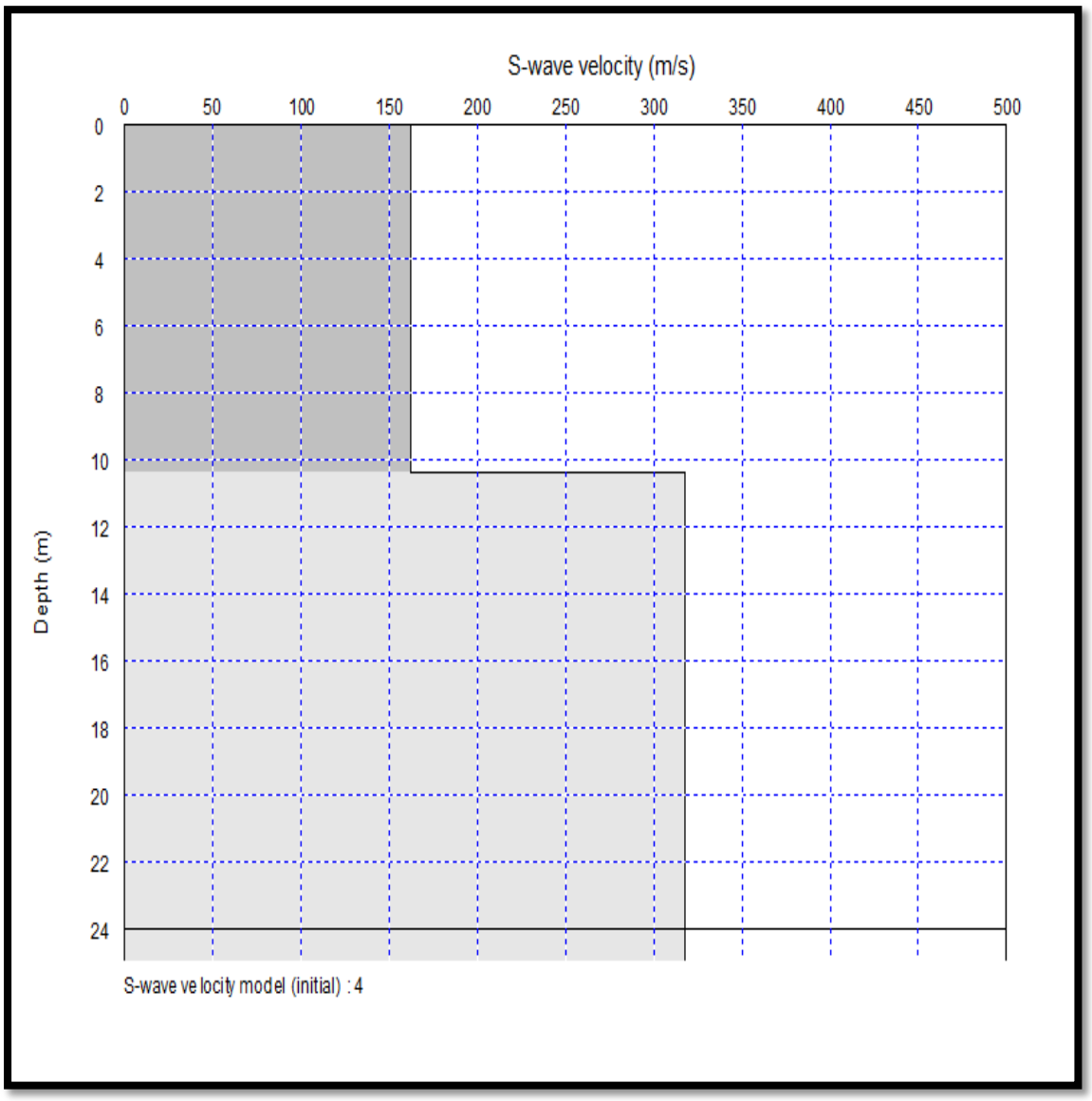

Fig. (4-8): Shows one-dimensional section of the shear velocity of the studied profile (first reading).

The Figure (4-8) illustrates the relationship between depth and shear velocity, as the greater the velocity the greater the depth. We notice that the depth through this figure is 10.39 m and the value of the shear velocity is 161.96 m/sec .The soil is rock.

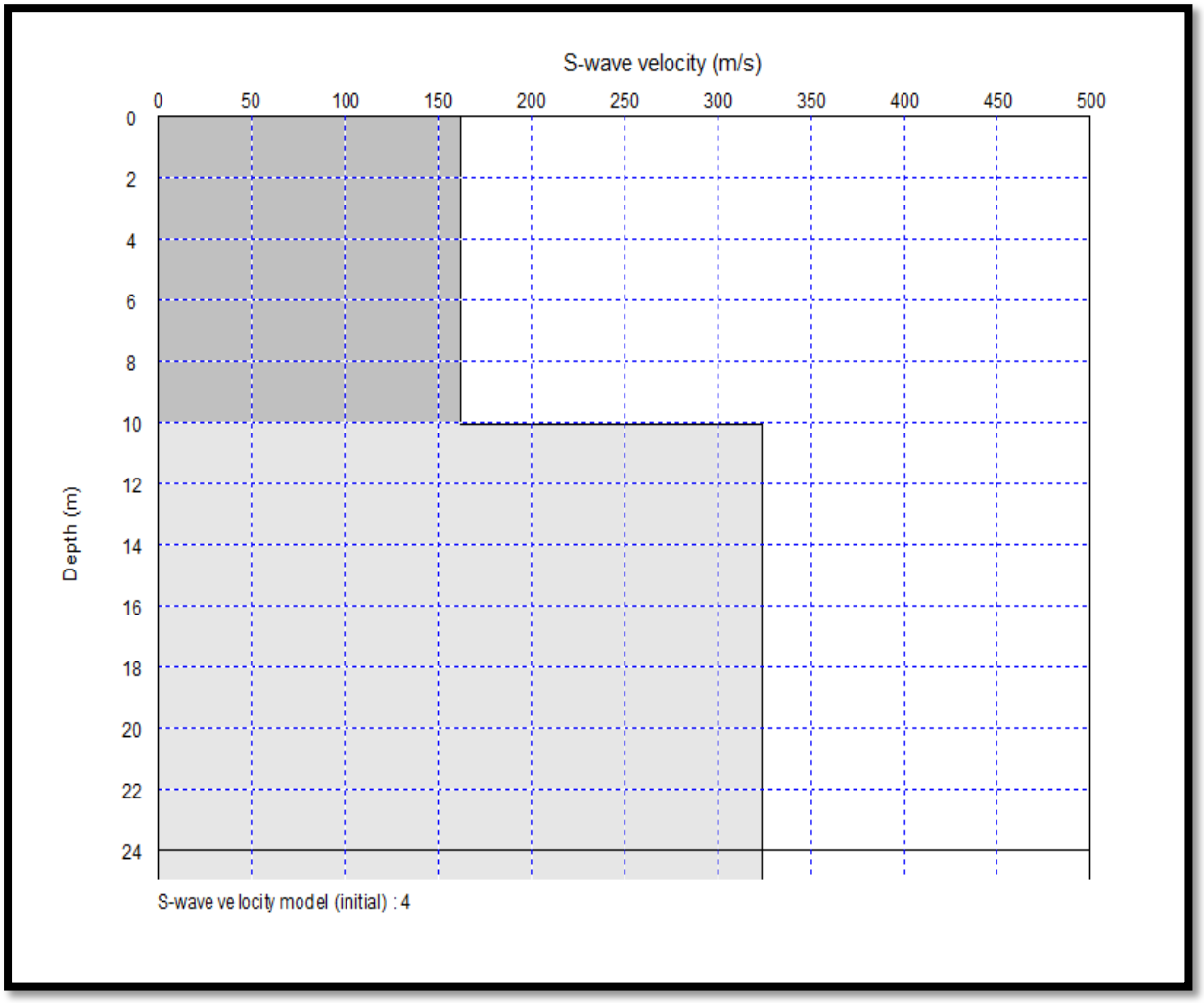

Fig. (4-9): Shows one-dimensional section of the shear velocity of the studied profile (second reading).

From the Figure (4-9) we notice that the depth through this figure is 10.061 m and the value of the shear velocity is 162.05 m/sec .The soil is rock.

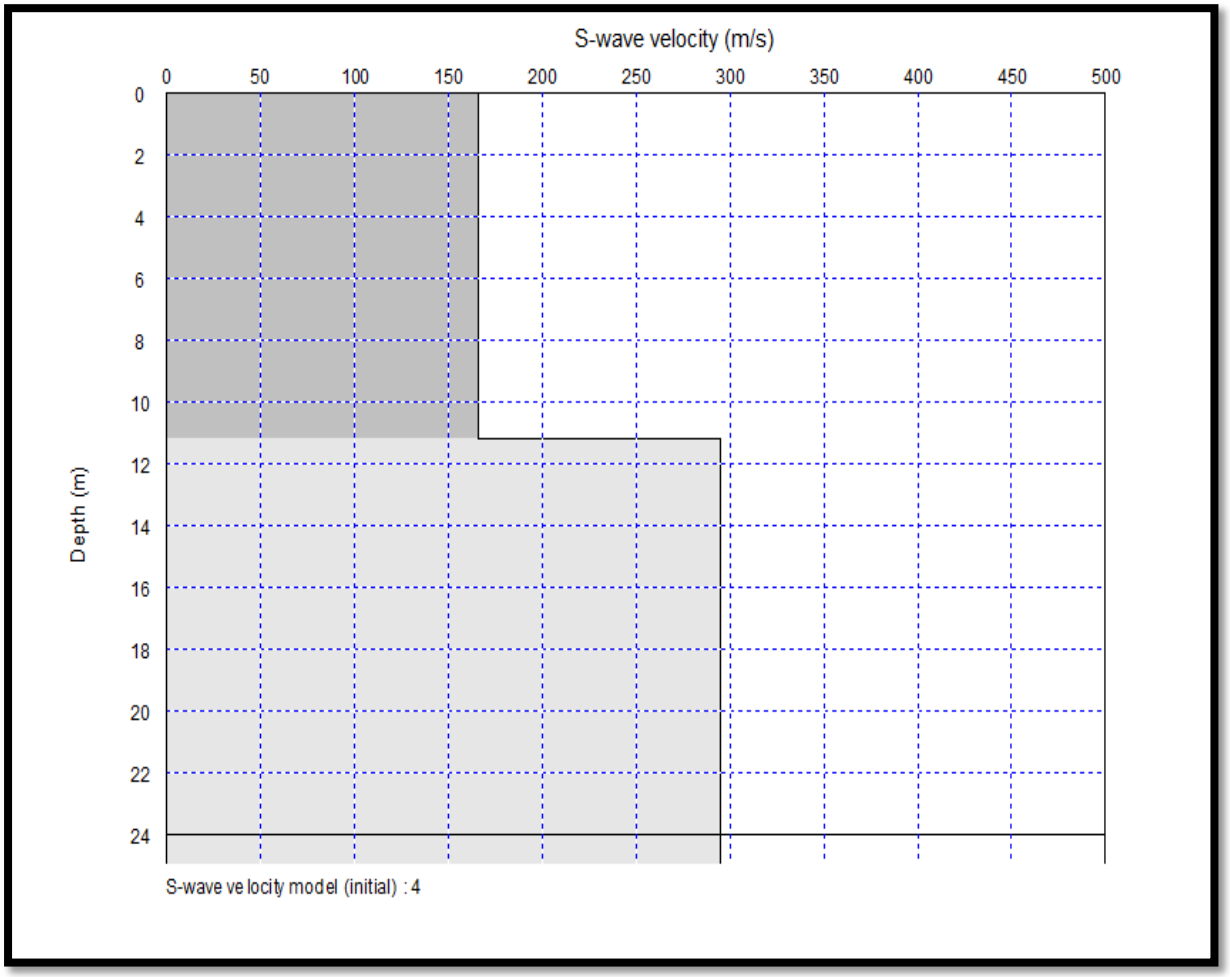

Fig. (4-10): Shows one-dimensional section of the shear velocity of the studied profile (third reading).

The Fig.(4-10) we notice that the depth through this figure is 11.231 m and the value of the first shear velocity is 166.05 m/sec, while the value for the second shear velocity is 295.24 m/sec. The soil is rock.

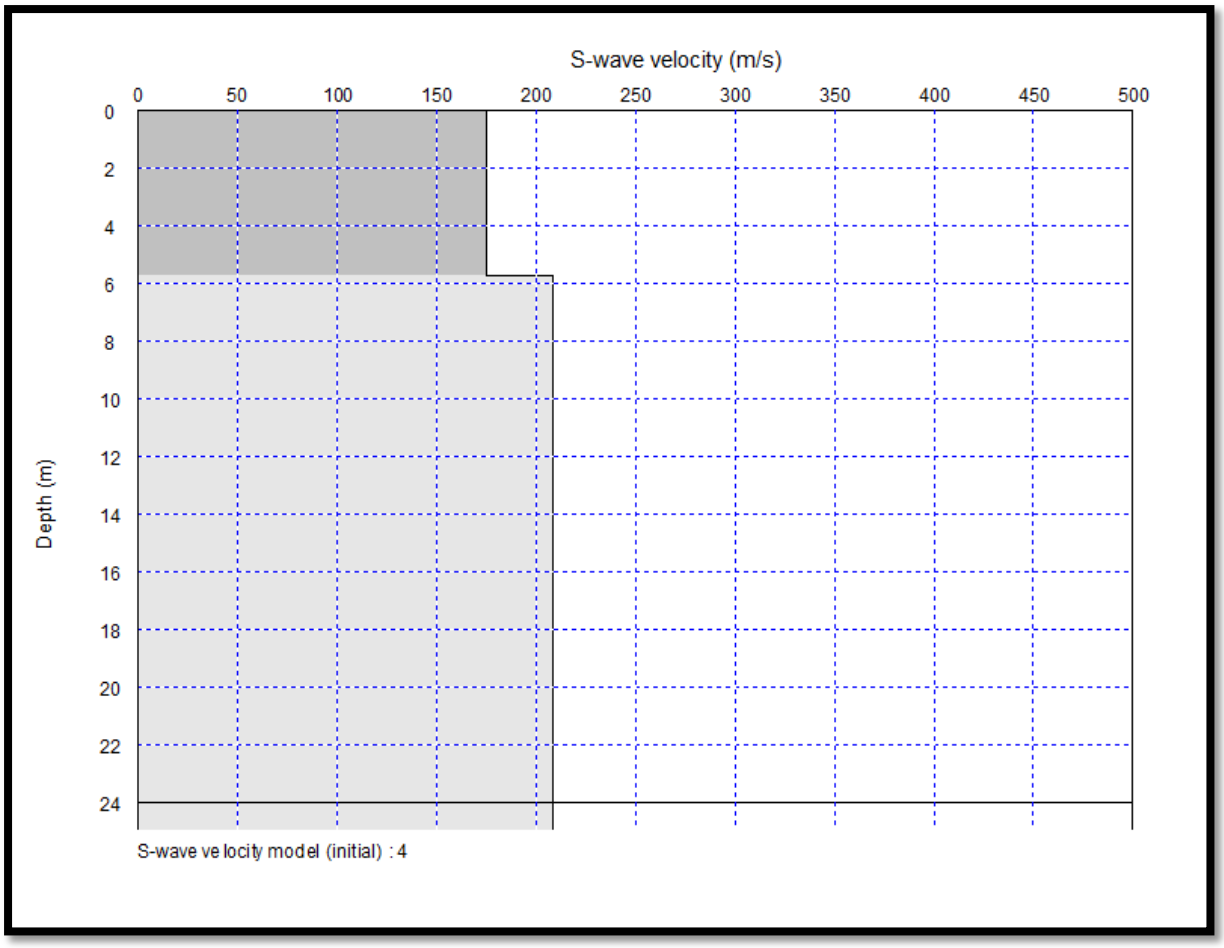

Fig. (4-11): Shows one-dimensional section of the shear velocity of the studied profile (fourth reading).

The Figure (4-11) illustrates the relationship between depth and shear velocity, the value of the shear velocity is 174.76 m/sec and value of the depth is 5.729 m, so the soil is stiff soil.

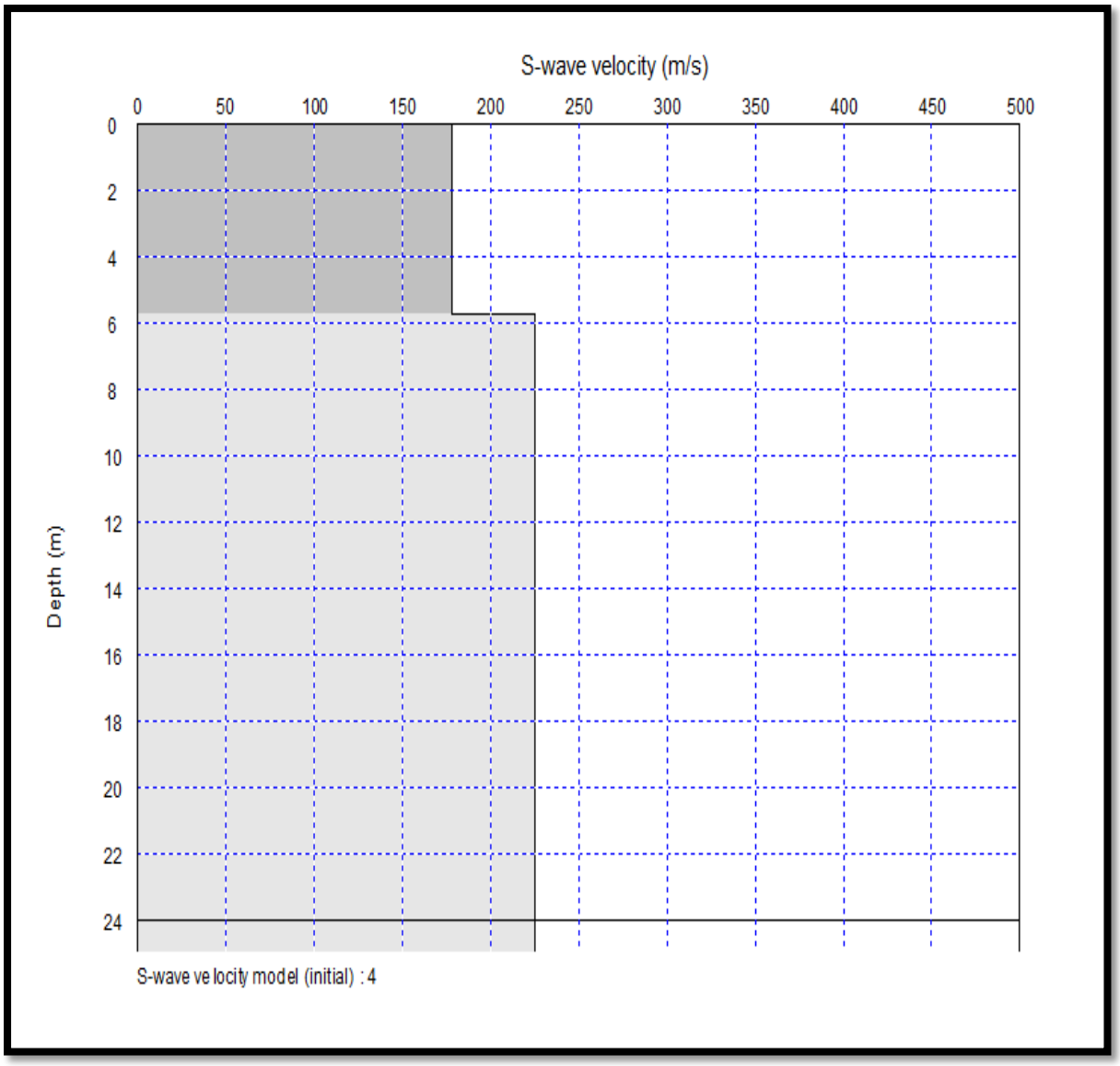

Fig. (4-12): Shows one-dimensional section of the shear velocity of the studied profile (fifth reading).

Also Fig. (4-12) show the relationship between shear velocity and depth. The value of the depth is (5.749) m and the value of the shear velocity is (177.38) m/sec. The soil is stiff soil.

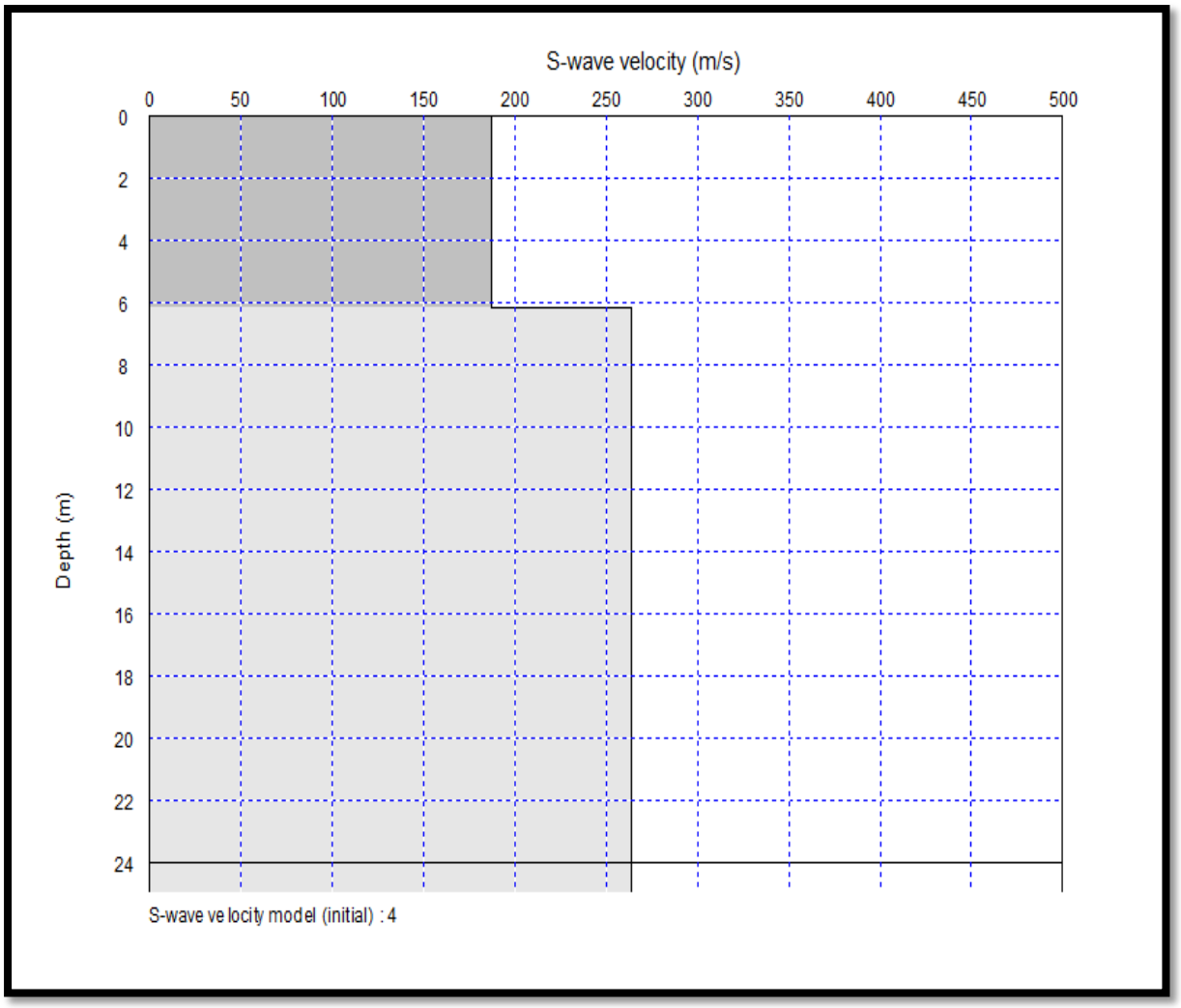

Fig. (4-13): shows one-dimensional section of the shear velocity of the studied profile(sixth reading).

In the Fig. (4-13) the value of the shear velocity is change and became 187.40 m/sec. Therefore, the value of the depth has changed for this reading (sixth reading) and became 6.181 m, so the soil is stiff soil.

These interpretations according to classify soil type according to estimated Vs, this classifation called NEHRP and IBC (Eker et al.,2012; ICC, 2006), Table (4-12).

Table (4-12): Classification of subsoil based on shear wave velocity as per NEHRP or IBC

Depth (m)	Vs (m/sec)	Type of soil
0-7	180>Vs>360	Stiff soil
7-8.9	360>Vs>760	Very dense soil, Soft rock
8.9-26.8	760>Vs>1500	Rock
26.8-30	Vs>1500	Hard rock

In this case, the second layer is the bed layer, which starts from a depth of 8.211 and above. As a result of these results, in order to establish the engineering structure, it must be done in two cases, either soil injection to a depth of 8 meters or stilts piles with a diameter of 80 cm.

The Surfer program is also used in this method in order to draw contour maps that show the distribution of shear waves velocity and variance, as well as the bearing capacity, the depth of the foundation and the thickness of the layer, and observing the extent of compatibility between each of them in the study area.

The Fig.(4-14a,b,c,d) represents a contour map obtained from the MASW profile in the study area, as it shows that the greatest shear wave velocity and bearing capacity is in the center of the study area, as it appears in the shape of lenses or layers separated by a horizontal distance in the contour map.

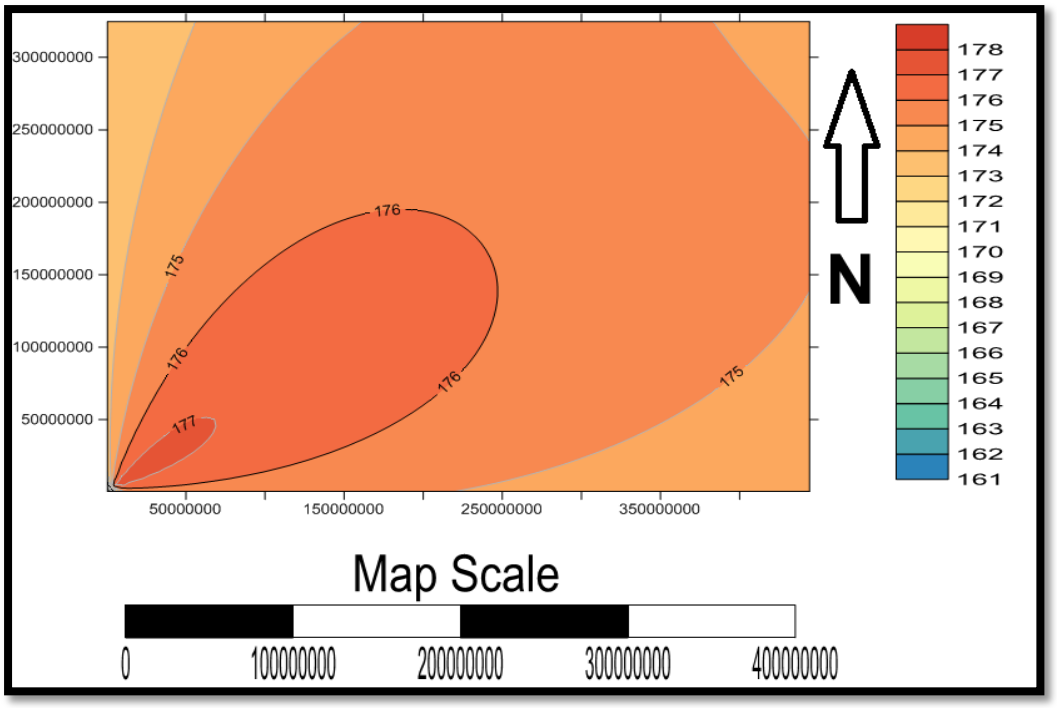

Fig. (4-14a): Shows contour map for distribution of shear waves velocity in study area for MASW profile.

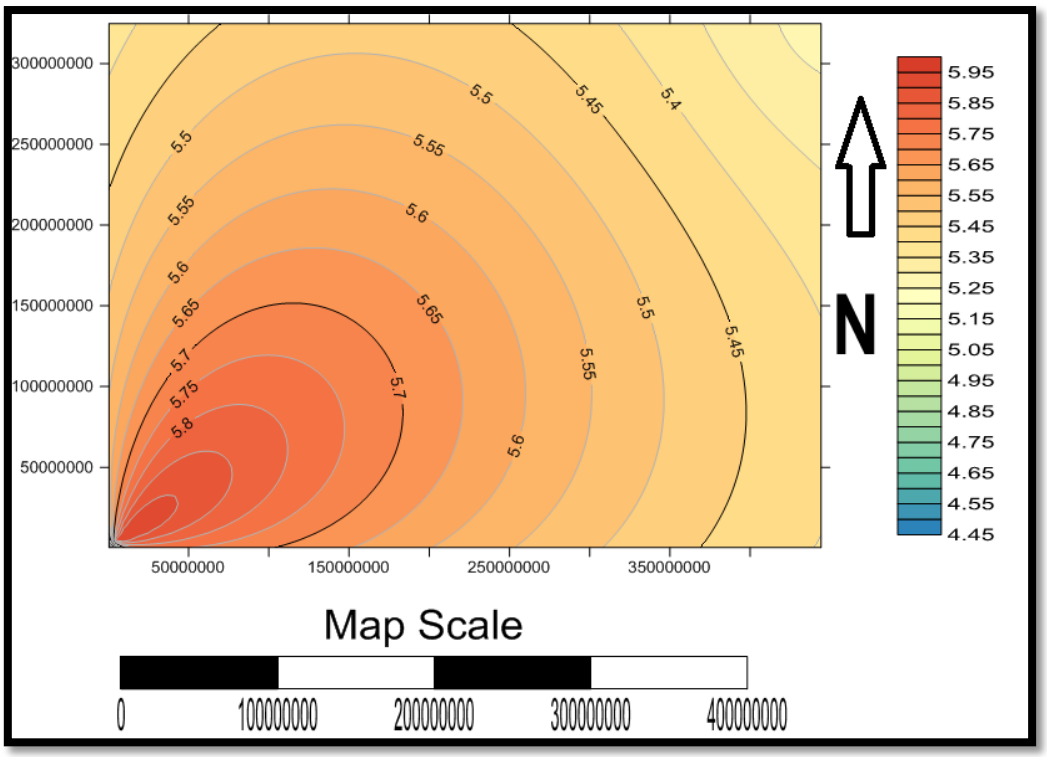

Fig. (4-14b): Shows contour map for distribution of bearing capacity in study area for MASW profile.

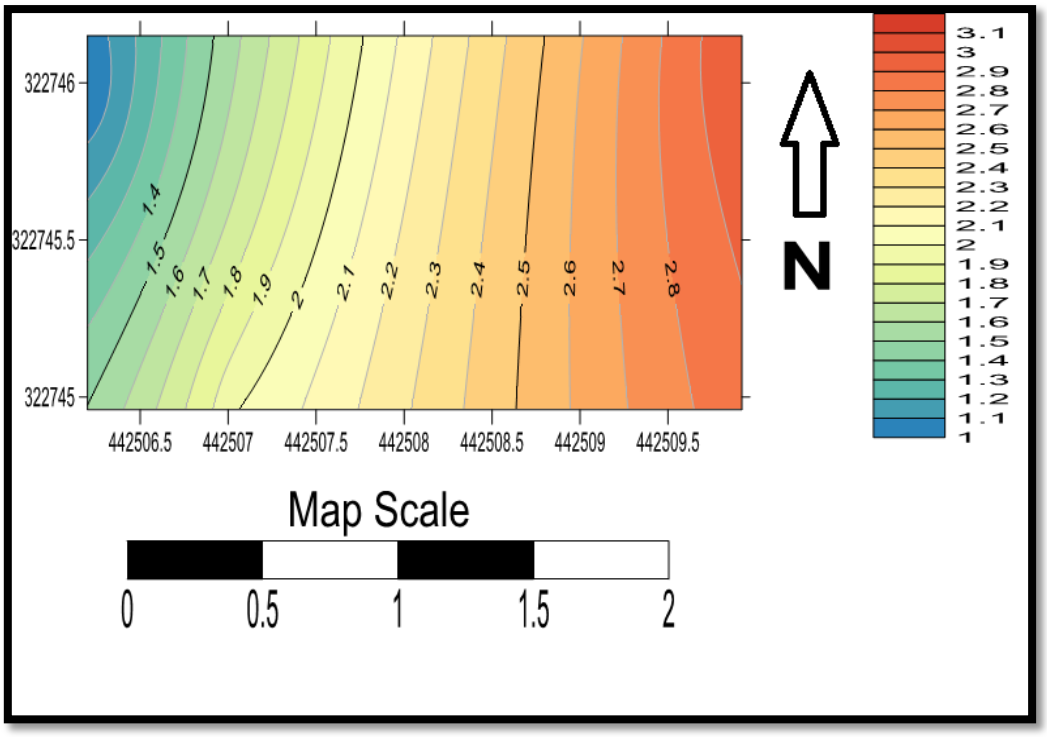

Fig. (4-14c): Shows contour map for distribution depth of foundation in study area for MASW profile.

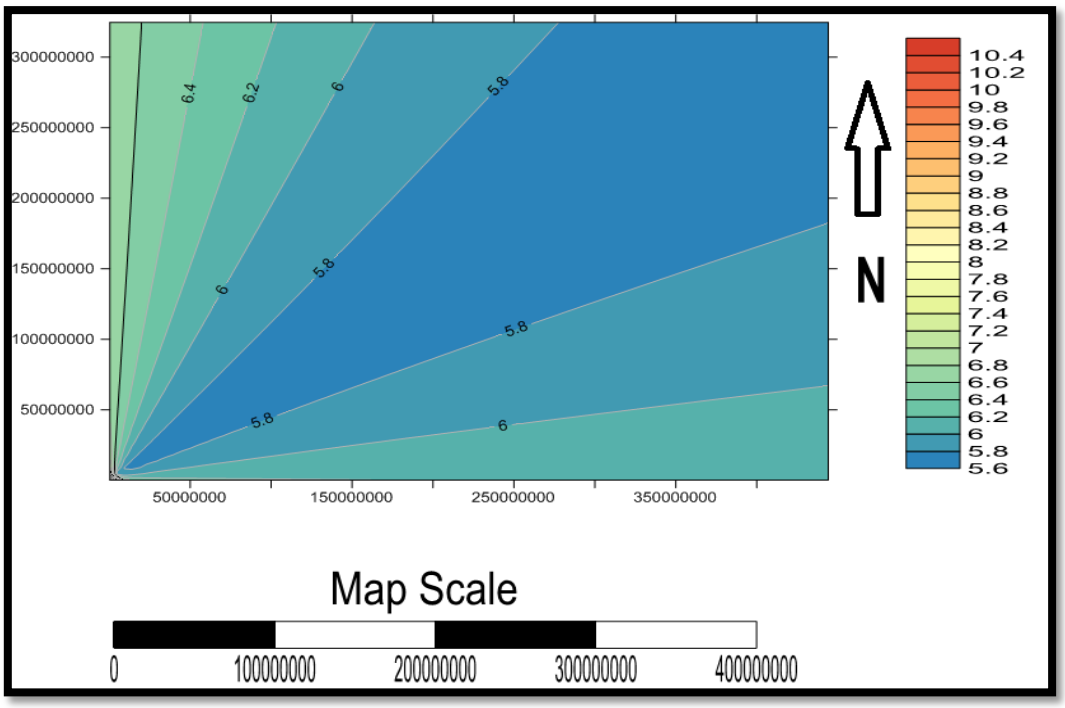

Fig. (4-14d): Shows contour map for distribution thickness in study area for MASW profile.

By using Excel software, the relationship between distance (m) and time (sec.) was plotted (graph) Fig(4-15a,b,c,d,e, and f). Through the graph, the number of layers, which are two layers, was clarified, and then the value of the velocity (m/sec) was calculated, which represents the distance over time (the law of slope according to the drawing), and then the value of the critical distance (X_c) is extracted from the end of the refraction of the first layer and the beginning of the second layer. By using the critical distance, the depth of the first layer is calculated using the equation (4-12) .

$$V_1 = \frac{X2-X1}{Y2-Y1} \quad \text{.....(4-10) (From drawing)}$$

$$V_2 = \frac{X2-X1}{Y2-Y1} \quad \text{.....(4-11) (From drawing)}$$

Where (V_1 is the velocity of the first layer, V_2 is the velocity of the second layer), (X_2, X_1 is the X axis from the drawing and representing the distance), (Y_2,Y_1 is the Y axis from the drawing and representing the time (T_2,T_1) alternately),

$$Z_1 = \frac{XC}{2}\sqrt{\frac{V2-V1}{V2+V1}} \quad \text{.....(4-12) (Sjögern, 1984)}$$

Where (Z1 is the depth of the first layer, X_C is cross-over distance).

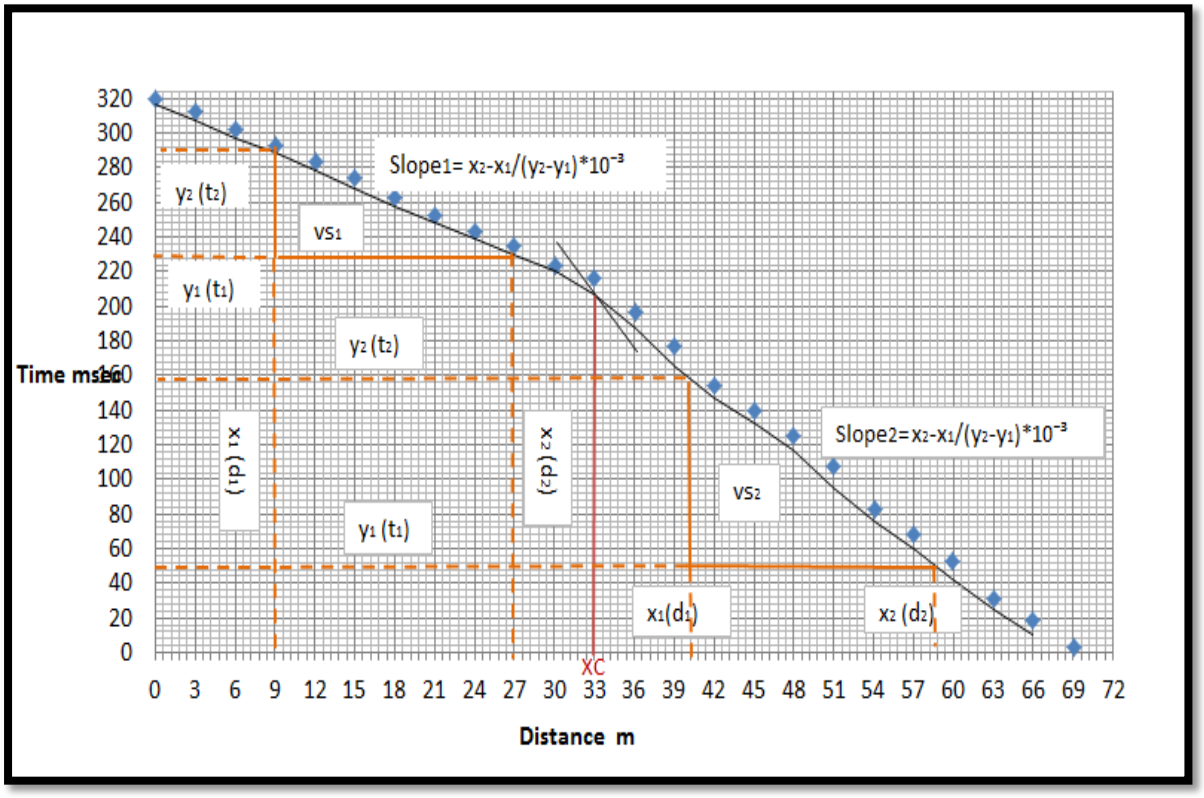

Fig. (4-15a): Shows the relationship between distance and time for the first reading (MASW profile).

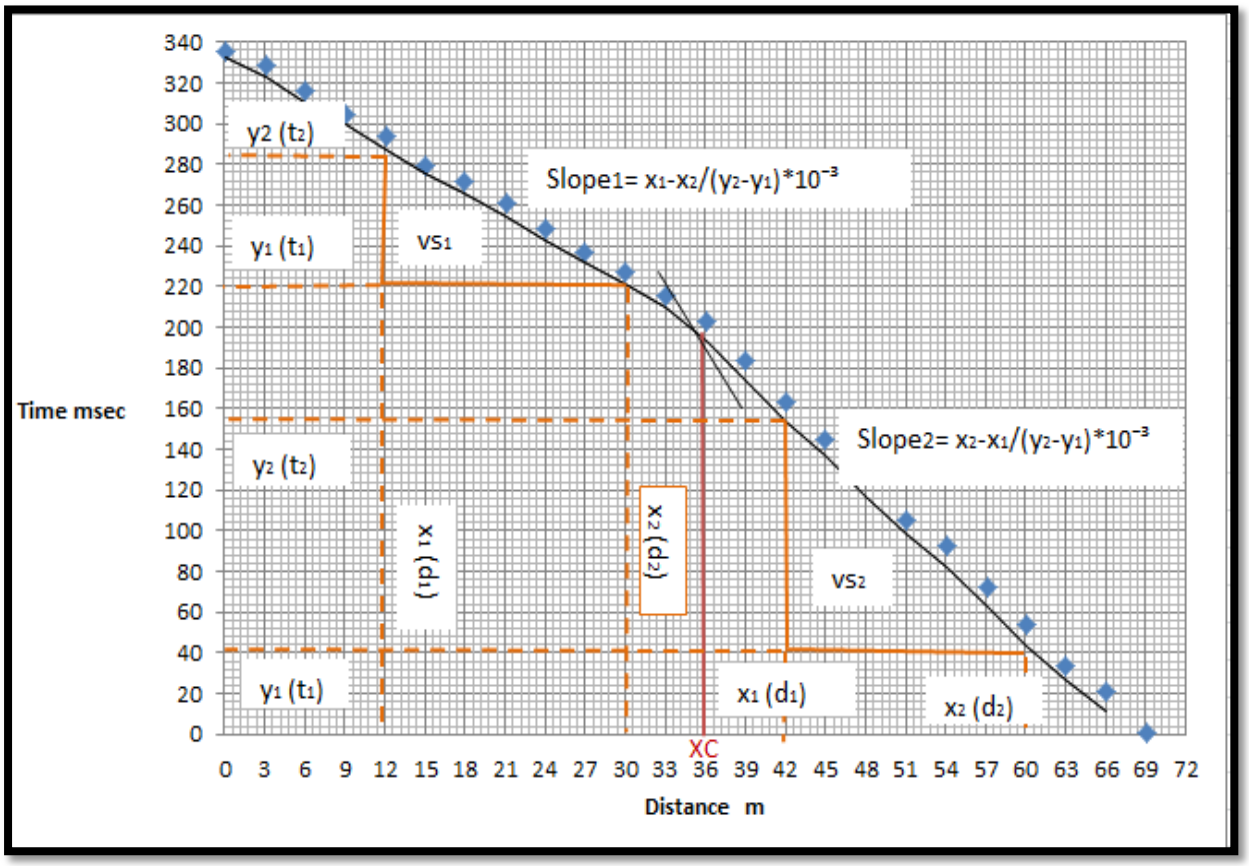

Fig. (4-15b): Shows the relationship between distance and time for the second reading (MASW profile).

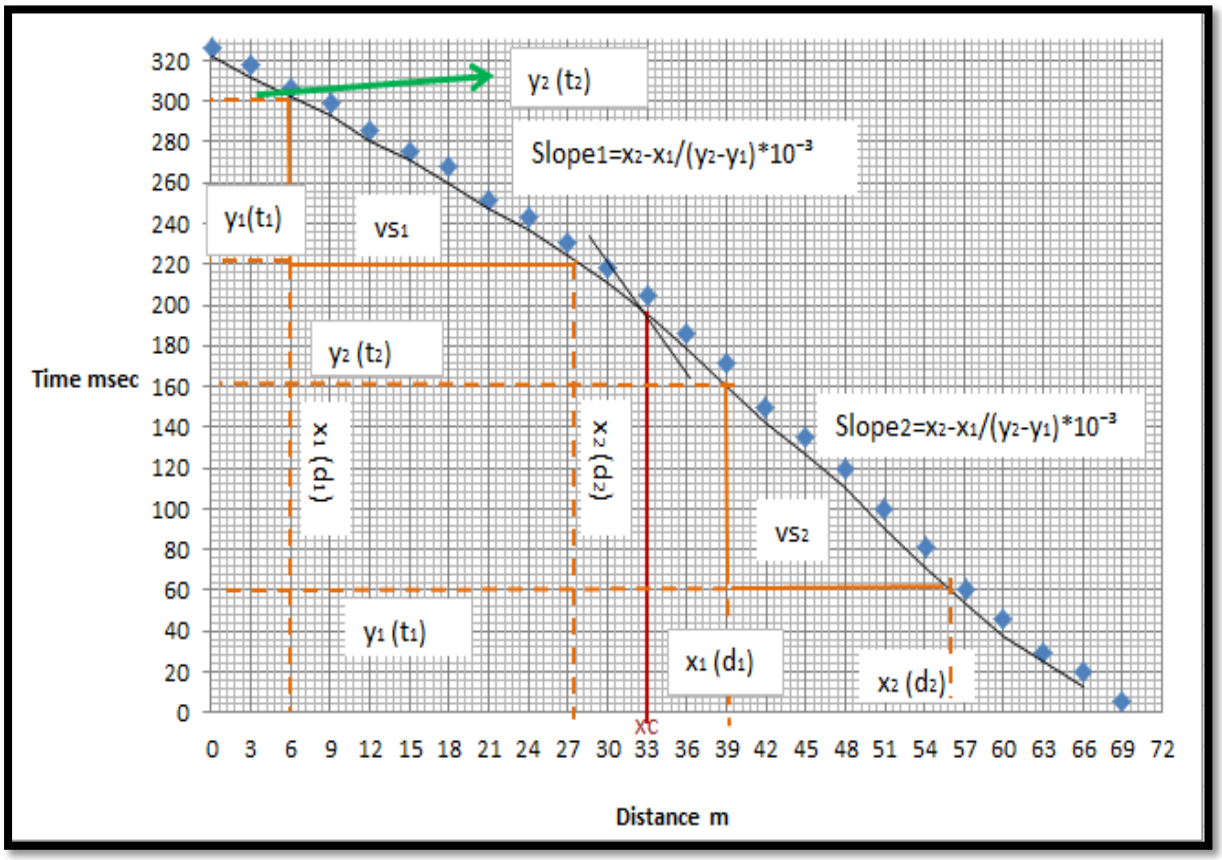

Fig. (4-15c): Shows the relationship between distance and time for the third reading (MASW profile).

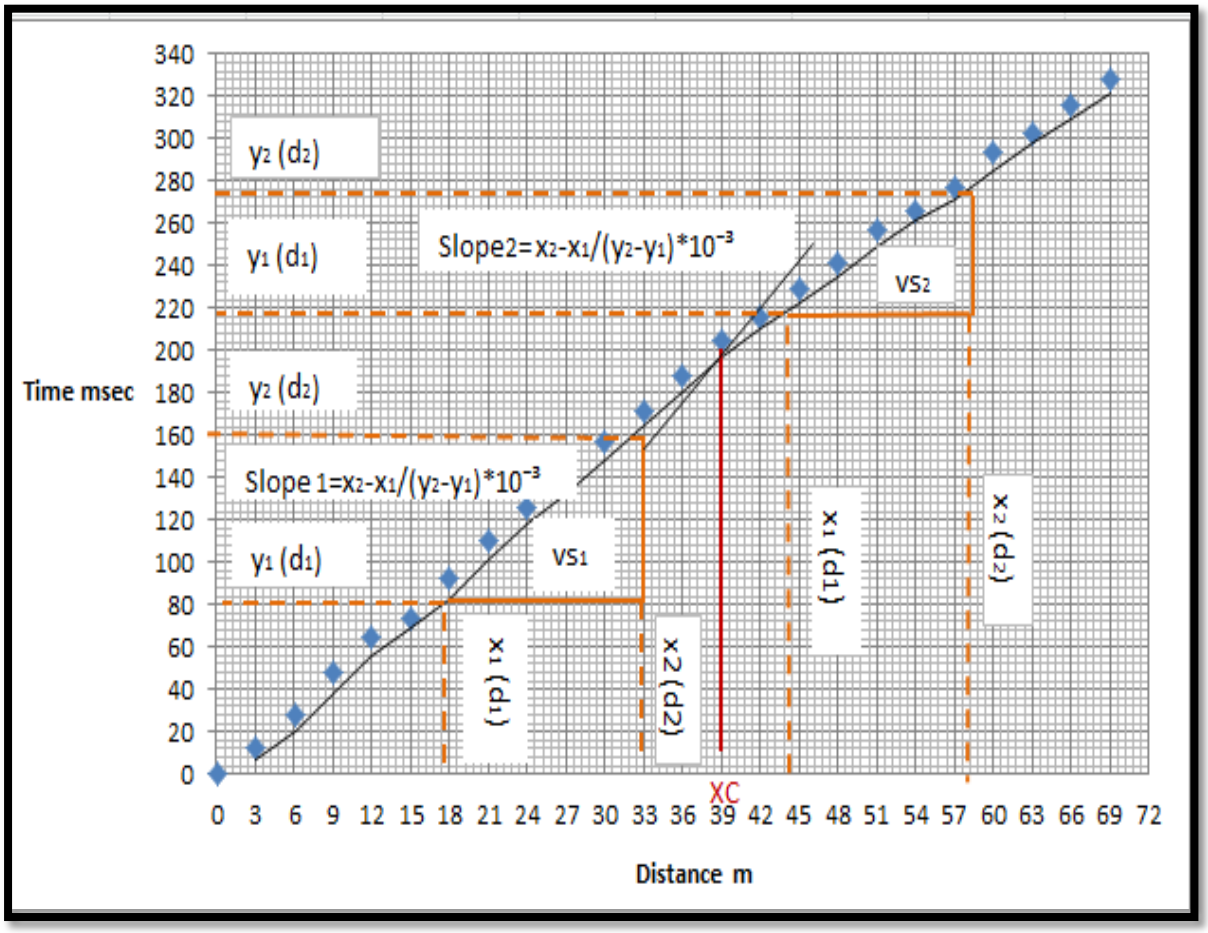

Fig. (4-15d): Shows the relationship between distance and time for the fourth reading (MASW profile).

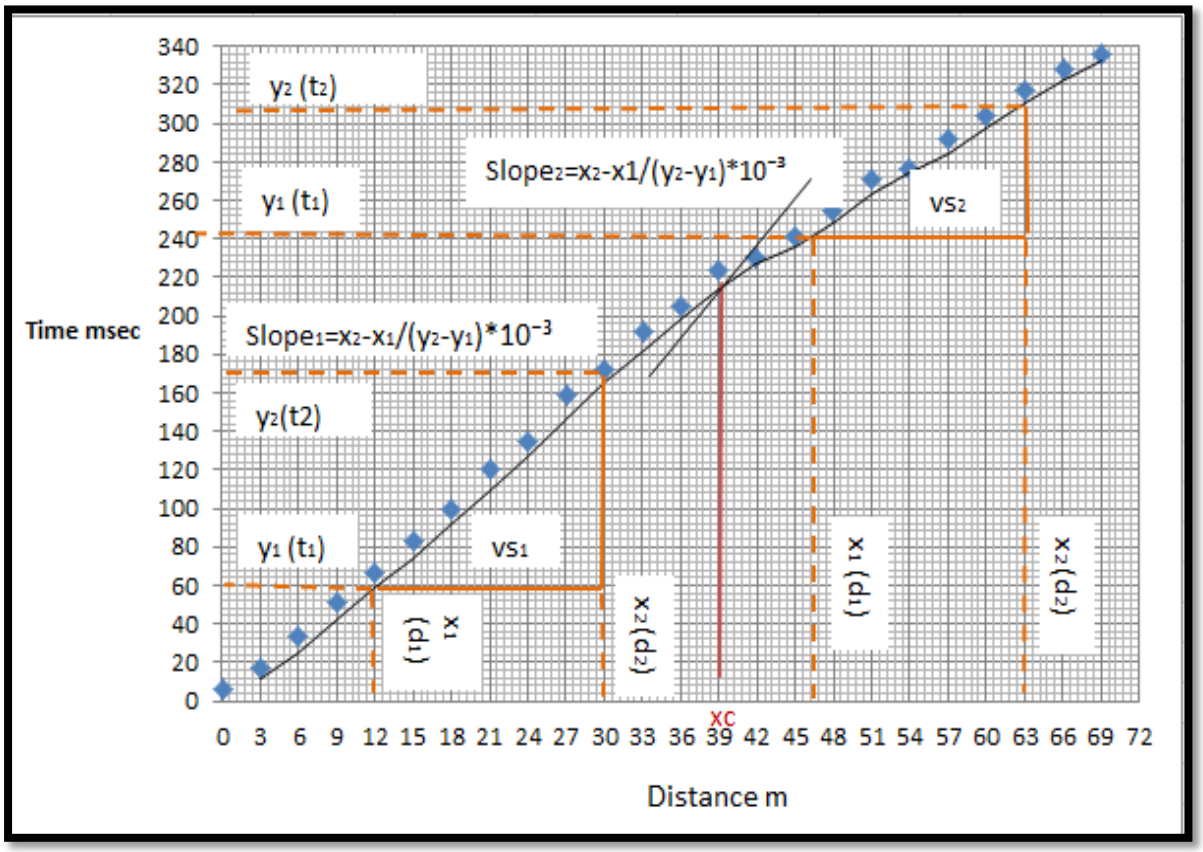

Fig. (4-15e): Shows the relationship between distance and time for the fifth reading (MASW profile).

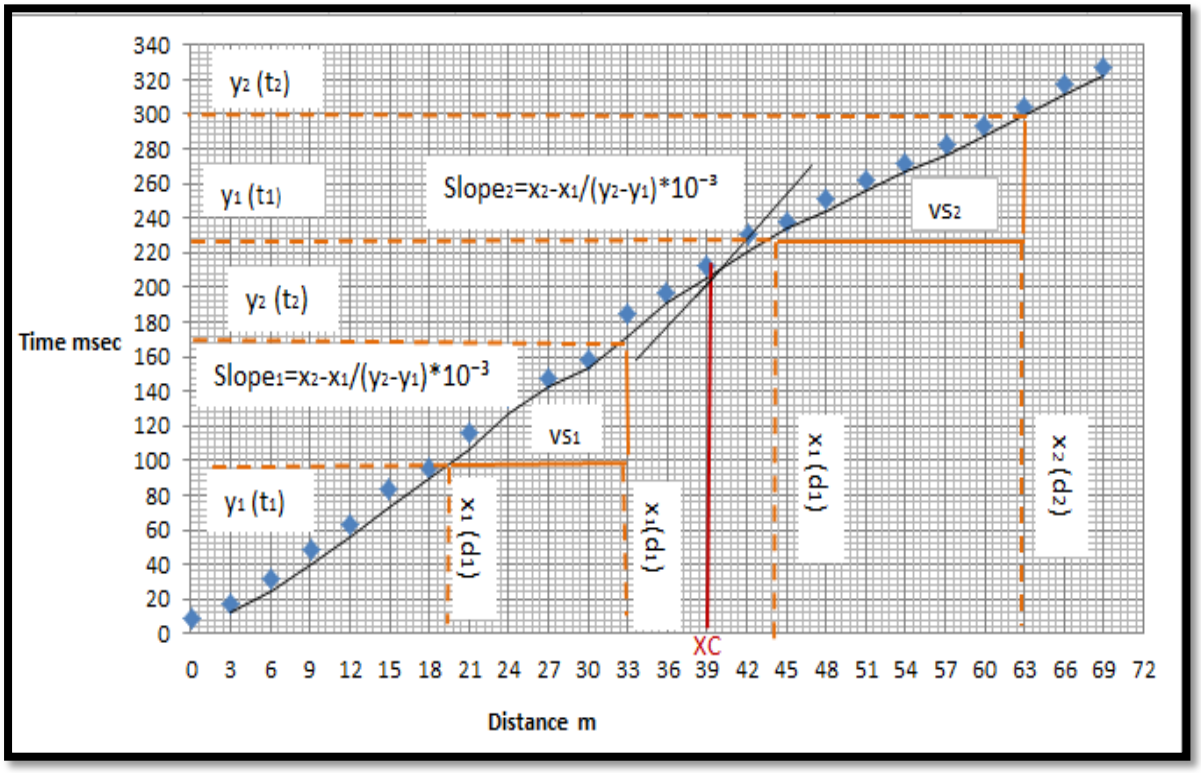

Fig. (4-15f): Shows the relationship between distance and time for the sixth reading (MASW profile).

The figures (4-15a,b,c,d,e, and f) show the relationship between the distance x that measured with meter unit and time t that measured with second unit. There are two layers in the study area. The value of the shear velocity for the first layer is 171.6 m/sec with thickness of 8.211 m and the value of the shear velocity for the second layer is 272.22 m/sec.

(4-11) Statistical relationships between Seismic Refraction Survey and the MASW method:

These relationships and comparisons is made between the two methods of refractive survey and MASW by means of the (Statistical Package for Social Sciences) (SPSS) program. The SPSS statistical analysis program is considered one of the most important statistical applications, and this program works within the Windows system, and the program consists of a set of menus as well as a set of tools that contribute to data analysis. The aim of this program is the analysis of all data related to the research. One of the most important terms of this program it is relationship between the variables and this mean correlation and degree of correlation https://www.maktabtk.com/blog/post/35/html.

When comparing the results and finding the correlation coefficient between the two methods (MASW and Refractive Survey), it is found that there is a positive relationship between the first shear velocities (first profile - first layer) in each of the two methods, Table (4-13), Fig.(4-16)

Table(4-13): The correlation between Vs1(first profile – first layer) for refractive survey and Vs1 (first layer) for MASW method.

Correlations			
		Vs1 (m/sec)	Vs1MASW (m/sec)
Vs1	Pearson Correlation	1	0.979
Vs1MASW	Pearson Correlation	0.979	1

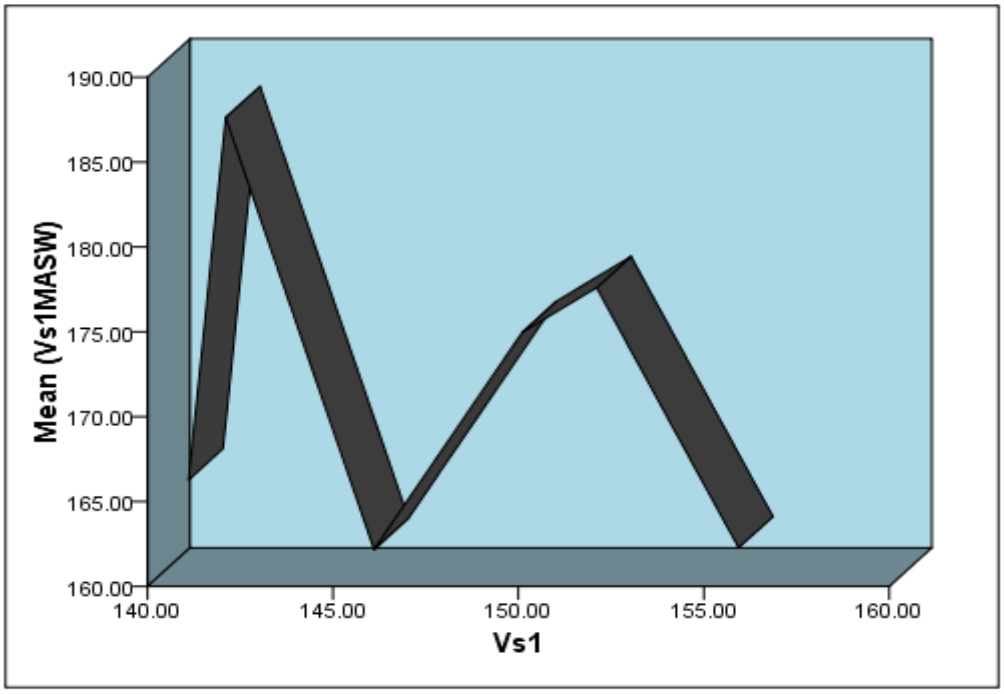

Fig.(4-16): Shows the relationship between Vs1(first profile-first layer) for refractive survey and Vs1(first layer) for MASW method.

Also the correlation coefficient between the second shear velocities (first profile – second layer) in each of the two methods has a positive relationship between them, Table (4-14), Fig.(4-17).

Table (4-14): The correlation between Vs2 (first profile - second layer) for refractive survey and Vs2(second layer) for MASW method.

Correlations			
		Vs2 (m/sec)	Vs2MASW (m/sec)
Vs2	Pearson Correlation	1	0.93
Vs2MASW	Pearson Correlation	0.93	1

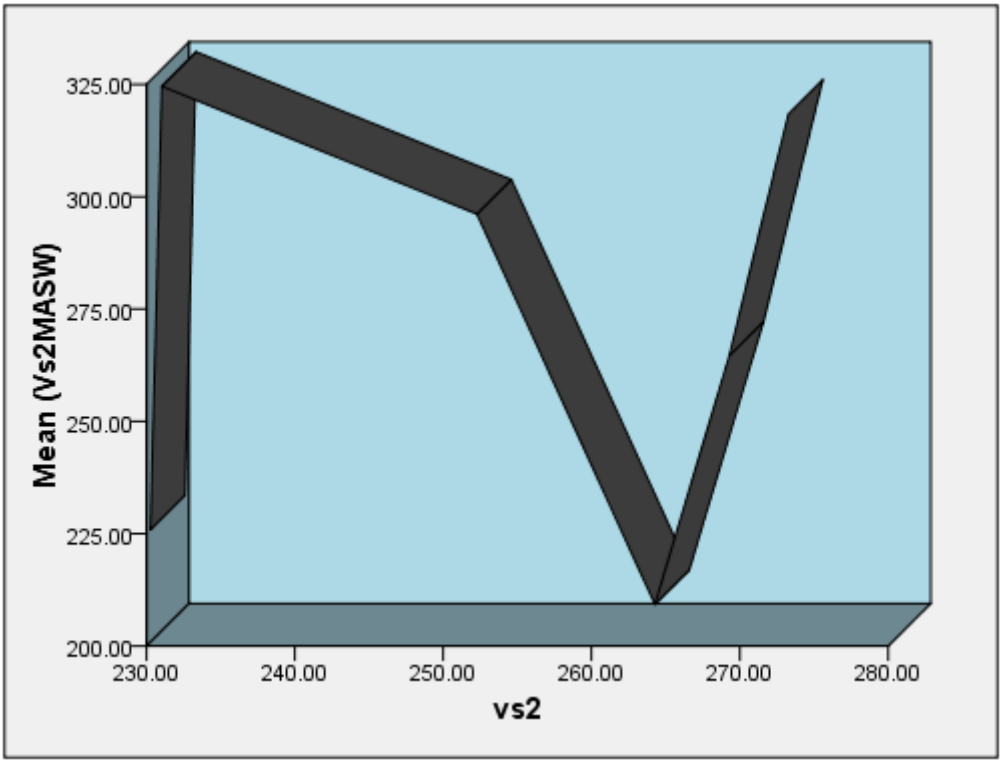

Fig.(4-17): Shows the relationship between Vs2(first profile- second layer) for refractive survey and Vs2(second layer) for MASW method.

And the correlation coefficient between the thickness of two methods is a strong positive relationship, Table (4-15), Fig.(4-18).

Table (4-15): The correlation between D_1 (Depth for first profile) for refractive survey and D_1 for MASW method.

Correlations			
		D1(m)	D1MASW(m)
D1	Pearson Correlation	1	0.956
D1MASW	Pearson Correlation	0.956	1

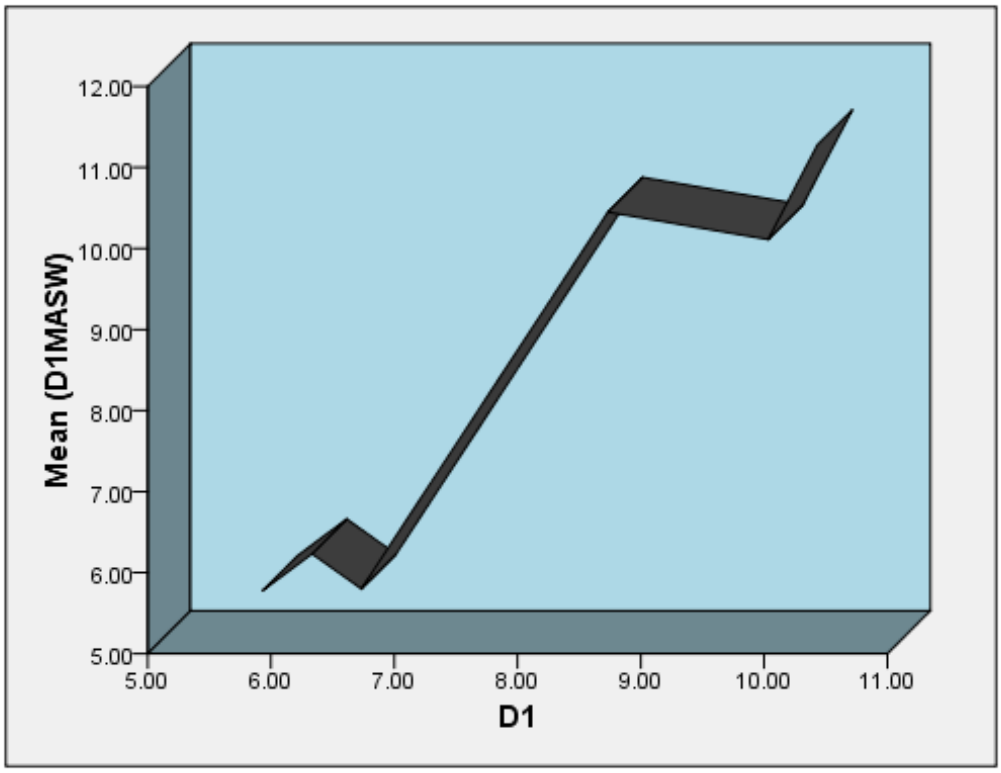

Fig.(4-18): Shows the relationship between D_1(Depth for first profile) for refractive survey and D_1 for MASW method.

For the first layer of the second profile and the MASW profile the correlation coefficient between Vs1 (for the refractive survey) and Vs1 (for MASW method) it is found that there is a strong positive relationship between of them, Table (4-16), Fig.(4-19).

Table(4-16): The correlation between Vs1(second profile – first layer) for refractive survey and Vs1(first layer) for MASW method.

Correlations			
		Vs1 (m/sec)	Vs1MASW (m/sec)
Vs1	Pearson Correlation	1	0.956
Vs1MASW	Pearson Correlation	0.956	1

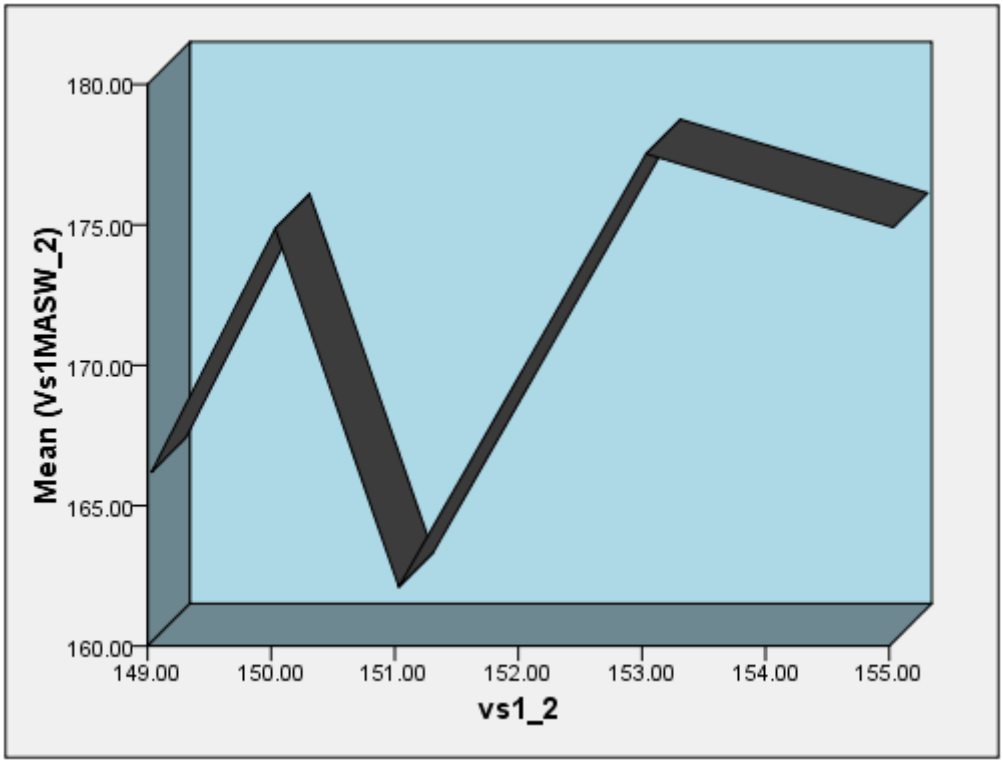

Fig.(4-19): Shows the relationship between Vs1(second profile - first layer) for refractive survey and Vs1(first layer) for MASW method.

The correlation coefficient for the same profiles (MASW and refractive survey) but for the second layer between (Vs_2 and Vs_2 MASW) it is found there is a positive relationship between them, Table (4-17), Fig. (4-20).

Table(4-17): The correlation between Vs2 (second profile- second layer) for refractive survey and Vs2(second layer) for MASW method.

Correlations			
		Vs2 (m/sec)	Vs2MASW (m/sec)
Vs2	Pearson Correlation	1	0.918
Vs2 MASW	Pearson Correlation	0.918	1

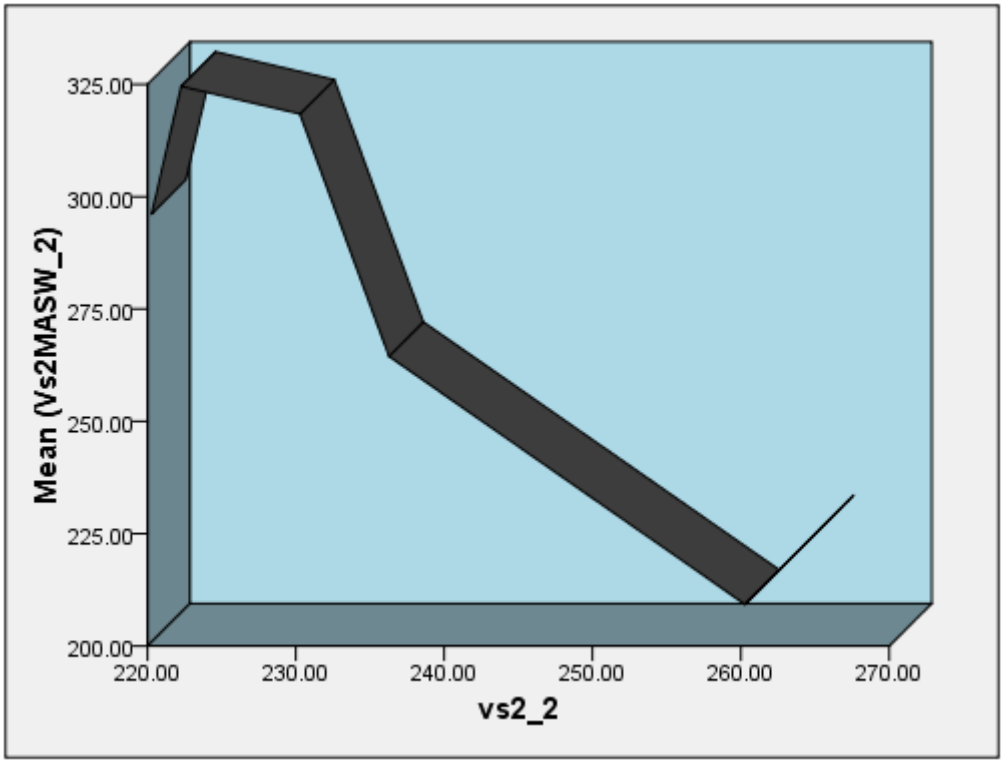

Fig.(4-20): Shows the relationship between Vs2(second profile - second layer) for refractive survey and Vs2(second layer) for MASW method.

And the correlation coefficient between the thickness of two methods is a strong positive relationship, Table(4-18), Fig.(4-21).

Table (4-18): The correlation between D_1 for refractive survey (second profile) and D_1 for MASW method.

Correlations			
		D_1(m)	D_1MASW(m)
D1	Pearson Correlation	1	0.996
D1MASW	Pearson Correlation	0.996	1

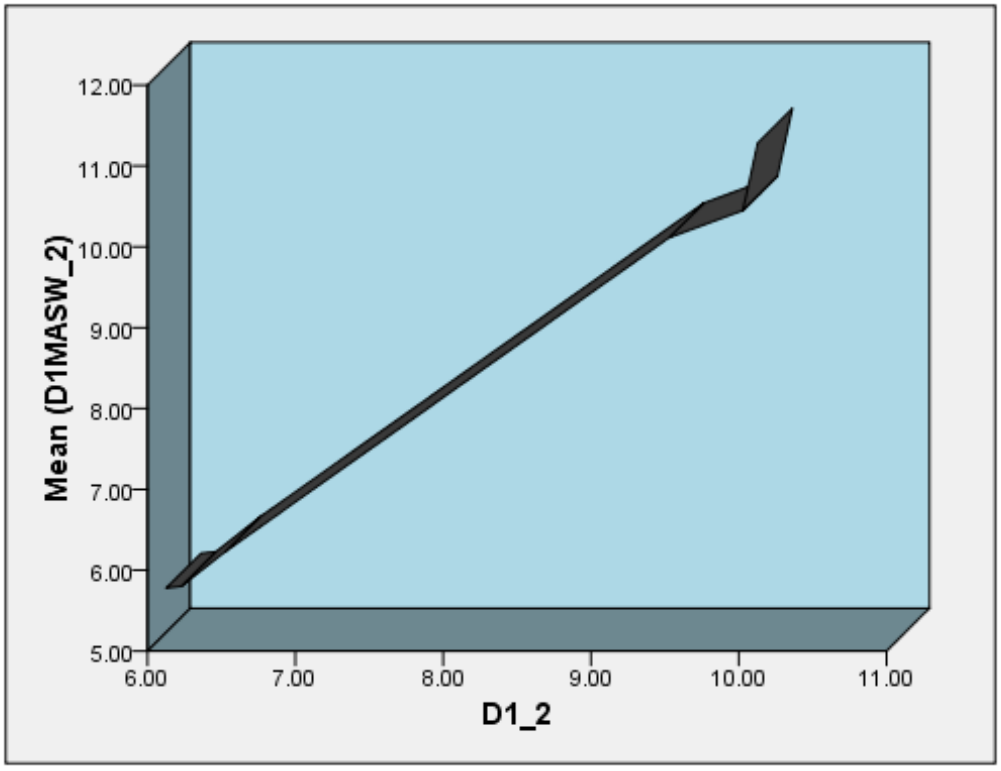

Fig.(4-21): Shows the relationship between D_1(Depth for second profile) for refractive survey and D_1 for MASW method.

Correlation coefficient equation between two methods (Refractive survey and MASW method) is :

$$r_{xy} = \frac{n\sum_{i=1}^{n} x_i\, y_i - \sum_{i=1}^{n} x_i \sum_{i=1}^{n} y_i}{\sqrt{\left[n\sum_{i=1}^{n} {x_i}^2 - \left(\sum_{i=1}^{n} x_i\right)^2\right]\left[n\sum_{i=1}^{n} {y_i}^2 - \left(\sum_{i=1}^{n} y_i\right)^2\right]}} \quad \ldots\ldots\ldots (4\text{-}13)$$

Where:

r_{xy} : Correlation coefficient (Pearson Correlation)

n : number of profiles

x , y : variables in profiles

And the results of correlation coefficient are illustrate in the Table (4-19) , Fig. (4-22):

Table (4-19): Shows Correlation table by percentage for refractive survey and MASW method according to (SPSS) program.

Sample_1	Sample_2	Correlation	Correlation percentages
Vs_1	Vs_1MASW	0.979	97.9%
Vs_2	Vs_2MASW	0.93	93%
D_1	D_1MASW	0.956	95.6%
Vs_1_2	Vs_1MASW_2	0.956	95.6%
Vs_2_2	Vs_2MASW_2	0.918	91.8%
D_1_2	D_1MASW_2	0.996	99.6%

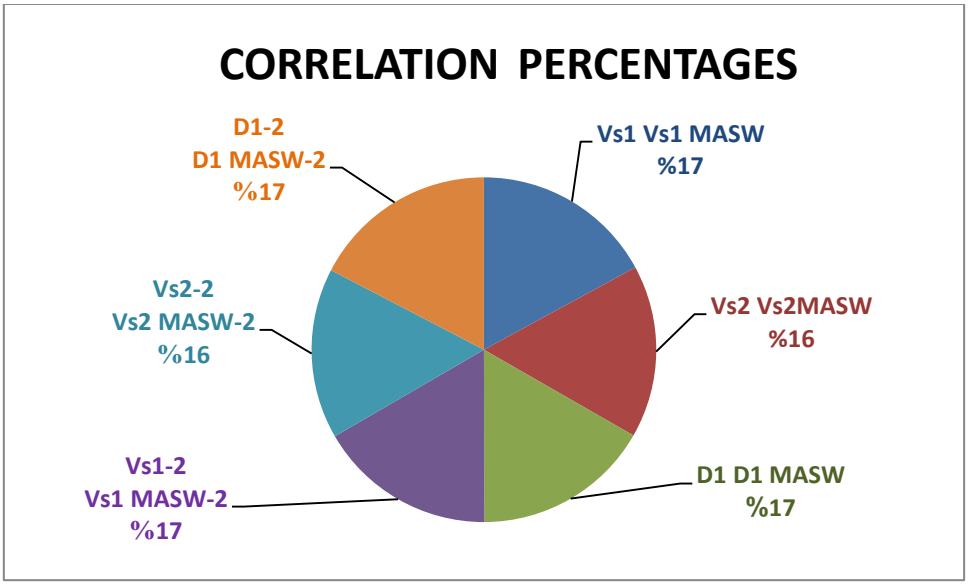

Fig. (4-22): Shows the correlation percentage for Refractive survey and MASW method.

References

المصادر العربية

١. أسحق، عبود سليمان أحمد (١٩٩٨): تحديد التراكيب الجيولوجية الضحلة وعمق المياه الجوفية في منطقة الحويجة بأستخدام الطريقة الزلزالية الأنكسارية. رسالة ماجستير، كلية العلوم - جامعة بغداد.

٢. الجريسي، بشار عزيز محمود (١٩٩٢): دراسة زلزالية أنكسارية لبعض مناطق سد صدام . رسالة ماجستير ، كلية العلوم، جامعة الموصل.

٣. الخفاجي، عمار محمد جاسم (٢٠٠٤أ): أستخدام الطرق الزلزالية في التحري عن أماكن الضعف والتقييم الجيوتكنيكي لتربة أسس مشروع ماء الحسين في كربلاء، رسالة ماجستير، كلية العلوم، جامعة بغداد.

٤. خورشيد، سلمان زين العابدين (١٩٨٦): دراسة الموجات الطولية والمستعرضة في الطبقات الرسوبية. رسالة ماجستير، كلية العلوم- جامعة بغداد.

٥. الربيعي، أسعد سلمان قنبر (١٩٩٥): الأستخدام الهندسي للطريقة الزلزالية الأنكسارية في موقع محطة كهربائية. رسالة ماجستير، كليه العلوم – جامعة بغداد (غير منشورة).

٦. الشجيري، صباح جاسم دحبوش (٢٠٠٨): د راسة جيوفيزيائية وجيوتكنيكية للتربة لموقعين في مدينة بغداد .رسالة ماجستير، كلية العلوم، جامعة الموصل ١١٧ صفحة.

٧. المولى، سلمان زين العابدين (١٩٩٦): أستخدام الطرق الجيوفيزيائية في تقييم الخواص الجيوتكنيكية لموقع سد العظيم. أطروحة دكتوراه، كلية العلوم - جامعة بغداد.

٨. الهيتي، أحمد جدوع رضا (٢٠١٤): مسح زلزالي أنكساري لموقع مشروع المستشفى التعليمي في جامعة الموصل. رسالة ماجستير غير منشورة ، كلية العلوم - جامعة الموصل ، ١٢٦ صفحة.

References:

1. Abd Al-Rahman, M. (1989). “Evaluation of the Kinetic Elastic Moduli of the Surface Materials and Application to Engineering Geologic Maps at Maba-Risabah Area (Dhamar Province), Northern Yemen”, Egypt. Journal of Geology. Vol. 33, No. 1–2, pp. 229–250..
2. Abd El-Aal, A. K. and Mohamed, A. A., (2009), Near-surface seismic refraction applied to exploring subsurface clay layer at a new mining area in southeast Cairo, Egypt: Arab J Geosci, Vol.3, No.2, pp.105-112.
3. Abd El-Rahman, M. (1991). “The Potential of Absorption Coefficient and Seismic Quality Factor in Delineating Less Sound Foundation Materials in Jabal Shib Az Sahara Area, Northwest of Sanaa, Yemen Arab Republic”, Egypt, M.E.R.C. Earth Sciences ,Vol. 5. Ain Shams University, pp. 181–187.
4. Abdel- Rahman, M.; Helal, A.N.M.A.; Mohamed, H.C. and Al-Malqi, I. (1994).Exploration Seismic for Site evaluation of the new city of El-Minya, Egypt- E.G.S. proc. of the 12th Ann. Meet. 59-74p.
5. ABEM Instrument (2009), Reference manual for ABEM Terraloc MK6. Sundbyberg , Sweden.
6. Aki, K. & Richards, P. G. (2002). Quantitative Seismology. (Second edition). Sausalito, CA: University Science Books.
7. Al-Awsi, M., Khorshid, S.Z. and AL-Banna, A., (2014): Geotechnical Evaluation to the Soil of Tikrit University Using Seismic Refraction Method, Diyala Journal Pure Sciences,10, 17 p.
8. Al-Bahadily, Haydar, A. (1997).The Use of Seismic Velocity Data for the Study of Stratigraphic Variation at Jambur Area. Unpublished M.Sc. Thesis, Collage of Science, Baghdad University,136p.

9. Al-Jiburi, H. K and Al-Basrawi, N. H., (2008). Hydrogeology-geology of Iraqi southern desert: Iraqi bull. geol. min. special issue, 2009. 77-91P.

10. Al-Kadhimi, J., Sissakian, V.K., Fattah, A.S. and Deikran, D.B., (1996). Tectonic Map of Iraq, scale 1: 1000 000, 2nd. ed., GEOSURV, Baghdad, Iraq.

11. Allaby, A. and M. Allaby,(1999). "cross-over distance." A Dictionary of Earth Sciences.

12. Al-Shimaree, A., Al-Khersan, E.H., and Al-Khalidy. (2012). Geophysical study for both hills-2 and karbala-2 gas power plants/ central Iraq with the assistance of the engineering information: international journal of 701 emerging technology and advanced engineering, ISSN 2250-2459, ISO 9001: Certified Journal, Vol 4.

13. Anbazhagan P. and Sitharam, T. G., (2008) Site Characterization and Site Response Studies Using Shear Wave Velocity, Journal of Seismology and Earthquake Engineering, Vol. 10, No.2, pp.53-67.

14. Barton, N. (2007). Rock quality, seismic velocity, attenuation and anisotropy. Taylor & Francis Group, London, UK.729p.

15. Barton, P.J., (1986), The relationship between seismic velocity and density in the continental crust − a useful constraint, Geophysics. J. Roy. astron. Soc. 87, 195-208.

16. Bessason, B. & Erlingsson, S. (2011). Shear wave velocity in surface sediments. Jökull 61, 51-64.

17. Birch, F. (1966). "Handbook of Physical Constants", Geological a Society of America. Memoir. 97, 613p.

18. Bowles, J.E. (1984): Physical and geotechnical properties of Soils. McGraw-Hill International Book Co., London, 578p.

19. Bowles, J. E.(1988). Foundation Analysis and Design.4th edition. a McGraw- Hill Book company.1004p.

20. Bowles, J. E. (1996). Foundation analysis and design. New York: McGraw-Hill.

21. Buday, T., (1980), The regional geology of Iraq, Stratigraphy Paleogeography, Dar Al-Kutub pub. House, Mosul, Iraq.

22. Buday, T. and Jassim, S.Z., (1984). Tectonic Map of Iraq, scale 1: 1000 000. GEOSURV, Baghdad Iraq.

23. Buday, T., and Jassim, S.Z., (1987). The Regional Geology of Iraq.Vol.2. Tectonism, Magmatism and Metamorphism. In: M.J., Abbas and I.I., Kassab (Eds.) GEOSURV, Baghdad, 352pp.

24. Clayton, C.R.I., Matthews, M.C. and Simons, N.E. (1995) Site Investigation. 2nd edition. London: Blackwell Science Ltd.

25. Dal Moro, G., Pipan, M., Forte, E., Finetti, I., (2003), Determination of Rayleigh wave dispersion curves for near surface applications in unconsolidated sediments, Expanded Abstract, Society of Exploration Geophysicists, pp.1247-1250.

26. Davies, A. and Schultheis, P.J., (1980): Seismic Signal Processing in Engineering Site Investigation a case history. Ground engineering.

27. Dobrin, M. B. (1976). Introduction to Geophysical Prospecting. McGraw Hill Book Co., 3rd edition. New York, 630p.

28. Dobrin, M.B. Savit, C.H, (1988): Introduction To Geophysical a Prospecting .4th Ed., McGraw Hill ,New York 867 p.

29. Evrett, M. E. (2013): Near-Surface Applied Geophysics. Cambridge: Cambridge University Press.

30. Foti, S. (2000): Multistation Methods for Geotechnical Characterization using Surface Waves. (Doctoral dissertation, Politecnico di Torino, Turin, Italy). Retrieved from http://porto.polito.it/2497212/1/S Foti PhDdiss. pdf

31. Foti S., Sambuelli L., Socco L.V., Strobbia C., (2003): Experiments of joint acquisition of seismic Refraction and surface wave data, near surface geophysics, pp.119-129 .

32. Foti, S., Parolai, S., Albarello, D. and Picozzi, M. (2011): Application of Surface Wave Methods for Seismic Site Characterization. Surveys in Geophysics, Vol.32, No.6, pp.777-825.

33. Fouad, S.F., (2010): " TECTONIC AND STRUCTURAL EVOLUTION OF THE MESOPOTAMIA FOREDEEP, IRAQ. Geo. Min., Special Issue. No. 2, p. 41 – 53.

34. Gadallah, M., R and Fisher, R.(2009). Exploration Geophysics. Springer-Verlag Berlin Heidelberg, 262p.

35. Gardner, G.H., Gardner, I.W., and A.R., Gregory,(1974), Formation Velocity and Density – The Diagnostic Basis for Stratigraphic Traps, Geophysics, Vol.39, pp. 770-780.

36. Gassman, F. (1973): Seismische Prospektion. Birkhaeuser Verlag, Stuttgart, 417p.

37. Gedge, M. & Hill, M. (2012): Acoustofluidics 17: Theory and applications of surface acoustic wave devices for particle manipulation. Lab Chip, 12 (17), 2998-3007.

38. George, N. J., Akpan, A.E., George, A. M., Obot, I. B.(2010): Determination of elastic properties of the overburden materials in Parts of Akamkpa, southeastern Nigeria using seismic Refraction Studies, Archives of Physics Research, 2010, Vol.1 No.2,pp.58-71

39. Gercek. H. (2006): Poisson's ratio values for rocks. International Journal of Rock Mechanics and Mining Sciences; Elsevier; Vol 44.(1). P 1-13.

40. Gerkens. J.C., (1987): Foundation of exploration geophysics. First edition Elsevier. 667 p.

41. Green, R., (1974), The seismic refraction method - a review. Geoexploration, 12: 259-284.

42. Haeni, F. P. (1986): Application of seismic Refraction methods in groundwater modeling studies in New England. Geophysics, vol. 51, No.2, pp.236-249

43. Hagedoorn, J.G., (1959): "The Plus-Minus Method Of Interpreting Seismic Refraction Section" , Geophysical Prospecting ,Vol.7 ,pp. 158-182.

44. Hasan, A. S., (2011): A contribution to the geotechnical properties of foundation soils for Kerbala and Baiji engineering construction sites. University of Baghdad.10-17PP

45. http://www.hinageo.en.alibaba.com

46. https://www.maktabtk.com/blog/post/35/html

47. http://www.masw.com/index.html

48. Iraqi meteorological organization., (2015): Climatic data for Al-Hilla station, for period from (1984-2014) (un published internal report).

49. Jassim, S.Z., and Goff, J.C., (2006). Geology of Iraq. Dolin, Prague and Moravian Museum, Brno. 341pp

50. Kaldal, L. S. (2007): Yfirborðsmælingar og ysjunarhætta. (Master's thesis). University of Iceland, Reykjavík.

51. Kearey, P., Brooks, M. and Hill, I. (2002): An introduction to Geophysical Exploration. 3rd edition, Blackwell Science Ltd, UK, 261p.

52. Khalil, M. H., Hanafy, S.M., (2008): Engineering application of a seismic refraction method: A field example at Wadi Wardan, Northeast Gulf of Suez, Egypt ,Journal of Applied Geophysics ,Vol.65, pp.132-141

53. Kilty, T.K., Norris, R., Mc Lamore, W.R.,Hennon,K.and Evge, K., (1986): Seismic Refraction at Horse Mesa Dam. An application of the generalized reciprocal method. Geophysics Vol.51, No.2,pp. 266- 275.

54. Lay, T and Wallace, T,C. (1995). Modern global seismology. Academic press, 521p.

55. Long,M. and Donohue,S.(2007): In situ shear wave velocity from multichannel analysis of surface waves (MASW) tests at eight Norwegian research sites, Canadian Geotechnical Journal, Vol.44,No.5, pp. 533-544.

56. Luna, R. & Jadi, H. (2000): Determination of Dynamic Soil Properties Using Geophysical Methods. Preceedings of the First International Conference on the Application of Geophysical and NDT Methodologies to Transportation Facilities and Infrastructure, St. Louis, December 2000.

57. Mashkori, M., and Al-Naimi, S., (1993): Geotechnical assessment of the site Qaqaa facility engineering hydrogeo study: Geoserv library, report 2176, Baghdad. (In Arabic).

58. Mota,L.,(1954): "Determination of Dip and Depth of Geological Layer By The Seismic Refraction Method", Geophysics ,Vol.19,pp.242-254.

59. Nafe ،J.E .and Drake, C.L. (1957): Variation with depth in shallow and deep water marine sediments of porosity،density and the velocities of compressional and shear waves. Geophysics ,Vol. 22, p.523-552. doi:10.1190/1.1438386

60. NEHRP and International Building Code(IBC 2000).

61. Ólafsdóttir, E. Á., (2014): Multichannel Analysis of Surface Waves Methods for dispersion analysis of surface wave data: University of Iceland.17P.

62. Palmer, (1981): An Introduction to the generalize reciprocal method of seismic refraction interpretation ,Geophysics ,Vol.46 , No. 11 ,pp. 1508-1518.

63. Parasnis, D. S., (1972): Principles of applied geophysics: 2nded, London, Chapman and Hall LTD. 214P.

64. Park, C. B., Miller, R. D. & Xia, J. (1997): Summary report on surface-wave project at Kansas Geological Survey (KGS). [Open-file Report]. Lawrence, KS: Kansas Geological Survey.

65. Park, C. B., Miller, R. D. & Xia, J. (1998): Imaging dispersion curves of surface waves on multichannel record. 68th Annual International Meeting Society of Exploration Geophysicists, Expanded Abstracts, 1377-1380.

66. Park, C. B., Miller, R. D. & Xia, J. (2001): Offset and resolution of dispersion curve in multichannel analysis of surface waves (MASW). Proceedings of the Symposium on the Application of Geophysics to Engineering and Environmental Problems (SAGEEP 2001), Denver, Colorado, SSM-4.

67. Park, C. B., Miller, R. D., Xia, J. & Ivanov, J. (2007): Multichannel analysis of surface waves (MASW) - active and passive methods. The Leading Edge, 26 (1), 60-64.

68. Park, C.B.Xia, J., Miller, R.D., and, (1999): Estimation of near-surface shear-wave velocity by inversion of Rayleigh waves: Geophysics, Vol. 64, No. 3, pp.691-700.

69. Rao, K.S. , Gupta,K.K. , Rathod ,G.W., Trivedi, S.S., (2009): Integrating Geophysical Studies With Engineering Parameters For Seismic Microzonation, Indian Geothechnical Society" (IGS), pp.52-56.

70. Redpath, B.B., (1973): Seismic refraction exploration for engineering site investigations, Technical Report E-73-4, U.S. Army Engineering Waterways Experiment Station Explosive Excavation Research Laboratory, Livermore, California.

71. Report of the Imam Hussainiya shrine for site Al-saidh Ruqayya Hospital Building project (2021).

72. Roma V. (2001): Soil Properties and Site Characterization by means of Rayleigh Waves. Ph.D. Dissertation, Politecnico di Torino (Italy).

73. Shaker, A. M., (2012): Geophysical and Geotechnical Study of a Proposed Tunnel Site at Al-Najaf City, Southern Iraq., Unpublished Ph.D. thesis, Collage of Science, Baghdad University, 108 pp.

74. Sharma, P.V., (1986): "Geophysical Method In Geology '",2nd Edition Elsevier, New York , 428 pp.

75. Sharma P.V., (1997): Environmental and Engineering Geophysics, Cambridge University Press, 475 pp.

76. Sheriff, R.E. and Geldart, L.P. (1986). "Exploration Seismology", Cambridge Univ. Press, Cambridge, pp. 316.

77. Sigbjörnsson, R.(2007): Continuum Mechanics. Lecture notes. Reykjavík: University of Iceland.

78. Sjogren, B. (1984): Shallow Refraction seismic. Chapman and Hall, London, 270pp

79. Socco L.V., Boiero D., Foti S., Piatti C.,(2010): Advances in surface wave and body-wave integration, In: Advances in near-surface seismology and ground-penetrating radar, Richard D. Miller, John H. Bradford, and Klaus Holliger, SEG (USA), , Vol. 15, pp. 55 – 73

80. Subramanian, N. (2008). Design of steel structures. New Delhi: Oxford University Press.

81. Tatham, R.H. (1982): "Vp/Vs and Lithology", Geophysics Vol.47,No. 3, pp. 336–344.

82. Uyanik, O. (2010): Compressional and shear-wave velocity measurements in unconsolidated top-soil and comparison of the results, Physical Sciences Vol. 5, No. 7, p. 1034-1039

83. Wair, B. R., DeJong, J. T. & Shantz, T. (2012): Guidelines for Estimation of Shear Wave Velocity Profiles. Berkeley, CA: Pacific Earthquake Research Center.

84. Wongpornchai ,P., Phatchaiyo, R. and Srikoch, N.,(2009): Seismic Refraction Tomography of Mae-Hia Landfill Sites, Mueang District, Chiang Mai, World Academy of Science, Engineering and Technology Vol.32 ,pp.678-681

85. www.geo.mtu.edu./UPSeis/waves.html

86. www.geosurviraq.iq

87. Xia J., Miller R.D., Park C.B., Wightman E. and Nigbor R., (2002): A pitfall in shallow shear-wave refraction surveying, Journal of Applied Geophysics, vol. 51, issue 1, 1-9 pp.

88. Xia, J., Miller R. D., Park C. B. & Tian G. (2003): Inversion of high frequency surface waves with fundamental and higher modes. Journal of Applied Geophysics, 52, 45-57.

89. Xia, J., Miller, R. D. & Park, C. B. (1999): Estimation of near-surface shear-wave velocity by inversion of Rayleigh waves. Geophysics, 64 (3), 691-700.

90. Xia, J., Miller, R. D., Park, C. B. & Ivanov, J. (2000): Construction of 2-D vertical shear-wave velocity field by the multichannel analysis of surface waves technique. Proceeding of the Symposium of the Application of Geophysics to Engineering Environmental Problems (SAGEEP 2000) Arlington, VA., February 20-24, 1197-1206.

91. Young, H. D. & Freedman, R. A. (2008): University Physics with Modern Physics. (12th Edition). San Francisco, CA: Pearson Addison-Wesley.

الملخص

أجريت دراسة هندسية جيوفيزيائية لمشروع بناية مستشفى السيدة رقية في مدينة الحلة بأستخدام طريقة المسح الزلزالي الأنكساري الأفقي وطريقة التحليل متعدد القنوات للموجات السطحية MASW لتحديد متوسط سرعة أمواج القص وعلاقتها بسمك الطبقة وعمق الأساس وقابلية التحمل وحساب المعاملات الهندسية للتربة في طريقة المسح الزلزالي الأنكساري الأفقي . حيث أجري هذا المسح الجيوفيزيائي بأستخدام جهاز ABEM Terraloc MK6 وبأستخدام جيوفونات لأستلام الموجات الزلزالية وكذلك أستخدام مطرقة حديدية وزنها 10 كغم .تم هذا المسح على أمتداد مسارين في المسح الزلزالي الأنكساري الأفقي للحصول على سرع الموجات الانضغاطية والقصية حيث ان طول المسار الواحد 72 م (أمامي وعكسي ومركزي) وتم حساب معاملات المرونة الديناميكية مثل نسبة بوازونν ومعامل يونكE والمعامل الحجميB ومعامل القصμ وأيضا ثابت لامي λ وعدد من المعاملات الهندسية مثل دليل المادةI_m ودليل التركيزI_c ومعامل الضغط الجانبيK_o و زاوية الأحتكاك الداخلي الفعالة Φ^o وأيضا" سعة التحمل المسموح بها Q_{all} بعد الحصول على قيم لسرع الموجات الانضغاطية V_p والقصية V_s في هذين المسارين، وبأستخدام برنامج Reflex 2D Quick تبين ان المسار الأول يتكون من طبقتين وكذلك المسار الثاني يتكون من طبقتين أيضا حيث ان معدل السرعة للموجات الأنضغاطية في المسار الأول للطبقة الأولى والثانية هو 277.768و460.001 م/ ثانية، على التوالي ومعدل السرعة للموجات القصية لنفس المسار ولنفس الطبقتين الاولى والثانية هو 152.423 و 252.734 م/ثانية وعلى التوالي أيضا". سمك الطبقة الاولى في المسار الاول هو 8 م. أما بالنسبة للمسار الثاني فكان معدل السرعة الأنضغاطية لهذا المسار وللطبقتين الأولى والثانية هو276.55 و 465.021 م/ثانية، على

التوالي بينما معدل السرع القصية لهاتين الطبقتين ولنفس المسار هو 152.149 و 250.735 م/ثانية، على التوالي ايضا". وسمك الطبقة الاولى في المسار الثاني هو 8.066 م. أما بالنسبة لطريقة التحليل المتعدد القنوات للموجات السطحية MASW حيث تم المسح بهذه الطريقة على أمتداد مسار واحد فقط وكان طوله 72 م لحساب متوسط سرعة أمواج القص وعلاقتها بعمق الأساس وبسمك الطبقة وقابلية التحمل. بأستخدام برنامج Reflex 2D Quick تبين أن هذا المسار يتكون من طبقتين أيضا" حيث ان قيمة معدل السرعة للموجة القصية في الطبقة الاولى هي 171.6 م/ثانية وبسمك 8.244 م، أما معدل السرعة القصية للطبقة الثانية هو 272.22 م/ثانية. وفي هذه الطريقة تم أستخدام برنامج SeisImager/SW للحصول على مقاطع تصويرية توضح منحنيات التشتت (بين التردد و طور السرعة) وكذلك من أجل رسم مقطع احادي البعد للسرع القصية. تم رسم خرائط كنتورية لتوضح توزيع كل من السرعة القصية، قابلية التحمل، عمق الأساس، وسمك الطبقة مع ملاحظة مدى التوافق بين كل منها. تم عمل علاقة احصائية باستخدام برنامج SPSS بين طريقة المسح الانكساري وطريقة MASW وكانت نسبة الارتباط عالية بين الطريقتين. من خلال النتائج الهندسية والجيوفيزيائية تبين أن الطبقة الثانية في كل المسارات هي الطبقة المقترحة لأقامة المنشأ الهندسي عليها.

وزارة التعليم العالي والبحث العلمي

جامعة بابل / كلية العلوم

قسم علم الارض التطبيقي

دراسة جيوفيزيائية هندسية بأستخدام الطرق الزلزالية الأنكسارية في موقع مستشفى السيدة رقية ـ مدينة الحلة ـ وسط العراق

رسالة مقدمة الى

مجلس كلية العلوم – جامعة بابل

كجزء من متطلبات نيل درجة الماجستير

في العلوم / علم الارض التطبيقي

من قبل

زينب محمد جواد سيفي وهيب

بكالوريوس علم الأرض التطبيقي٢٠١٣

دبلوم عالي في العلوم/ علم الأرض التطبيقي ٢٠١٥

الإشراف

أ. د. عامر عطية لفته الخالدي

2023م **1444هـ**